Development and Characterization of Branching Enzymes for Improving Industrial Starches

by

Jessica Kristyn Victoria White

A thesis
presented to
The University of Guelph

In partial fulfillment of requirements
for the degree of
Master of Science
in
Molecular and Cellular Biology

Guelph, Ontario, Canada

© Jessica Kristyn Victoria White, May, 2018

ABSTRACT

DEVELOPMENT AND CHARACTERIZATION OF BRANCHING ENZYMES FOR IMPROVING INDUSTRIAL STARCHES

Jessica Kristyn Victoria White
University of Guelph, 2018

Advisor:
Dr. Ian J. Tetlow

Starch is a plant-based polyglucan made of branched amylopectin and linear amylose, and is used in many food and non-food applications. The linear component forms undesirable gels during industrial processing at temperatures below 100^{o}C. This thesis describes the development and characterization of branching enzymes with potential to minimize gelling by branching starch. Site-directed mutants of *Deinococcus radiodurans* glycogen branching enzyme (DrGBE) were made (Gln205His, Ala310Gln, Ala310Gly, Ala312Thr). Relative to wild-type, Ala312Thr exhibited increased activity with amylopectin and increased substrate-affinity for amylose and amylopectin, whereas the other mutants exhibited decreased activity with amylose and amylopectin, and Gln205His and Ala310Gln exhibited increased substrate-affinity for amylopectin. An attempt to study DrGBE activity with amylose and amylopectin within starch was unsuccessful, because changes in amylopectin masked changes in amylose. Unsuccessful attempts were made to improve activities of chimeric enzymes previously made with *Zea mays* and *Thermus thermophilus* branching enzyme domains by modifying protein expression/purification/refolding.

ACKNOWLEDGEMENTS

Firstly, I would like to thank Dr. Ian Tetlow for his continual support, encouragement, patience, and advice throughout my project. I am also thankful for my committee members, Dr. Michael Emes and Dr. Steffen Graether, for their advice and encouragement.

I would like to thank Dr. Lily Nasanovsky for providing the *E. coli* cells containing the vectors used to express wild-type *Deinococcus radiodurans* glycogen branching enzyme and the chimeric enzymes, and for her patience when training me, continual technical and personal advice, encouragement, and friendship. I am also thankful for Jacqueline Farr, Kimberly Beech, Alexandra Everette, and Michelle-Rose Goodman, who helped me perform several experiments and who made lab work more fun during their time as undergraduate project students or volunteers. I am thankful for the encouragement and technical advice given by Dr. Jenelle Patterson, Gregory MacNeil, Cecily Costain, Dr. Amina Makhmoudova, Sahar Mehrpooyan, Noel Mano, Matthew Carswell, Dr. Fushan Liu, You Wang, and Liping Wang throughout our time as coworkers.

I am also thankful to my family Jocelyn and Jonathan Collings and Richard, Marlene, Jaclyn, and Joshua White for their continual support, personal and professional advice, and friendship throughout my project.

I would also like to thank the Ontario Ministry of Agriculture, Food and Rural Affairs for funding my research.

TABLE OF CONTENTS

LIST OF FIGURES

LIST OF TABLES

LIST OF ABBREVIATIONS

λ_{max}	Wavelength of maximum absorption
Abs.	Absorbance
BE	Branching enzyme
BSA	Bovine serum albumin
DMSO	Dimethyl sulfoxide
DOPE	Discrete Optimized Protein Energy
DrGBE	*Deinococcus radiodurans* glycogen branching enzyme
DTT	Dithiothreitol
GBE	Glycogen branching enzyme
GH13	Glycoside hydrolase 13
GH57	Glycoside hydrolase 57
GPC	Gel permeation chromatography
IPTG	Isopropyl-β-D-thiogalactoside
KAN	Kanamycin sulfate
K_d	Dissociation constant, inversely related to substrate-affinity
MOPS	3-(N-morpholino)propanesulfonic acid
mSBE	Maize starch branching enzyme
PBS	Phosphate buffered saline
SBE	Starch branching enzyme
SDM	Site-directed mutagenesis
SDS	Sodium dodecyl sulfate
SDS-PAGE	SDS polyacrylamide gel electrophoresis
TEMED	Tetramethylethylenediamine
Tris	Tris(hydroxymethyl)aminomethane
TtGBE	*Thermus thermophilus* glycogen branching enzyme
$TtGBE_{cat}$-$mSBEI_{COO-}$	Chimeric enzyme with the catalytic domain of TtGBE and the carboxyl-terminal domain of mSBEI
$TtGBE_{cat}$-$mSBEI_{NH2}$	Chimeric enzyme with the catalytic domain of TtGBE and the amino-terminal domain of mSBEI
U	Unit for the iodine-binding assay; decrease in absorbance at λ_{max} of the glucan-iodine complex of 1 per min

CHAPTER 1: INTRODUCTION

Starch is the major energy and carbon storage compound in plants, algae and some cyanobacteria. Starch is composed of chains of glucose residues arranged into compact, water-insoluble granules, allowing starch to store high levels of glucose without affecting osmotic potential within plant cells. Plants contain starch within their seeds, fruits, roots, and tubers. In these organs, it serves as either short- or long-term storage. Short-term (transient) starch accumulates in leaf chloroplasts during the day and is degraded at night, whereas long-term (storage) starch accumulates in seed, root, and tuber amyloplasts.

Structure of Starch

Starch is composed of glucose residues joined by linear α-1,4-glycosidic linkages and non-linear α-1,6-glycosidic branches (Figure 1). Most starches contain 20-30% amylose, a mostly linear component with 0.1-1% branching, and contain 70-80% amylopectin, a branched component with ~4-5% branching (Buléon *et al*., 1998; Hizukuri *et al*., 1981; Manners, 1989). Amylose weighs around 10^5-10^6 Da, whereas amylopectin is much larger, weighing around 10^7-10^9 Da (Ball *et al*., 1996; Manners, 1989). As amylopectin composes the majority of starch, it has a greater effect than amylose on the structure and physical properties of starch.

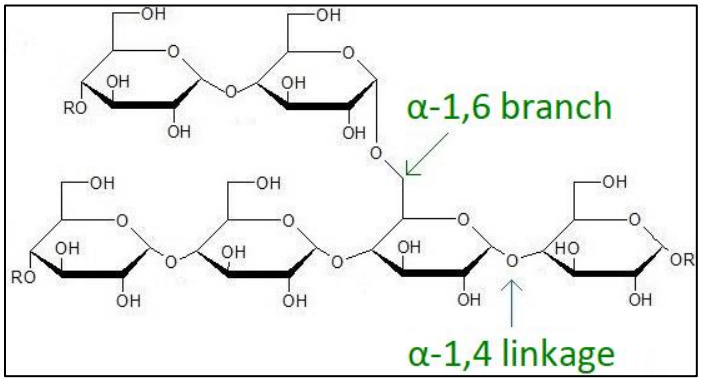

Figure 1: α-1,4-glycosidic linkages and α-1,6-glycosidic branches found in polyglucans. Figure made using ChemSketch.

In unbranched chains containing ten or more glucose residues, hydrogen bonds can form between the hydroxyl groups of neighboring chains, forming crystalline and water-insoluble double helices (Gidley and Bulpin, 1987; Sarko and Wu, 1978). These helices form readily in

amylose due to its low branch frequency. Branches within amylopectin are clustered, and therefore crystalline helices form in unbranched regions (crystalline lamellae) but do not form in branched regions (amorphous, hydrated lamellae) (Figure 2A, B) (Bertoft, 2004; Bertoft *et al*., 2011; Hizukuri, 1986; Robin *et al*., 1974).

The majority of amylopectin is crystalline, giving starch a water-insoluble, granular structure (Figure 2) (Jenkins *et al*., 1993; Waduge *et al*., 2013). Long chains of amylopectin are thought to connect the crystalline lamellae by extending either through or along the crystalline lamellae (cluster or backbone models respectively, shown in Figure 2A, B) (Hizukuri, 1986; Robin *et al*., 1974; Bertoft, 2004, 2017; Bertoft *et al*., 2010, 2011). Alternating layers of amorphous and crystalline lamellae radiate away from the center of the starch granule, forming discrete semi-crystalline blocklets that accumulate to form growth rings (Figure 2C, D) (Gallant *et al*., 1997; Jane, 2009; Waduge *et al*., 2013).

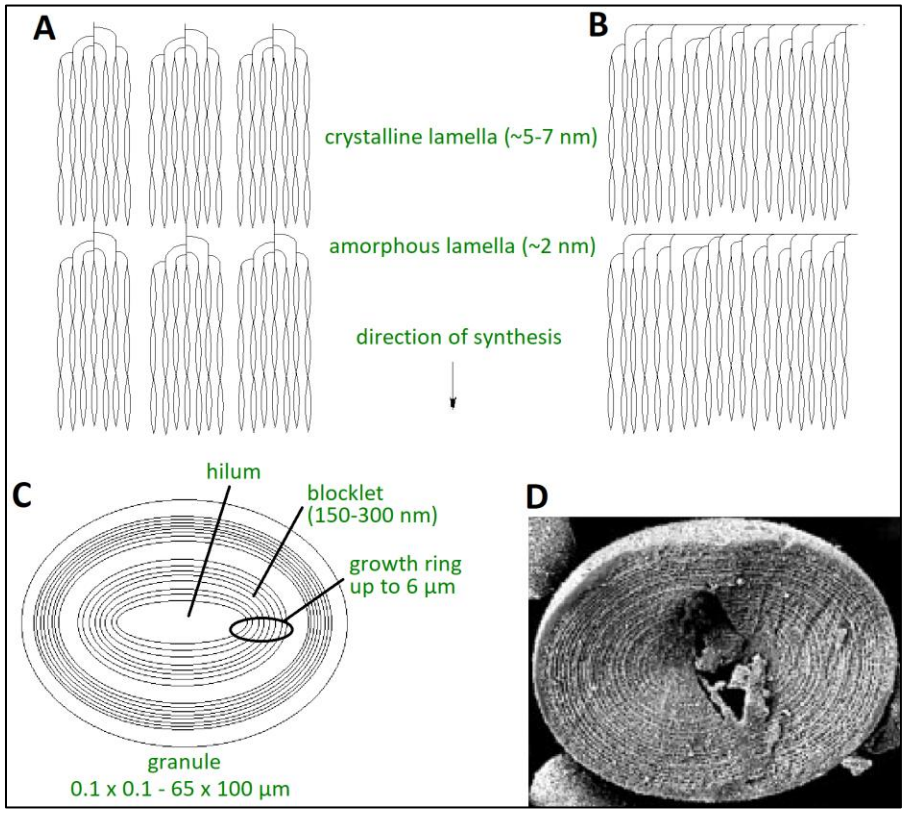

Figure 2: Starch structure. Alternating layers of amorphous and crystalline lamellae according to the cluster model (A) or backbone model (B), radiating away from the center of the granule (hilum), forming blocklets that accumulate into growth rings (C); scanning electron microscopy image of a starch granule showing growth rings (D). Parts A-C were made using ChemSketch. Part D was taken from Pilling and Smith (2003).

Starch granules within plants vary in size, texture, shape, and distribution (individual or aggregated), depending on the plant species, genotype, and developmental stage (Baum and Bailey, 1987; Forsyth *et al*., 2002; Jane *et al*., 1994; Singh and Kaur, 2004; Utrilla-Coello *et al*., 2010). These differences affect how starch is used in industry (Park *et al*. 2005; Singh and Kaur, 2004; Soh *et al*., 2006). Starch also contains proteins and phosphorous, and their potential roles in the starch granule have been discussed in earlier reports (Blennow *et al*., 2002; Denyer *et al*., 1993; Hizukuri *et al*., 1970; Lampitt *et al*., 1948; Lim *et al*., 1994; Schoch, 1942; Soni *et al*., 1990; Tabata and Hizukuri, 1971; Takeda and Hizukuri, 1982).

Starch Biosynthesis and Degradation

Starch biosynthesis involves five major reactions. A specific enzyme class carries out each reaction, and each enzyme class contains several isoforms. The first reaction, catalyzed by ADP-glucose pyrophosphorylase, is the synthesis of ADP-glucose *via* the following reaction: ATP + glucose-1-phosphate ⇌ pyrophosphate + ADP-glucose (Ghosh and Preiss, 1966). Next, starch synthases elongate polyglucan chains by transferring glucose from ADP-glucose to the C4 non-reducing end of another glucose, forming an α-1,4 glycosidic linkage (Recondo and Leloir, 1961). Starch branching enzymes (SBEs) convert specific α-1,4 linkages into α-1,6 branches (Martin and Smith, 1995). Starch debranching enzymes then hydrolyze specific α-1,6 branches to allow crystalline helices to form (Figure 3) (Pan and Nelson, 1984). Disproportionating enzyme transfers glucose residues between amylopectin chains by cleaving and reforming α-1,4-linkages, but it is not known how this contributes to the synthesis of amylopectin (Colleoni *et al*., 1999). For a detailed review of starch biosynthesis, see Tetlow and Emes (2017).

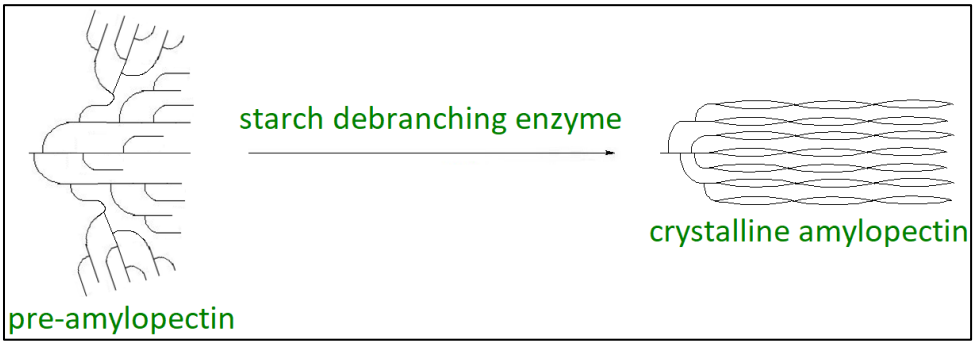

Figure 3: Conversion of pre-amylopectin to amylopectin *via* reaction with starch debranching enzyme. Figure made using ChemSketch.

Glucan water dikinases appear to initiate starch degradation by phosphorylating the glucan so that it is soluble and accessible to endo-amylases that hydrolyze the polymer into maltodextrins (Baunsgaard *et al*., 2005; Beck and Ziegler, 1989; Blennow *et al*., 2002; Lorberth *et al*., 1998; Ritte *et al*., 2002). Other hydrolytic enzymes (*e.g.* isoamylase) appear to degrade the maltodextrins into glucose that is used in sucrose synthesis (Beck and Ziegler, 1989; Trethewey and Rees, 1994a, 1994b; Yu *et al*., 2001).

Uses of Starch

Starch is important to the human population. Approximately forty-nine million tons of starch are produced per year (Jobling, 2004). Starch is the major source of calories to the human population, is found in high quantities in staple foods (*e.g.* bread, pasta, and porridge), and is used in animal feed. Starch is also used as a thickener, stabilizer, coating agent, and fat mimetic in food products such as yogurt and canned goods (Ačkar *et al*., 2015; Alting *et al*., 2009; Burrell, 2012).

A significant amount of starch is also used for non-food purposes. Starch is biodegradable, non-toxic, widely available, cheap, and renewable, and can be modified to alter its properties, giving it a wide range of applications (Jia *et al*., 2011; Kümmerer *et al*., 2011; Yu *et al*., 2007). Starch is often converted to fermentable sugars that are used to make biofuels (Flach *et al*., 2013). Starch is also used as a gelation agent, adhesive, disintegrate, diluent, settling agent, and/or additive in paints, pharmaceuticals, textiles, papers, cement, and biodegradable plastics (Burrell, 2003; Copeland *et al*., 2009; Hajji, 2011; Ochubiojo and Rodrigues, 2012; Otegbayo *et al*., 2014; Stagner *et al*., 2011). In addition, starch is used as a blood plasma volume expander for victims of blood loss and cancer, and is also used in bone tissue engineering and in the production of artificial red blood cells (Ochubiojo and Rodrigues, 2012).

Industrial Processing of Starch

Harvested starch is often processed to make it suitable for end applications. Before processing, starch is commonly dissolved in hot solvents at temperatures above 75^{o}C ("solubilized" or "gelatinized"). Solubilization disrupts the crystalline helices between

neighboring glucan chains, increasing starch solubility and increasing the accessibility of reactive hydroxyl groups within starch for subsequent modification (Figure 4) (Jobling, 2004). However, upon cooling, insoluble helices between glucan chains form again, resulting in a gel that is distinct from natural starch in a process known as retrogradation (Figure 4) (Alcázar-Alay and Meireles, 2015).

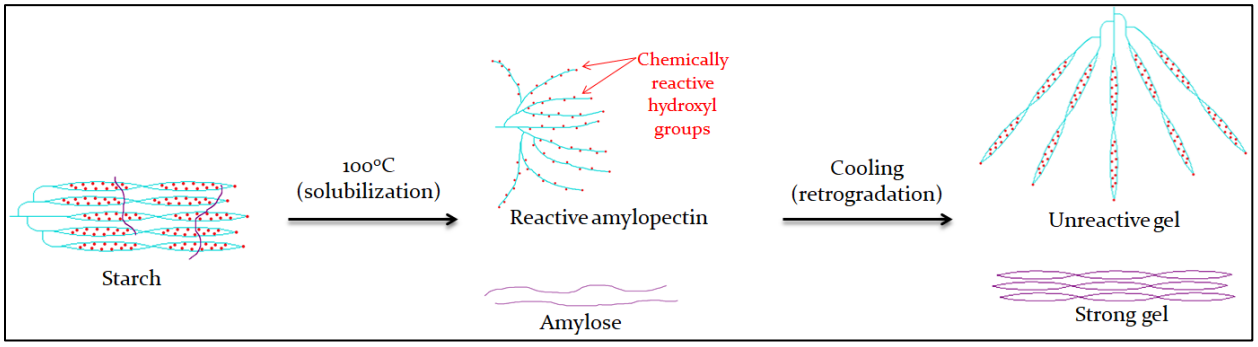

Figure 4: Solubilization and retrogradation of starch. Figure made using ChemSketch.

Retrograded starch decreases the quality of starch-based products and increases manufacturing and transportations costs; for example, retrograded starch deposits unevenly onto products and forces industries to shut down and clear equipment (Nichols, 2002). Industries are often forced to use starch solutions at lower concentrations than desired to minimize retrogradation, which is concentration-dependent, reducing the range of end applications for starch (Nichols, 2002).

Amylose is more susceptible than amylopectin to retrogradation due to its low branching frequency and long chains that favour helix formation (Abbas *et al*., 2010; Alcázar-Alay and Meireles, 2015). Therefore, industries often desire amylose-free or low-amylose starches (*waxy* starches). *Waxy* starches are acquired from mutant varieties of maize, wheat, potato, rice, and barley in which a specific starch synthase isoform (granule bound starch synthase) has reduced or absent activity (Ball *et al*., 1998; Hovenkamp-Hermelink *et al*., 1987; Nakamura *et al*., 1998; Shure *et al*., 1983; Vrinten and Nakamura, 2000).

However, *waxy* starch is expensive ($3.94-$13.78 more for *waxy* corn than regular corn per metric ton in America from 2001-2005). Farmers also require that *waxy* crops be contracted a year before they are grown, forcing industries to predict how much they need far in advance (U.S. Grains Council, 2006). This is because the *waxy* trait is recessive, requiring farmers to

isolate *waxy* crops from wild-type crops, to grow *waxy* crops on soil not used the previous year for wild-type crops, and to perform quality control procedures to prevent contamination (Hofreiter *et al*., 1978; Pauley *et al*., 2000; U.S. Grains Council, 2006). Additionally, *waxy* varieties are best grown in Southern regions such as Indiana and Illinois, and must therefore be transported to Ontario if used locally, which is also expensive (U.S. Grains Council, 2006). Low-amylose starches from mutant crops with downregulated debranching enzyme (as opposed to downregulated starch synthase) are not widely used because these crops synthesize excessively-branched, water-soluble polyglucan ("phytoglycogen") that cannot efficiently accumulate in plants due to osmotic effects on the cell (Anderson and Singh, 2003; Bi *et al*., 2011a, 2011b; Burton *et al*., 2002; Delatte *et al*., 2005; James *et al*., 1995; Mouille *et al*., 1996; Wattebled *et al*., 2005; Wong *et al*., 2003). Because low-amylose starch from mutant crops is expensive, industries instead use starch from wild-type crops that has been modified post-harvest to reduce its susceptibility to retrogradation. Starch modification can be done chemically, physically, or enzymatically.

Chemical modification is a common method used to hinder starch retrogradation in food, paper, textile, plastic, coating, and adhesive industries; chemical modification involves derivatization of the starch hydroxyl groups to reduce molecular linearity and increase hydrophilicity, or involves cross-linking of starch hydroxyl groups to strengthen starch and prevent solubilization (examples are shown in Table 1). Physical modification of starch is common in food/feed, paper, and textile industries, and involves heat, pressure, and/or mechanical treatment (in the presence of absence of water) (see Table 2 for examples). Enzymatic modification of starch is a newer technique involving treatment with enzymes that shorten and/or branch glucan chains (decreasing amylose content and susceptibility to retrogradation) (see Table 3).

Table 1: Examples of chemical modifications of starch performed in industry.

Modification *	Examples**	Advantages and Disadvantages
Oxidation	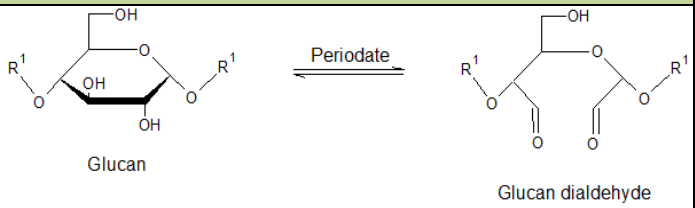 Alternatively: reaction with H_2O_2, potassium permanganate, or acidic bromate, or photo oxidation	Decreases retrogradation and viscosity Increases solubility Use or release of toxic chemicals Depolymerization
Acetylation	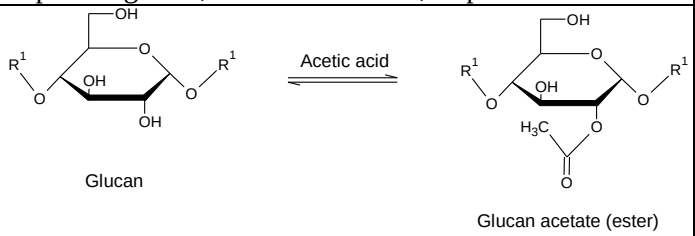 Alternatively: reaction with acetic anhydride, or vinyl acetate	Decreases retrogradation and viscosity Increases solubility Use of toxic, carcinogenic, and/or expensive chemicals
Succinylation	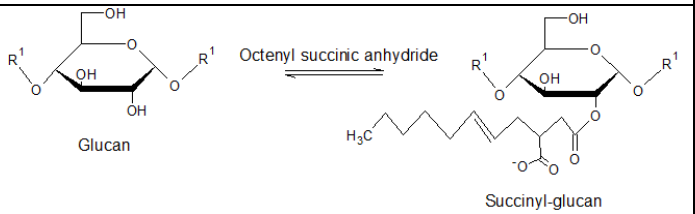	Decreases retrogradation Increases or decreases viscosity depending on starch source Use of toxic, carcinogenic, and/or expensive chemicals
Cross-linking	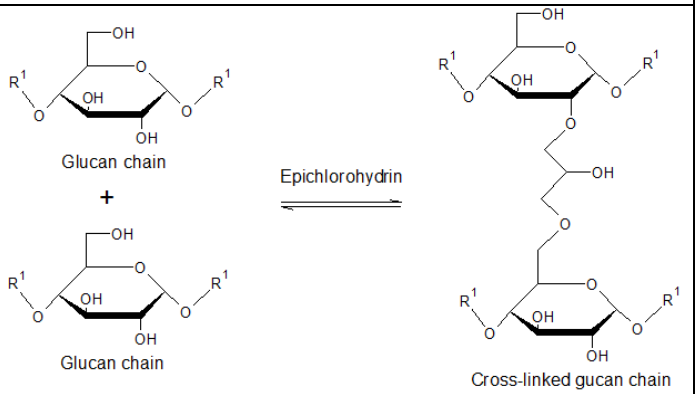 Alternatively: reaction with monosodium phosphate, phosphoryl chloride, or vinyl chloride	Strengthens starch granules, decreasing solubilization and subsequent retrogradation Increases viscosity Use of carcinogenic chemicals

*References: Ačkar *et al*. (2015); Bhandari and Singhal (2002); El-Sheikh *et al*. (2009); Komulainen *et al*. (2013); Korma *et al*. (2016); Lawal (2004); Lewicka *et al*. (2015); Malmsjo *et al*. (2012); Muhamedbegović *et al*. (2012); Olayinka *et al*. (2011); Sodhi and Singh (2005); Tharanathan (2005).
** Reaction images were made using ChemSketch.

Table 2: Examples of physical modifications of starch performed in industry.

Modification*	Process	Applications	Disadvantages
Pregelatinization (or precooking)	Solubilization (130-135^{o}C, pressure, often in steam-heated rollers) followed by drying and grinding (in a drum drier containing rollers)	Fragments starch Increases solubility Can decrease retrogradation	Depolymerization Retrogradation decreases only in some starches
Extrusion	Fractionation (pushing through a hole the size of desired end material), followed by cooking (in an extruder)	Increases solubility	Depolymerization
Heat-moisture treatment	Heating to temperature required for solubilization, but with almost no water present	Can increase solubility	Solubility increases only in some starches

*References: Colonna *et al*. (1984); Doublier *et al*. (1986); Jyothi *et al*. (2010); Takahashi and Ojima (1969); Yadav *et al*. (2013).

Table 3: Examples of enzymes used to modify starch.

Enzyme (and source)	Effect on starch*	Reference
α-amylases & glucoamylases (bacteria and fungi)	Decreased retrogradation and molecular weight Increased branching	Hofreiter *et al*., 1978
α-amylase (*Bacillus licheniformis*)	Decreased viscosity and molecular weight	Skuratowicz *et al*., 2009
α-amylase (*B. licheniformis*)	Decreased molecular weight	Pauley *et al*., 2000
α-amylase (*Bacillus stearothermophilus*)	Increased solubility Decreased molecular weight	Brumm, 1997
Putative glycogen branching enzyme (*Streptococcus mutans*)	Decreased retrogradation and molecular weight Increased branching	Kim *et al*., 2008
Glycogen branching enzyme (*Geobacillus thermoglucosidans*)	Decreased retrogradation Molecular weight not analyzed	Li *et al*., 2016
Cyclomaltodextrinase (*Bacillus* sp.)	Decreased retrogradation, amylose content, and molecular weight	Auh *et al*., 2006
Glycogen branching enzyme (*Rhodothermus obamensis*)	Increased solubility and branching Decreased molecular weight	Jensen *et al*., 2013
Disproportionating enzyme (*Thermotoga maritima*)	Increased solubility Decreased amylose content and molecular weight	Oh *et al*., 2008
Amylomaltase (*Thermus thermophilus*)	Decreased amylose content and molecular weight	van der Maarel *et al*., 2005
Glycogen branching enzyme (*Bacillus subtilis*)	Decreased amylose content and molecular weight	Le *et al*., 2009
Glycogen branching enzyme (*Acidothermus cellulolyticus*)	Decreased amylose content and molecular weight	Li *et al*., 2014
Amylomaltase (*T. thermophilus*)	Decreased molecular weight	Hansen *et al*., 2008

*Starches from wild-type, *waxy*, or high-amylose maize, rice, potato, or cassava root were tested at 30-85^{o}C

As detailed in Tables 1-3, current modifications of starch have some disadvantages. Chemical modification often requires or releases harmful chemicals, is expensive, and depolymerizes glucans. Depolymerization is problematic because the low-molecular weight products generated are lost during industrial washing and filtering of glucans, reducing yield by up to 15% (Pauley *et al*., 2000). Additionally, C1 reducing ends generated during glucan depolymerization react with the nucleophilic amino groups that are present during starch processing (Maillard reaction), producing a brown colour that is undesirable in several industries, especially paper-making industries. Physical modification causes unpredictable results depending on starch type and can cause glucan depolymerization. Enzymatic modification in industry most commonly uses α-amylases that non-selectively depolymerize (hydrolyze) glucans and yield unnatural amylopectin (Hofreiter *et al*., 1978). Enzymatic treatment can produce glucans as small as 2 x 10^4 Da (compared to amylopectin that is 10^7-10^9 Da) (Brumm, 1997).

Hofreiter *et al*. (1978) avoided shortening amylopectin while decreasing retrogradation by cross-linking non-selective α-amylase (from *B. subtilis*) to a porous carrier that preferentially absorbs amylose, so that α-amylase would access and hydrolyze amylose and not amylopectin. However, their method still generated short-chain oligosaccharides containing one to eight glucose residues, and these oligosaccharides must be removed from the sample prior to specific applications. Additionally, optimal cross-linking required the use of phenol-formaldehyde, which is made from and can degrade into toxic compounds (Hofreiter *et al*., 1978). Skuratowicz *et al*. (2009) attempted to reduce retrogradation while maintaining high molecular weight compounds by utilizing starch hydrolyzing enzymes (such as α-amylases, isoamylases, and enzyme mixtures) and conditions that favour hydrolysis of the starch into long oligosaccharides instead of small sugars. However, their method still reduced molecular weight to at least 2.5-20 x 10^4 Da, which is much smaller than amylopectin (10^7-10^9 Da).

Branching Enzymes for Modifying Starch

Branching enzymes (BEs) can potentially improve the properties of industrial starches. Unlike α-amylases that hydrolyze glucans, BEs hinder retrogradation *via* branching, which shortens glucan chains and introduces steric hindrance with minimal glucan depolymerization (Figure 5) (Abbas *et al*., 2010; Alcázar-Alay and Meireles, 2015; van der Maarel *et al*., 2002).

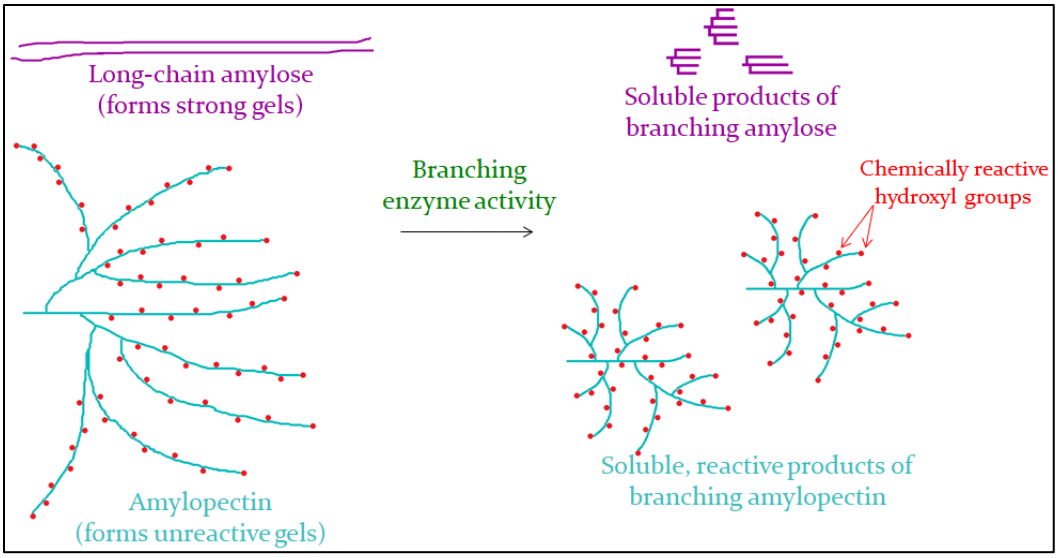

Figure 5: Ability of branching enzyme to reduce retrogradation and increase reactivity of industrial starches by forming branches and shortening chains. Figure made using ChemSketch.

The ability of prokaryotic BEs to improve the properties of harvested starch is being studied because these enzymes can be isolated from thermostable species and thus withstand the high temperatures required for processing starch while avoiding retrogradation (Fan *et al*., 2016; Palomo *et al*., 2011; Shinohara *et al*., 2001; Takata *et al*., 2003). For example, BEs from *R. obamensis* and *Aquifex aeolicus* have optimal activities at 65-80^{o}C (van der Maarel *et al*., 2003; Shinohara *et al*., 2001; Takata *et al*., 2003). BEs from *S. mutans*, *G. thermoglucosidans*, and *R. obamensis* have already been shown to decrease retrogradation (see Table 3).

Prokaryotic BEs are naturally involved in glycogen biosynthesis and are referred to as glycogen branching enzymes (GBEs). Glycogen is the energy and carbon storage compound of most prokaryotes and non-plant eukaryotes (for example, bacteria and humans), and, similarly to starch, is composed of glucose residues joined *via* α-1,4 linkages and α-1,6 branches. However, relative to starch, glycogen branching is more frequent (8-12% as opposed to 4-5%) and is evenly distributed (amylopectin branches are clustered), giving glycogen an open, soluble, osmotically active structure that can be degraded and used more rapidly (Ball and Morell, 2003; Roach *et al*., 2012). Glycogen synthesis is similar to starch synthesis (glycogen synthases elongate glucan chains using UDP-glucose, and GBE branches the glucan chains (Farkass *et al*., 1991; François and Parrou, 2001; Leloir *et al*., 1959, 1961). However, bacteria and humans contain one GBE isoform per species, whereas dicots and monocots each contain two or three BE isoforms: SBEI and SBEII in dicots, and SBEI, SBEIIa, and SBEIIb in monocots (Boyer and

Preiss, 1978; Dang and Boyer, 1988). Each BE isoform has unique properties, such as substrate preference and optimum temperature for catalysis, which affect how the enzyme can be used industrially. Examples of the distinct properties of BE isoforms within and between different species have been reported by Guan and Preiss (1993), Guan *et al*. (1997), Palomo *et al*. (2009), and Takeda *et al*. (1993).

Branching Enzyme Structure and Reaction Mechanism

Nearly all BEs are members of the glycoside hydrolase 13 (GH13) α-amylase family of enzymes (based on their amino acid sequences) (Henrissat, 1991; Janeček, 1994). The GH13 family of enzymes includes most enzymes that hydrolyze or transglycosylate α-1,4 linkages and/or α-1,6 branches, including most α-amylases, isoamylases, and cyclodextrin glucanotransferases (Baba *et al*., 1991; Svensson, 1988; Takata *et al*., 1992). GH13 family enzymes contain three domains: an amino-terminal domain, a central and catalytic $(\beta/\alpha)_8$-barrel domain, and a carboxyl-terminal domain (Figure 6) (Abad *et al*., 2002; Buisson *et al*., 1987; Katsuya *et al*., 1998; Matsuura *et al*., 1984). However, some GBEs, such as those from the bacterium *Thermus thermophilus* and the Archaeon *Thermococcus kodakaraensis*, belong to the glycoside hydrolase 57 (GH57) α-amylases family of enzymes (Henrissat and Bairoch, 1996; Murakami *et al*., 2006; Palomo *et al*., 2011). GH57 family enzymes have two domains: a catalytic amino-terminal $(\beta/\alpha)_7$-domain and a carboxyl-terminal domain (Figure 6) (Imamura *et al*., 2003).

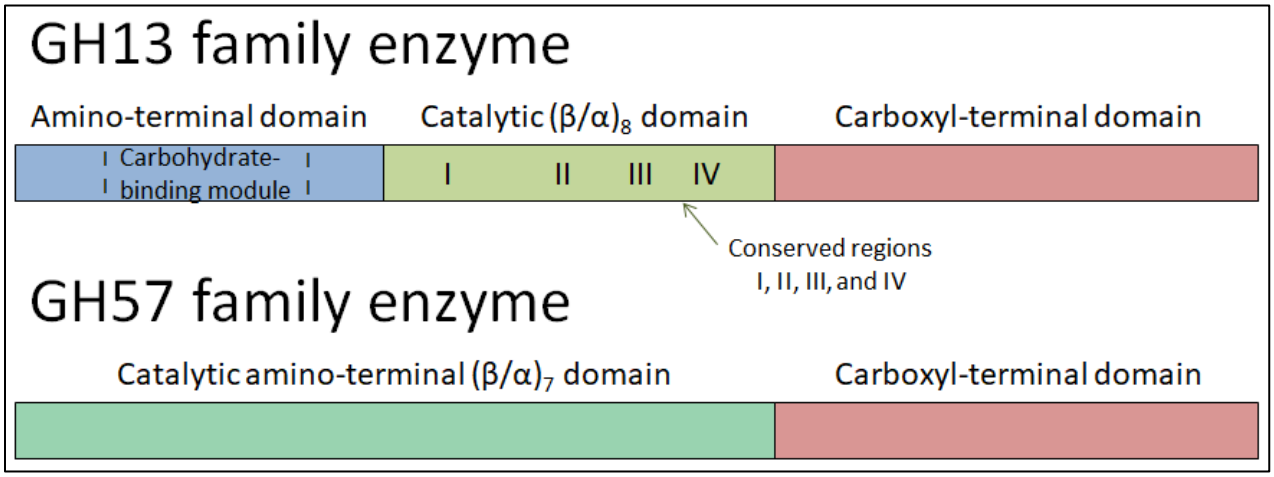

Figure 6: Domains within GH13 *versus* GH57 family enzymes.

Structure and Reaction Mechanism of GH13 Family Branching Enzymes

The catalytic domain of GH13 family branching enzymes is more highly conserved than either terminal domain, and contains four highly conserved regions with three catalytic residues, which are thought to catalyze reaction *via* a mechanism similar to GH13 family α-amylases, based on structural studies (Figures 6-9) (Baba *et al*., 1991; Buisson *et al*., 1987; Kuriki *et al*., 1991; MacGregor *et al*., 2001; Mathupala *et al*., 1993; Matsuura *et al*., 1984; Mosi *et al*., 1997; Nagashima *et al*., 1992; Nakajima *et al*., 1986; Pal *et al*., 2010; Uitdehaag *et al*., 1999). The proposed BE mechanism begins with a glutamic acid residue within BE protonating a glycosidic oxygen within a glucan. Next, an aspartic acid residue performs a nucleophilic attack on the anomeric carbon (carbon 1) in the same glucose residue, yielding an intermediate which is stabilized by another aspartic acid residue. The carbon 6 hydroxyl group on the original chain or another chain then performs a nucleophilic attack on the carbon 1, forming a branch point (intra- or inter-chain transfer respectively) (Borovsky *et al*., 1976). In some cases, a hydroxyl group from water (not glucan) performs the final nucleophilic attack on the original glucan carbon 1, resulting in glucan amylolysis ("inefficient branching" or "hydrolysis") instead of branching. Amylolysis is generally a minor component of BE activity (for example, below 1% in GBE from *Deinococcus radiodurans* (Palomo *et al*., 2009)).

Several non-catalytic residues within the catalytic domain are also important in BE properties including substrate-binding, catalytic rate, and thermostability (see Table 8 in Results for details). The catalytic domain is electronegative, which is important in its ability to interact with α-glucans (Abad *et al*., 2002).

	Conserved region 1	Conserved region 2	Conserved region 3	Conserved region 4
		Putative nucleophile ↓	Putative proton donor ↓	Putative stabilizer ↓
Thermostable GBEs				
Deinococcus radiodurans	239 DWVPGH	305 GLRV**D**AVAS	360 **E**EST	422 LAISH**D**
Rhodothermus marinus	235 DWVPSH	301 GLRV**D**AVAS	356 **E**EST	418 LPLSH**D**
Geobacillus thermoglucosidans	239 DWVPGH	305 GFRV**D**AVAN	352 **E**DST	415 LPFSH**D**
Non-thermostable GBEs				
Escherichia coli	335 DWVPGH	401 ALRV**D**AVAS	458 **E**EST	521 LPLSH**D**
Mycobacterium tuberculosis	341 DWVPAH	407 GLRV**D**AVAS	464 **E**EST	527 LPLSH**D**
Homo sapiens	286 DVVHSH	353 GFRF**D**GVTS	412 **E**DVS	476 YAESH**D**
SBEs				
Zea mays IIb	315 DVVHSH	382 GFRF**D**GVTS	441 **E**DVS	504 YAESH**D**
Oryza sativa I	270 DVVHSH	340 GFRF**D**GVTS	399 **E**DVS	463 YAESH**D**
Arabidopsis thaliana 2.2	380 DIVHSH	447 GFRF**D**GVTS	506 **E**DVS	569 YAESH**D**

Figure 7: Conserved regions and catalytic residues within GH13 branching enzymes. Alignment was made using Clustal Omega, and catalytic residues are shown in red.

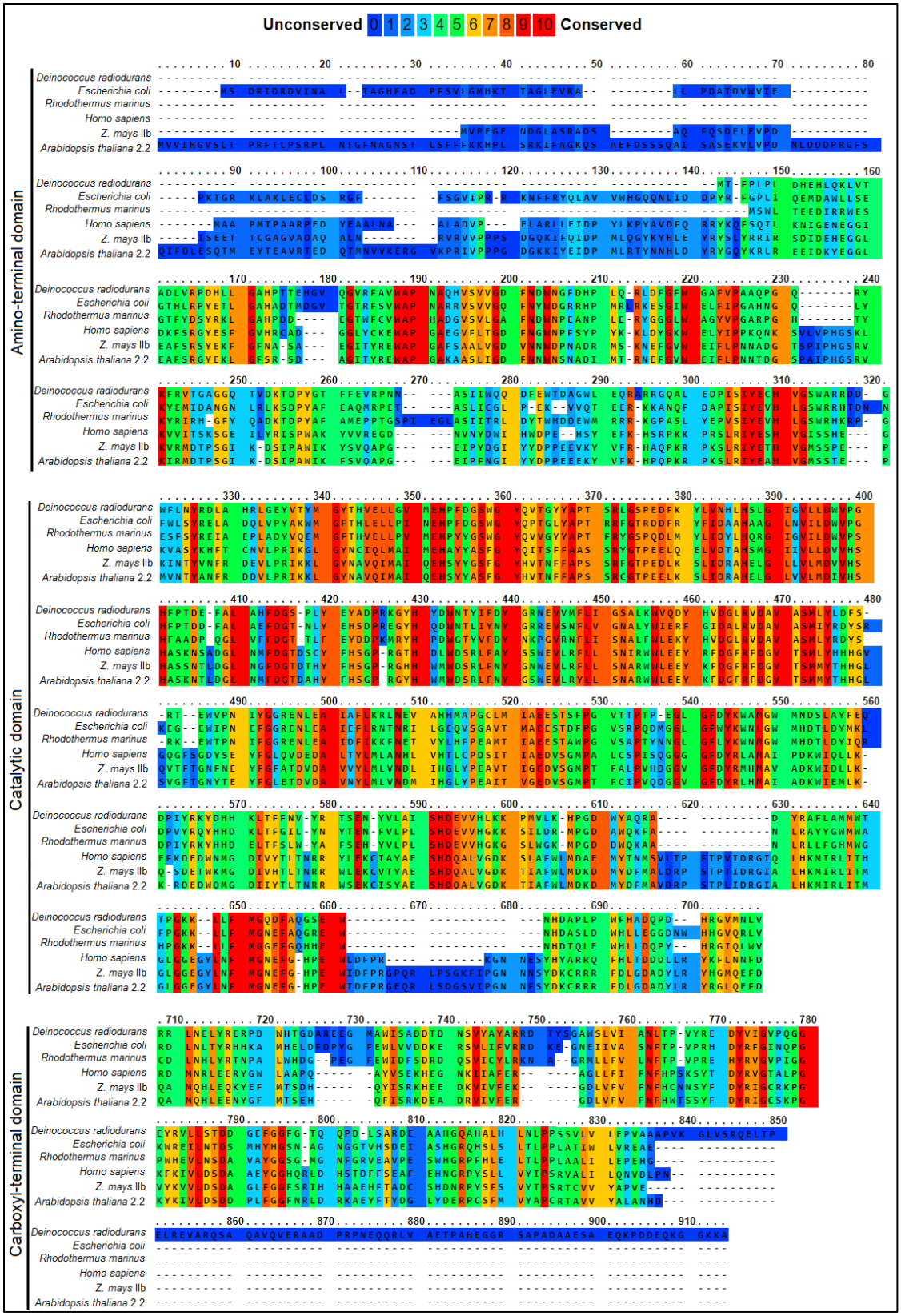

Figure 8: Sequence conservation among select GH13 branching enzymes. The colour scale is shown at the top of the figure. Figure was made using PRALINE.

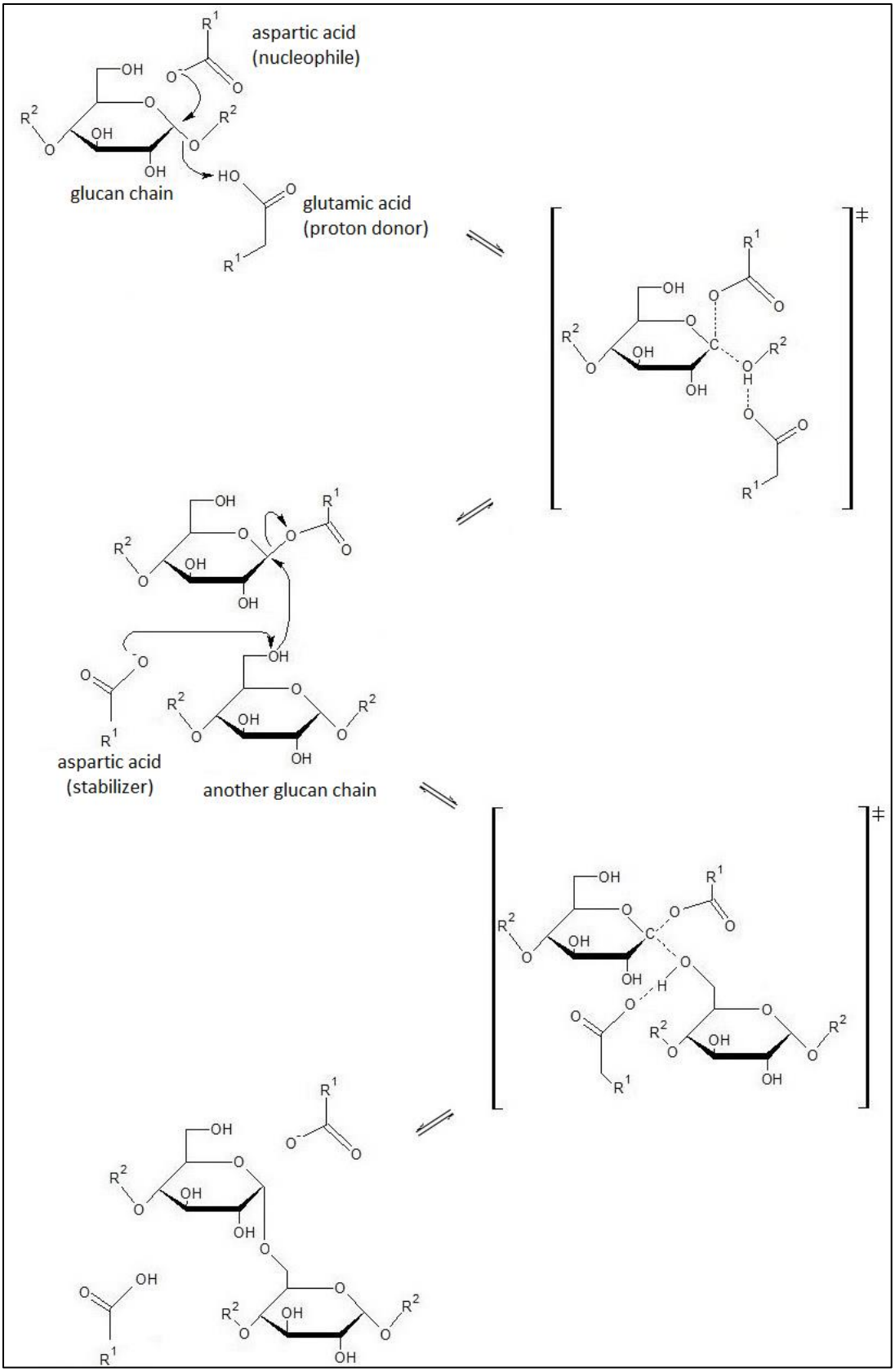

Figure 9: Proposed catalytic mechanism of GH13 family branching enzymes.

The amino- and carboxyl-terminal domains of GH13 enzymes are less conserved than the catalytic domain (Figure 8). The amino-terminal domain contains a carbohydrate-binding module (CBM48, Figure 6) (Chaen *et al*., 2012; Koay *et al*., 2007), and this domain may be important in determining the lengths of the transferred glucan chains in some BEs. This was first suggested by a domain-swapping experiment performed by Kuriki *et al*. (1997), in which a chimeric enzyme containing the amino-terminal domain from mSBEI and the central- and carboxyl-terminal domains from mSBEII was able to transfer chains of similar length as those transferred by mSBEI (Figure 10). Another experiment showed that truncation of the amino-terminal domain of *E. coli* GBE altered the length of glucan chains transferred (Binderup *et al*., 2002). Studies of the amino-terminal domain of *Deinococcus radiodurans* GBE and *Deinococcus geothermalis* GBE also suggested that the amino-terminal domain affects the product branching pattern, in addition to the substrate specificity of the enzymes (Palomo *et al*., 2009). However, domain-swapping experiments performed using SBEs from *Phaseolus vulgaris* L. (kidney beans) suggested that the amino-terminal domain is important in catalytic activity but not in determining the length of chains transferred, suggesting that the function of the domain may vary between BEs (Hamada *et al*., 2007). Domain-swapping experiments using maize and kidney bean BEs suggested that the carboxyl-terminal domain affects catalytic rate, substrate-binding, and/or the length of chains transferred, whereas experiments using *D. radiodurans* and *D. geothermalis* GBEs suggested that the domain does not affect substrate-binding or branching pattern (an example is shown in Figure 10) (Hong and Preiss, 2000; Ito *et al*., 2004; Kuriki *et al*., 1997; Palomo *et al*., 2009).

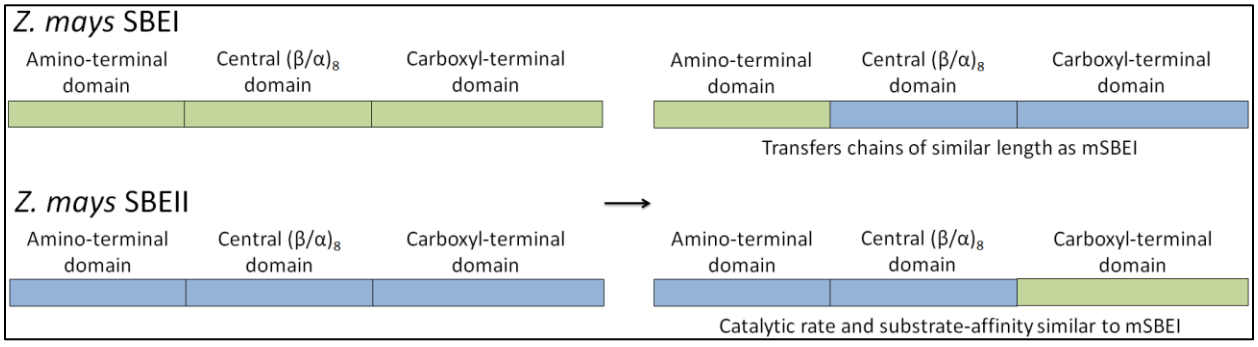

Figure 10: Starch branching enzyme domain-swapping experiment performed by Kuriki *et al*. (1997).

Structure and Reaction Mechanism of GH57 Family Branching Enzymes

GH57 family enzymes contain several conserved amino acid residues, two of which are hypothesized to be catalytic (Table 4). The proposed reaction mechanism for this family is similar to that of GH13 family enzymes, except the glutamic acid acts as the nucleophile, and the aspartic acid acts as the proton donor (as opposed to *vice versa* for GH13 family enzymes) (Imamura *et al*., 2001; Murakami *et al*., 2006; Palomo *et al*., 2011). In *T. thermophilus* GBE, the amino-terminal $(\beta/\alpha)_7$-domain is required for substrate-binding in addition to catalysis (Palomo *et al*., 2011). The function of the carboxyl-terminal domain is not known.

Table 4: Conserved and catalytic residues within GH57 family enzymes.

Residue (*T. thermophilus* numbering)	**Conserved**	**Catalytic (hypothesized)**	**References**
Glu183 and Asp354	Yes	Yes	Imamura *et al*. (2001); Murakami *et al*. (2006)
His10, His145, Trp270, Trp407, Trp416	Yes	Not determined	

***Deinococcus radiodurans* Glycogen Branching Enzyme**

GBE from the extremophilic bacterium *Deinococcus radiodurans* (DrGBE) is an attractive candidate for large-scale modification of starch-based polyglucans, as the enzyme is naturally able to withstand extreme conditions which are commonly used in industry. DrGBE also has high catalytic activity relative to most other GH13 GBEs, which could allow lower amounts of DrGBE to be used to reduce polyglucan retrogradation relative to other BEs, minimizing protein production costs (Palomo *et al*., 2009). Additionally, bacterial proteins are generally easier to produce recombinantly within *E. coli* than are plant SBEs.

DrGBE is active from pH 7-9, has a temperature optimum at 34^{o}C, and can remain fully active at 50^{o}C for one hour, making it more useful in industry than less thermotolerant BEs, such as those from maize (Palomo *et al*., 2009; Takeda *et al*., 1993). Nasanovsky (2017) showed that treatment of an industrial polyglucan with DrGBE reduced glucan susceptibility to retrogradation, increased glucan branching, and caused no glucan amylolysis (degradation). While DrGBE naturally prefers to catalyze reactions with branched substrates, such as glycogen or amylopectin instead of amylose, DrGBE can potentially be modified to increase substrate-affinity for and

activity with amylose to maximize decreases in retrogradation while minimizing changes to amylopectin (see Goal 1) (Palomo *et al*., 2009).

Chimeric Enzymes

Chimeric enzymes containing domains from multiple enzymes may also have potential for improving industrial starches. Chimeric branching enzymes have been made containing domains from mSBEI and *T. thermophilus* GBE (TtGBE), with the intention that the mSBEI domains would impart substrate-affinity for starch-like polymers and the TtGBE domains would impart thermostability (TtGBE has optimal activity at 65^{o}C and can remain active for up to one hour at 80^{o}C) (Boyer and Preiss, 1978; Guan and Preiss, 1993; Guan *et al*., 1997; Nasanovsky, 2017; Palomo *et al*., 2011). The chimeric enzymes contain the catalytic domain of TtGBE and either the amino- or carboxyl-terminal domain of mSBEI ($TtGBE_{cat}$-$mSBEI_{NH2}$ and $TtGBE_{cat}$-$mSBEI_{COO-}$ respectively) (Figure 11). While the chimeric enzymes were partially characterized previously, complete characterization was not possible due to their low expression yields and low catalytic rates (Nasanovsky, 2017).

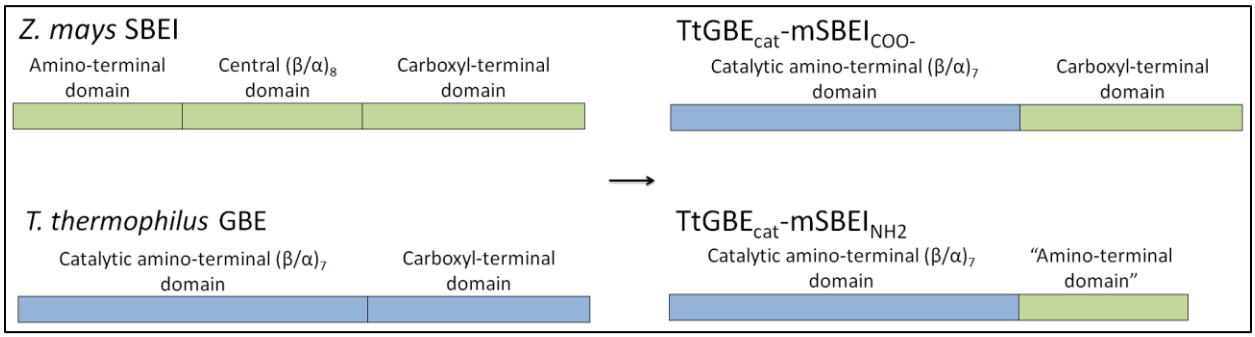

Figure 11: Chimeric branching enzymes made by Nasanovsky (2017).

Purpose and Hypotheses

The following M.Sc. project developed and characterized branching enzymes with potential for improving industrial starches. The project consisted of two goals:

Goal 1:

- Purpose: Create and analyze site-directed DrGBE mutants with increased substrate-affinity for and activity with amylose (regardless of whether or not amylopectin is present)
- Hypothesis: Relative to wild-type, the DrGBE mutants will exhibit higher substrate-affinity for amylose and higher activity with amylose
- Practical implications: Increased activity with amylose will allow DrGBE to reduce amylose content and thus retrogradation of industrial starches while minimizing reductions in the molecular weight of amylopectin

Goal 2:

- Purpose: Optimize production of $TtGBE_{cat}$-$mSBEI_{NH2}$ and $TtGBE_{cat}$-$mSBEI_{COO-}$
- Hypothesis: The chimeric enzyme expression yields and catalytic rates can be improved by altering protein expression, purification, or protein refolding
- Practical implications: The chimeric enzymes may have increased catalytic activity with amylose and thermostability relative to their native counterparts, providing enzymes with increased ability to reduce retrogradation of industrial starches, even at high temperatures

CHAPTER 2: MATERIALS AND METHODS

Protein Expression

Recombinant DrGBE and DrGBE variants for mutagenesis studies were expressed from the pET28a vector as fusions to amino-terminal His-tags. Recombinant $TtGBE_{cat}$-$mSBEI_{COO-}$, $TtGBE_{cat}$-$mSBEI_{NH2}$, and DrGBE (for comparison to chimeric enzymes) were expressed from the pTXB1 vector as fusions to carboxyl-terminal intein tags (Cat# N6707 from New England Biolabs; Chong *et al*., 1997). Recombinant proteins were expressed in *E. coli* BL21(DE3) cells. Nasanovsky (2017) provided the *E. coli* cell lines containing the vectors used for expression of wild-type DrGBE and the chimeric enzymes. Cell lines were stored between use at -80°C in 40% (v/v) glycerol + 60% (v/v) LB Broth containing appropriate antibiotic (100% (v/v) LB broth contained 10 g/L tryptone, 5 g/L yeast extract, 5 g/L NaCl, and 100 or 50 μg/mL of ampicillin sodium salt or kanamycin sulfate (KAN) for cells hosting pTXB1 or pET28a vectors respectively).

Overnight cultures of *E. coli* were grown in 100% (v/v) LB broth containing the appropriate antibiotic (described in the paragraph above) for 16h at 37°C and 220-250 rpm (in the Innova®40 from the New Brunswick Scientific Incubator Shaker Series). The next morning, each culture was diluted into LB Broth without antibiotic (exact volumes are shown in Table S1 on page 82). The cultures were subsequently incubated for another 3 h at 37°C and 250 rpm (in the Innova®44 from New Brunswick Scientific) until the cells reached mid-to-late log phase (when the absorbance of the cultures at 600 nm reached 0.4-0.6). 1 mL of cells was then harvested for SDS-PAGE analysis (*via* centrifugation at 16,000 rpm for 2 min at room temperature, using the Beckman Coulter™ Microfuge 22R Centrifuge). Expression of the T7 promoter upstream of the gene for DrGBE or either chimeric enzyme was then induced using 0.4 mM isopropyl-β-D-thiogalactoside (IPTG), and the cultures were incubated another 3 h with shaking at 220-250 rpm, and 34°C for DrGBE expression or 30-34°C for chimeric enzyme expression (reduced shaking and/or temperature was used in attempt to reduce protein aggregation). The cells were subsequently harvested at 4,500 or 10,000 x*g* for 20-30 min at 4°C (using the Beckman Coulter Allegra X-22R Centrifuge 5415D or the Beckman Coulter Avanti™ J-25I Centrifuge and JA-10 rotor respectively), depending on equipment availability. Cell pellets (each containing cells from 100-600 mL aliquots of *E. coli* culture) were resuspended and

washed in ~5-10 mL phosphate buffered saline (PBS, Cat# PD0435 from BioBasic), pelleted at 4,500 rpm for 15-20 min at 4°C, and stored at -80°C until cell lysis at a future date.

$TtGBE_{cat}$-$mSBEI_{COO-}$ was in some cases expressed in the presence of arginine, following an established protocol (Wang and Li, 2014), in an attempt to prevent aggregation of recombinant protein. In these cases, *E. coli* cultures were grown for 3 h after being subcultured, and IPTG was subsequently added along with 28.7 mM arginine (Cat# A5006 from Sigma-Aldrich, added from a solution previously adjusted to pH ~7-8) and 27.8 mM glucose. Cultures were subsequently incubated for 24 h at 34°C and with shaking at 250 rpm.

Cell Lysis

Cells were lysed using BugBuster Protein Extraction Reagent (Cat# 70584 from Millipore) and the Bacterial Protein Extraction kit (Cat# BS596 from Bio Basic Canada Inc.). Each cell pellet (each containing cells from 100-600 mL aliquots of *E. coli* culture) was gently resuspended in 3-25.9 mL of cell lysis buffer (from the Bio Basic kit) or BugBuster Protein Extraction Reagent containing protease inhibitor (~1 mM phenylmethyl sulfonyl fluoride (from the kit) or 1-2% (v/v) ProteaseArrest (G-Biosciences Cat# 786-437)), ~0.95 mg/mL lysozyme (from the kit), and ~0.008 mg/mL DNase/RNase (from the kit or Cat# EN0525 from ThermoFisher Scientific). The resuspended cells were incubated at room temperature for 40-60 min at 20 rpm (using the SB2 rotator from Stuart Equipment) until the solution became fluid.

Insoluble debris was removed from the cell lysate solution by centrifugation at 16,000 x*g* for 20 min at 4°C. The inclusion bodies were saved for SDS-PAGE analysis or protein refolding and purification (described below). 20 µL of the soluble protein fraction was saved for SDS-PAGE analysis and the remaining soluble fraction was used for purification of recombinant protein (described below).

Protein Refolding

Attempts were made to refold intein-tagged $TtGBE_{cat}$-$mSBEI_{COO-}$ and $TtGBE_{cat}$-$mSBEI_{NH2}$ from the inclusion bodies from the *E. coli* cell lysate. The refolding protocol was based on a protein refolding kit (Cat# 70123-3REF from EMD Chemicals Inc.), with some modifications.

Aliquots of inclusion bodies (4 or 8 µL) were washed 5-8 times in ~1.8-2.2 mL of inclusion body wash buffer (20 mM tris(hydroxymethyl)aminomethane (Tris)-HCl pH 7.5, 10 mM ethylenediaminetetraacetic acid, 1% (v/v) Triton X-100). Each wash was followed by centrifugation for 2-5 min at 10,000-16,000 x*g* and 4^{o}C and removal of the supernatant.

Washed pellets were resuspended and solubilized in 1-5 mL of solubilization buffer (50 mM *N*-cyclohexyl-3-aminopropanesulfonic acid pH 11, 0.3-0.6% (w/v) N-lauroylsarcosine, 5 mM dithiothreitol (DTT)) for 10-35 min at 20 rpm and room temperature until the solution became a dilute yellow colour. Solubilized protein was subsequently centrifuged at 10,000 x*g* for 10 min at room temperature or 4^{o}C. In most cases, protein content in the supernatant was too low to be measured using the Bradford assay but was detected using SDS-PAGE analysis. Solubilized protein was transferred *via* dialysis or direct dilution into refolding buffer (50 mM 3-(*N*-morpholino)propanesulfonic acid (MOPS)-NaOH pH 7), which was in some cases supplemented as described below.

For dialysis, 1-5 mL aliquots of solubilized protein (up to 90 µg/mL protein) were transferred into 50 kDa cut-off dialysis tubes (G235034 or G235058 Float-A-Lyzer® from Spectra/Por®). Dialysis tubes containing solubilized protein were subsequently placed into a beaker containing 0.5-1 L of refolding buffer (50 mM MOPS-NaOH pH 7) (up to two dialysis tubes per beaker), and kept at 4^{o}C with slow mechanical stirring (so that dialysis tubes barely moved). The refolding buffer was changed twice, with at least 4 h between/after every buffer change. A 15-31 µL aliquot of refolded protein was taken for SDS-PAGE analysis, and the remaining refolded protein was used for purification of chimeric enzyme using chitin resin. In attempt to prevent protein aggregation, the refolding buffer in some rounds of dialysis was supplemented with one of the following: 0.1% (v/v) Triton X-100 + 5 mM DTT, 0.1% (v/v) Triton X-100, or 1 M arginine pH ~8.4.

For direct dilution, 0.1-1 mL of solubilized protein (13 µg/mL protein) was added into 150 mL of refolding buffer, which was kept at 10^{o}C with 100 rpm shaking (in the Innova®44). The dilution step was repeated again at 6.5, 6, 1.5, and 1 h hour intervals (a minimum of 1 h between dilutions). The refolding buffer in some rounds of dilution was supplemented with 0.4 mg/mL maltodextrins (Cat# 419672 from Sigma-Aldrich) and/or 0.4 M arginine (the solubilization buffer used for these samples also contained 0.4 M arginine).

SDS-PAGE analysis showed that following protein refolding, the chimeric enzymes remained fused to their intein tags and their samples contained either degradation products and/or contaminating protein (Figure S1). Therefore, intein tag purification was performed to remove the intein tag and possibly increase sample purity.

Purification of Intein-tagged Protein

Protein-intein-tag fusions were purified using chitin resin, for which the intein tag has affinity. Econo-Pac® Chromatography Columns (14 x 1.5 cm, BioRad Cat# 7321010) were packed with 50% (w/v) chitin resin slurry in 20% (v/v) ethanol (Cat# S6651L from New England Biolabs) (volumes of chitin resin used are indicated in Table S2). Each column was subsequently equilibrated with 50-60 mL of column buffer (20 mM Tris-HCl pH 8.5, 500 mM NaCl, previously filtered through a 0.2 µm filter (Filtropur BT50, Cat# 83.1823.101 from Sarstedt)).

Impure protein samples were mixed with column buffer and loaded onto the prepared columns through 0.45 µm polyethersulfone filters (previously Cat# 83.1826 from Sarstedt) (volumes added are shown in Table S2). The columns were subsequently incubated at 4^{o}C and 20 rpm rotation for ~16 h to allow the intein tag to bind to the chitin resin (incubation time was reduced down to ~4 h throughout troubleshooting of chimeric enzyme purification in attempt to minimize protein misfolding). After incubation, the columns were drained using gravity flow (~30 µL of the flow-through was collected for SDS-PAGE analysis). The columns were subsequently washed with ~150-400 mL of wash buffer (column buffer + 1% (v/v) Triton X-100), during which the chitin resin was agitated *via* pipette-aspiration 5-7 times, to improve removal of contaminating proteins (details are shown in Table S2). Columns were subsequently washed with ~33-50 mL of column buffer to remove Triton X-100. 100 µL of resin (50% (w/v) in buffer) was then taken for SDS-PAGE analysis.

Each column was subsequently incubated with 3-7 mL of cleavage buffer (column buffer + 50 mM DTT), without shaking, in order to induce self-cleavage of the intein tag from the recombinant protein (Chong *et al.*, 1996, 1997). Columns containing protein from the soluble fractions of cell lysate were incubated at 23^{o}C for ~61-68 h. Columns containing protein from

refolded inclusion bodies were incubated at 4^{o}C for 36-62 h (temperature was lowered in attempt to reduce protein misfolding).

After cleavage, 60 mL of 50 mM MOPS-NaOH pH 7 (for DrGBE) or 20-65 mL of column buffer (for chimeric enzymes) per column was used to elute intein-free recombinant protein. The eluate was concentrated *via* centrifugation using 15 mL 50 kDa cut-off spin columns (EMD Millipore Amicon Ultra centrifugal filters, Cat# UFC905024) at 4,500 rpm and 4-8^{o}C, each round lasting 3-7 min (unless Triton X-100 was present (as described below), in which case each round lasted 30 min due to filter clogging). Eluted samples that contained detectable DTT odor were mixed with up to 14.9 mL of MOPS and further centrifuged within the spin columns to remove DTT. This was repeated until DTT odor was no longer detected (using up to 105 mL of MOPS).

Chimeric enzyme eluates after centrifugation contained ~0.15-1 mL of solution with 0-0.90 mg/mL protein. DrGBE eluates after centrifugation contained 0.2-2 mL of solution with a maximum protein concentration of ~11 mg/mL (not concentrated further to prevent protein aggregation). Eluate containing ~10 µg of protein (or simply 50 µL of eluate if protein concentration was undetectable) and 100 µL of chitin resin after elution (50% (w/v) in buffer) was taken for SDS-PAGE analysis. Protein was stored in 50 mM MOPS-NaOH pH 7 at -20^{o}C (short-term) or -80^{o}C (long-term) in 0.05-1 mL aliquots.

Intein tag purification of refolded protein was in some cases modified. Proteins refolded from inclusion bodies in the presence of Triton X-100 were purified in the presence of this detergent (1% (v/v) during column equilibration and loading and 0.1% (v/v) during intein tag cleavage and protein elution). Proteins refolded from inclusion bodies using direct dilution were concentrated from 150 mL to 5 mL (~1.3 – 13 µg/mL protein) using 50 kDa cut-off spin columns prior to purification, except samples with maltodextrin, which were only concentrated to 94 mL (70-700 ng/mL protein), 10 mL of which was used for purification (due to maltodextrin clogging the filters used to concentrate the samples).

Purification of His-tagged *Deinococcus radiodurans* Glycogen Branching Enzyme

His-tagged DrGBE and His-tagged DrGBE variants were purified from the soluble protein fractions of cell lysate using chromatography, based on the affinity of the His-tag to

nickel. Poly-Prep Chromatography Columns (Cat# 731-1550 from Bio-Rad) were packed with 225 μL of 50% (w/v) HisPur^{TM} Ni-NTA resin slurry in 20% (v/v) ethanol (Cat# 88221 from Thermo Scientific), optimized to reduce non-specific protein binding. The columns were drained by gravity flow to remove ethanol and subsequently equilibrated with 450 μL of equilibration buffer (20 mM NaH_2PO_4-NaOH pH 7.4, 300 mM NaCl, 10 mM imidazole). Protein samples were filtered through 0.45 μm filters and applied onto the columns as 50% (v/v) mixtures with equilibration buffer (~15 mL solution total). The columns were drained using gravity flow, and the eluate was reapplied onto the columns once (to increase binding of the DrGBE-His-tag fusions to the resin). The columns were again drained and subsequently washed with 15-24 mL wash buffer (PBS-HCl pH 7.4, 24 mM imidazole). The columns were then incubated with 1-2.5 mL of elution buffer (PBS-HCl pH 7.4, 250 mM imidazole) for 5 min and subsequently drained. Incubation and elution was repeated once or twice into the same collection tube (one collection tube per DrGBE variant), until protein concentration in the eluate drops was below 0.11 mg/mL. The eluates were then washed with 60-96 mL of 50 mM MOPS-NaOH pH 7 through 15 mL 50 kDa cut-off spin columns using centrifugation at 4,500 rpm to remove imidazole (each round of centrifugation lasted 8 min).

Bradford Assay

Protein concentrations were determined using the Bio-Rad Protein Assay (Bio-Rad Cat# 5000006), which is based on the Bradford assay (Bradford, 1976). The assay was performed as per the manufacturer's instructions.

SDS-PAGE Analysis

The purity of affinity-purified protein was determined using sodium dodecyl sulfate polyacrylamide gel electrophoresis (SDS-PAGE, Laemmli, 1970). The Mini-Protean® Tetra Handcast Systems (Bio-Rad Cat# 1658037-41 and 1653303-04) were used to cast 10-well, polyacrylamide gels and to perform electrophoresis. The resolving gels contained 10.2% (w/v) acrylamide, 390 mM Tris pH 8.8, 0.1% (w/v) sodium dodecyl sulfate (SDS), 0.1% (w/v) ammonium persulfate, and 0.1% (v/v) tetramethylethylenediamine (TEMED) (in water). The

stacking gels contained 5.04% (w/v) acrylamide, 128 mM Tris pH 6.8, 0.1% (w/v) SDS, 0.112% (w/v) ammonium persulfate, and 0.08% (v/v) TEMED (in water).

Samples for analysis were prepared with water and a final volume of ~20% (v/v) Laemmli loading buffer (313 mM Tris-HCl pH 6.8, 50% (v/v) glycerol, 25% (v/v) 2-β-mercaptoethanol, 10% (w/v) SDS, 0.04% (w/v) 3',3",5',5"-tetrabromophenolsulfonphthalein (bromophenol blue)), as indicated in Table S3. Samples were subsequently boiled for 5-10 min and loaded onto the gels. 5 µL of BLUeye prestained protein ladder (FroggaBio Cat# PM007-0500) or Precision Plus Protein™ All Blue or Dual Color Standards protein ladder (Cat#s 161-0373-4 from Bio-Rad) were loaded onto the gels as molecular weight standards.

Electrophoresis was performed in running buffer (25 mM Tris, 192 mM glycine, 0.1% (w/v) SDS) at ~120 V for 1-2 h. The gels were then stained in Coomassie stain (0.5 mg/mL Pierce Coomassie Brilliant Blue G-250 Dye (Thermo Scientific™) in 40% (v/v) MeOH, 10% (v/v) glacial acetic acid in water) for ~ 0.5-19h and destained in 30% (v/v) MeOH for 1-4h.

Design of *Deinococcus radiodurans* Glycogen Branching Enzyme Mutants

The amino acid sequences of plant SBEs, prokaryotic GBEs, and a mammalian GBE were aligned to identify amino acid residues that may impart desirable qualities within each class of isoforms, and therefore potential mutagenic targets within DrGBE. Sequence alignments were made using Clustal Omega (EMBL-EBI, 2016). A 3D DrGBE model was built to determine which of these residues are potentially near the substrate-binding and/or catalytic sites. The model was built using MODELLER version 9.16, and the results were visualized using PyMOL (Fiser *et al.*, 2000; Marti-Renom *et al.*, 2000; Sali and Blundell, 1993; Schrödinger, 2016; Webb and Sali, 2014, 2016). MODELLER creates initial models by threading the amino acid sequence of a protein with unknown structure into the known structure of a homologous protein and subsequently makes corrections to accommodate spatial constraints derived from the sequence-template structure alignment.

The template with the highest percent identity and percent coverage and lowest Expect value when compared to DrGBE was used for threading (selected from the PDB database). The Expect value indicates how likely amino acid sequence similarity between two proteins occurs due to chance. Scores greater than one suggest that similarity occurred by chance, which is

common for short sequences with many common amino acids. Scores less than $10x10^{-10}$ suggest that similarity occurred due to close homology, which is common for similar sequences that are long and/or have less common amino acids. MODELLER generated five models. Discrete Optimized Protein Energy (DOPE) score analysis, which estimates the negative free energy of folding (spontaneity of folding) based on properties such as solvent exposure and hydrogen bond geometry, was performed on the five models using MODELLER. The model with the most negative total score (suggesting the most favourable protein conformation) was used for subsequent analysis. DOPE score analysis was performed on each residue within this model and within the template to indicate how realistic each region of the model was relative to the template.

VSL2 was used to predict 3D disorder within DrGBE using PONDR set to a threshold of 0.5 (Molecular Kinetics Incorporation, 2003; Peng *et al*., 2006). VSL2 predicts disorder by comparing the amino acid sequence of a protein to structural data generated using various methods of characterization (*e.g.* NMR, circular dichroism), and is optimized to detect both short and long regions of disorder.

To position potential substrates within the DrGBE model, the model was aligned using PyMOL to four known structures with co-crystallized polyglucans. Structures used for alignment were selected from the NCBI database so that they shared at least 20% sequence identity and 70% coverage with the modelled region of DrGBE, with an Expect value below $10x10^{-10}$, and so that they contained distinct and long substrates (to visualize a higher number and more diverse range of potential substrate-interaction sites).

Site-directed Mutagenesis

Site-directed mutagenesis (SDM) was performed on the DNA encoding His-tagged DrGBE directly within the pET28a vector acquired from Nasanovsky (2017). His-tagged mutants were made instead of intein-tagged mutants (and compared to His-tagged wild-type DrGBE) to save time due to the high number and in many cases low activities of the mutants (the His-tag purification protocol requires a few hours, whereas that of the intein tag requires five days).

SDM PCR reactions were performed using the PCR conditions and primers indicated in Tables S4-S6, and PCR products were DpnI-digested to remove non-methylated (non-mutated)

DNA. The digestion reactions for Q205H and A312T contained 1.8 μL of FastDigest DpnI (Cat# FD1703 from ThermoFisher) and 18 μL of PCR product. The reactions for A310Q and A310G contained 12 μL water, 4 μL 10X fast digest buffer (Cat# FD1703 from ThermoFisher), 2 μL of 20 mg/mL bovine serum albumin (BSA), 2 μL DpnI, and 20 μL PCR product. Each DpnI-digest reaction was incubated at 37^{o}C for 5h. DpnI-digested PCR products were analyzed using agarose gel electrophoresis to confirm that PCR amplification had been successful.

DpnI-digested SDM products were transformed into competent DH5α *E. coli* cells. A positive colony from each transformation was grown in 5 mL LB broth-KAN overnight. DNA was isolated from each culture and sequenced to confirm that the desired SDM product was present with no unintentional, non-silent mutations or parental (non-mutated) DNA. DNA was isolated using the Presto^{TM} Mini Plasmid Kit (Cat# PDH300 from Geneaid) as per the manufacturer's instructions. Sequencing was performed by the University of Guelph Lab Services department using the sequencing primers shown in Table S6 and a specific protocol for GC-rich DNA.

Agarose Gel Electrophoresis

Agarose gels were made to a final concentration of 1% (w/v) agarose (Cat# A87 from FroggaBio) and 1.5% (v/v) UltraPure^{TM} Ethidium Bromide (Cat# 15585011 from ThermoFisher) in TAE buffer (40 mM Tris-acetate pH 8.0, 1 mM ethylenediaminetetraacetic acid). Samples containing 5 μL of PCR product and 1.67 μL of 6x DNA loading dye (Cat# R0611 from Thermo Scientific) were electrophoresed in agarose gels alongside a 1kb ladder (Cat# DM010-R500 from GeneDire). Electrophoresis was performed in TAE buffer at 95V for ~1.5 hours.

Making Competent Cells

To make competent cells, a 1 mL overnight culture of DH5α or BL21 *E. coli* cells (in LB broth) was subcultured into 100 mL of LB broth and grown at 37^{o}C for 4-6.5h until the cells reached mid-to-late log phase. The cells were then centrifuged at 3,500 x*g* at 4^{o}C for 5 min. The pelleted cells were resuspended in 30 mL cold, filtered (through 0.45 μm) TFB1 buffer (30 mM potassium acetate-acetic acid pH 5.8, 100 mM RbCl, 50 mM $MnCl_2$, 10 mM $CaCl_2$, 15% (v/v) glycerol) and incubated on ice for 90 min. The cells were then re-pelleted by centrifugation

(4,000 x*g*, 4°C, 5 min), resuspended in 4 mL cold, filtered TFB2 buffer (10 mM MOPS-KOH pH 6.8, 10 mM RbCl, 75 mM $CaCl_2$, 15% (v/v) glycerol), immediately frozen in liquid nitrogen, and stored at -80°C until use.

Transformations

Competent DH5α or BL21 *E. coli* to be transformed were thawed on ice and subsequently mixed with the desired vectors (volumes used are indicated in Table S7). The mixtures were immediately and briefly swirled, left on ice for 30 min, and then incubated at 42°C for 60s or 45s to heat-shock the cells (Table S7). The samples were subsequently cooled on ice for 1-2 min and mixed with SOC broth (20.0 g/L tryptone, 5.0 g/L yeast extract, 0.5 g/L NaCl, 5 g/L magnesium sulfate·$7H_2O$, 3.6 g/L D-glucose, pH 7.0±0.2) (400 µL SOC broth was used for DH5α cells, and 700 µL was used BL21 cells). Cells were then incubated at 37°C and 250 rpm for 1 h and subsequently pelleted at 16,000 x*g* for 2 min. Pelleted cells were plated onto LB agar-KAN plates (10 g/L tryptone, 5 g/L yeast extract, 5 g/L NaCl, 50 µg/mL KAN, 15 g/L agar). Plates were incubated at 37°C overnight, and positive clones were subsequently used for production of plasmids and/or protein.

Iodine-binding Assay

BE activity was semi-quantitatively measured using the iodine-binding assay. This assay estimates BE activity based on decreases in absorbance of glucan-triiodide complexes at wavelengths of maximum absorption (λ_{max}), which occur as glucan chains are shortened throughout BE-induced branching (Archibald *et al*., 1961; Bailey and Whelan, 1961; Bourne *et al*., 1945; Hanes, 1937; John *et al*., 1983; Rundle and Baldwin, 1943; Rundle and French, 1943; Swanson, 1948).

Glucan for the iodine-binding assays was dissolved in NaOH or DMSO at 95°C, as described in Table 5 (temperature controlled using an Eppendorf heater (Fisher Scientific Isotemp® Cat# 11-715-145D) (DMSO was only used for early studies because it caused amylopectin to form a gel, even at high temperatures). Dissolved glucan was diluted to the desired final concentration using 50 mM MOPS-NaOH pH 7 (previously heated to 60°C in a

water bath) (Table 5), and retrograded glucan was removed using centrifugation (16,000 x*g*, 2 min).

Table 5: Variations of the iodine-binding assay.

<table>
<tr><th colspan="4">Preparation of glucan stocks</th></tr>
<tr><th colspan="4">For analysis of DrGBE and chimeric enzymes purified from soluble protein fractions</th></tr>
<tr><td colspan="4">4.8-5 mg amylose or amylopectin[1] was dissolved in 300 µL of 0.3 M NaOH for 60-75 min with 1 vortex in the middle, diluted with 690 µL MOPS, and brought to pH to 7 using ~6.8 µL concentrated HCl</td></tr>
<tr><th colspan="4">For analysis of chimeric enzymes purified from inclusion bodies</th></tr>
<tr><td colspan="4">12.5 mg amylose[1] was dissolved in 100 µL DMSO for ~30 min and diluted to 0.5-12.5 mg/mL using MOPS</td></tr>
<tr><th colspan="4">Reaction ingredients</th></tr>
<tr><th colspan="4">For analysis of DrGBE and chimeric enzymes purified from soluble protein fractions</th></tr>
<tr><th colspan="2">Ingredients added</th><th colspan="2">Final concentrations</th></tr>
<tr><td colspan="2">1.3-8.7 µL of 1-1,600 µg/mL DrGBE + 190-200 µL glucan stock</td><td colspan="2">0.042-26 µg/mL DrGBE[2] + 0.89-1 mg/mL glucan[2] in 202 µL MOPS</td></tr>
<tr><td colspan="2">10 µL of 0.08-0.6 mg/mL chimeric enzyme + 90 µL glucan stock</td><td colspan="2">8-60 µL/mL chimeric enzyme + 3 mg/mL glucan in 100 µL MOPS</td></tr>
<tr><th colspan="4">For analysis of chimeric enzymes purified from inclusion bodies</th></tr>
<tr><th colspan="2">Ingredients added</th><th colspan="2">Final concentrations</th></tr>
<tr><td colspan="2">1-20 µL of chimeric enzyme (undetectable concentration) + 80-99 µL glucan stock</td><td colspan="2">Undetectable chimeric enzyme concentration + ~0.4 mg/mL amylose + ~0.31% (v/v) DMSO in 100 µL MOPS</td></tr>
<tr><th colspan="4">Reaction and Analysis</th></tr>
<tr><th>Reaction Temperature and Time</th><th colspan="3">Assay Inactivation & Addition of I_2/KI</th></tr>
<tr><td rowspan="2">34°C for 5-20 min (DrGBE);
34 or 64°C for 20 min (chimeric enzymes)[3]</td><td colspan="3">His-tagged DrGBE & chimeric enzymes purified from soluble protein fractions: 22 µL aliquots of reaction were mixed with 88 µL 10 mM HCl and 88 µL I_2/KI</td></tr>
<tr><td colspan="3">Chimeric enzymes purified from inclusion bodies: reactions were boiled for 5 min and mixed with 400 µL 10 mM HCl and 400 µL I_2/KI</td></tr>
</table>

[1]Potato amylose and corn amylopectin (Cat# A0512 and A7780 from Sigma Life Science respectively).
[2]Exact concentrations for studying each mutant are indicated in Figure 21.
[3]Chimeric enzymes purified from inclusion bodies were analyzed at 30 and 23, 60, or 80°C.

BE reactions were activated by adding enzyme to the prepared glucan and were incubated at variable temperatures and 500 rpm (to keep components of the reaction mixed well) using an Eppendorf Thermomixer (volumes and concentrations are shown in Table 5). Reactions were inactivated using10 mM HCl (and/or boiling in an Eppendorf heater), and glucan chain lengths were visualized using I_2/KI (0.0125% (w/v) I_2 + 0.04% (w/v) KI) (details are shown in Table 5). Absorbance of the glucan-iodine complex was immediately read at λ_{max} (620 or 510 nm for amylose or amylopectin dissolved using NaOH respectively, or 660 nm for amylose dissolved using DMSO) using the Multiskan Go Spectrophotometer (Thermo Scientific Cat# 51119300). One unit (U) of activity was defined as a decrease in absorbance of 1 per min (relative to a glucan control without protein). Glucan controls did not routinely contain boiled protein because

preliminary studies showed this to yield the same results as controls containing no protein. T-tests (2-tailed, type-3, p-value threshold set to 0.05) comparing the activities DrGBE and its variants were performed using Excel.

Affinity Gel Electrophoresis

The substrate-affinity of DrGBE and its variants was measured using affinity gel electrophoresis. In this technique, BEs are electrophoresed through non-denaturing gels containing varying substrate concentrations, and their migration is lowered in proportion to their affinity for the substrate.

Non-denaturing resolving gels with 8% (v/v) acrylamide and 0.02-0.49 mg/mL glucan were cast and electrophoresis was performed using the apparatuses described for SDS-PAGE analysis. For each resolving gel, a solution was made with 2.6 mL 30% (w/v) acrylamide, 2.6 mL of 1.5 M Tris-HCl pH 8.8, 0.1 mL 10% (w/v) ammonium persulfate, and 0.01 mL TEMED. A 4.7 mL mixture of glucan stock and/or glucan-free solution otherwise chemically identical to the glucan stock was added to each solution. ~7.2 mL of solution was used for each gel.

Glucan stocks were prepared as they were for the iodine-binding assay of DrGBE (see Table 5 on page 29) so that retrograded glucan could be easily removed before gel preparation using centrifugation (16,000 x*g*, 2 min). A single stock of amylose or amylopectin was used for making triplicate gels because using triplicate stocks gave variable results due to irreproducible glucan solubilization.

Ammonium persulfate and TEMED were added to the resolving gel solutions immediately before casting the gels (ammonium persulfate was added to three solutions at a time, and TEMED was added to one solution at a time). This is because the gels solidified quickly thereafter (unlike SDS-PAGE gels). 1-butanol was added above each gel as it solidified to give a straight interface between the stacking and resolving gels (using water gave an uneven interface and resulted in inaccurate comparison of protein migration between different lanes). Ten-well stacking gels were made as they were for SDS-PAGE analysis, but with the volume of SDS replaced with water.

Samples were prepared with 0.36 µg of DrGBE or 1 µg of BSA and 6 µL of native loading dye (320 mM Tris-HCl pH 6.8, 40% (v/v) glycerol, 0.027% (w/v) bromophenol-blue) in

a final volume of 26 µL of 50 mM MOPS-NaOH pH 7. DrGBE and BSA samples were electrophoresed alongside 3 µL of BLUeye ladder (FroggaBio Cat# PM007-0500) to confirm that BSA migration was unaffected by glucan concentration. Gels were electrophoresed at 120 V and 4^{o}C for 2.5h in native running buffer (25 mM Tris, 192 mM glycine), stained overnight in Coomassie stain, and destained in 30% (v/v) MeOH for ~2.5h. Migration of each protein was measured at the bottom of its band (bottom band if 2 bands were seen).

The relative mobility of each DrGBE variant through each gel was calculated relative to BSA (relative mobility = $\frac{mobility_{DrGBE}}{mobility_{BSA}}$) (mobility was measured relative to BSA instead of the running front to eliminate error associated with marking (visualizing) the running front and to allow for increased electrophoresis times and thus resolution). The reciprocal of BE mobility was plotted against substrate concentration in a plot wherein the negative of the x-intercept equals the dissociation constant (K_d), which is inversely related to substrate-affinity (Matsumoto *et al*., 1990; Takeo and Nakamura, 1972). T-tests (2-tailed, type-3, p-value threshold set to 0.05) comparing the dissociation constants of DrGBE and its variants were performed using Excel.

Gel Permeation Chromatography

Gel permeation chromatography (GPC) was used to separate the components of starch, in order to visualize the effects of BE activity on amylose and amylopectin within their natural milieu (starch). GPC uses porous agarose beads to separate small molecules (which get trapped within the beads and thus elute late) from large molecules (which cannot fit within the beads and therefore elute early).

GPC was used similarly as described by Forsyth *et al*. (2002) and Bertoft *et al*. (2008). Glass pipettes (chromatography columns) were packed with Sepharose® CL-2B (50% (w/v) cross-linked beads in 20% (v/v) ethanol, from Sigma-Aldrich) to a final bed volume of 8.28-8.57 mL (3 mm radius and 293-303 mm height). Columns were connected to the low flow rate peristaltic pump BT100-2J with the YZ II15 pump head and tubing with inner diameters of 1.6, 3.1, and 6.4 mm (#14, 16, and 17 from the YZ1515 series) (from Langer Instruments by BioChem Fluidics). The mobile phase (0.01 M NaOH, 0.02 M NaCl) was applied onto the column top down (to avoid suction and thus air bubbles caused by pulling mobile phase through the column). The 1.6 mm inner diameter tubing (cut to a length of 1,993 mm) was connected to

the mobile phase reservoir at one end, the peristaltic pump in the middle, and the 3.1 mm inner diameter tubing (cut to a length of 22.5 mm) at the other end. The 3.1 mm inner diameter tubing was connected to the 6.4 mm inner diameter tubing (cut to a length of 38 mm), which was connected to the column. The reducing connectors had 1.59-3.18 or 3.18-6.35 mm inner diameters and were made from polypropylene or kynar (Cat# EW-40622-23 or EW30703-50 from Cole-Parmer).

Mobile phase was pumped at ~0.128-0.133 mL/min (0.6 rpm setting on the pump) until changes in bed height could no longer be visually detected. The rpm setting was calculated using the maximum rpm and flow rate for the pump (Langer Instruments, 2016) (approximate rpm = $\frac{desired\ flow\ rate\ \left(=0.4\frac{mL}{min}\right) * max\ rpm\ (=100\ rpm)}{\max flow\ rate\ (=380\frac{mL}{min})}$), and subsequently adjusted to reduce elution time without compromising resolution.

Columns were stored in mobile phase for a few days or in 20% (v/v) ethanol for up to five months. Columns contained no visible air bubbles and were kept at room temperature to avoid formation of air bubbles caused by temperature changes.

Potato amylose, corn amylopectin, *waxy* corn starch (amylopectin from *waxy* corn varieties that do not produce amylose, that is free of amylose contamination), and starch for chromatography were purchased from Sigma Life Science (Cat# A0512, A7780, S9679, and S9679 respectively; identity of Cat# S9679 was altered from *waxy* starch to regular starch when the supplier for the product changed). Glucans were dissolved in 95^{o}C NaOH (amounts used are shown in Table 6), with periodic vortexing, for up to 1.5h until the glucan had fully dissolved. MOPS-NaOH pH 7 (60^{o}C) was added to the dissolved glucan, and concentrated HCl was subsequently added to bring the pH to ~7 (details are shown in Table 6). Starch concentrations were higher than amylose and amylopectin concentrations, so that the low amylose content of starch (~25-30%) could be detected within the GPC eluates.

Table 6: Variations in the glucan stocks used for gel permeation chromatography.

Glucan	Ingredients used to prepare glucan stock						Glucan loaded onto column (in 200 µL) (mg)
	Glucan (mg)	NaOH		MOPS		Concen-trated HCl (µL)	
		Volume (µL)	Concen-tration (M)	Volume (µL)	Concen-tration (mM)		
Amylose	10	300	0.3	692	50	~8-8.7	2
Amylopectin	10	300	0.3	692	50	~8-8.7	2
Starch	31-35	400	2	528	95	~70-75	6-7

For DrGBE treatment, 242 µL of glucan solution described above, 6.5 µL of 50 mM MOPS-NaOH pH 7, and 1.6 µL of 0.3 mg/mL DrGBE (0.488 µg) were incubated together for 10 min at 35^{o}C and 300 rpm shaking within an Eppendorf Thermomixer (final concentrations of 30 mg/mL starch and 1.95 µg/mL DrGBE (activity units with starch are unknown)). Reactions were inactivated by boiling for 10 min. The reaction conditions mentioned above were used because higher enzyme concentrations or longer reaction times resulted in glucan products that were too short (due to BE activity) to bind to and therefore be detected using iodine (*i.e.* after GPC, all fractions mixed with iodine showed an absorbance of 0 relative to the blank).

Untreated or DrGBE-treated glucans were centrifuged (16,000 x*g*, 2 min), yielding a light yellow supernatant for amylose or a cloudy white supernatant for amylopectin and starch. 200 µL of the supernatant was immediately loaded onto the GPC column, which had been previously nearly dried using gravity flow (mg amounts of glucan loaded are shown in Table 6). Once the glucan solution had dripped through the column and the column bed was nearly dry, the column was filled to the top with mobile phase and connected to the tubing, which was full of mobile phase (this step was repeated if air bubbles were introduced). Chromatography was performed using a mobile phase flow rate of ~0.128-0.133 mL/min, and fractions were collected every 2.5 min for 80 min (32 fractions total; after checking that no glucan eluted after this point for up to 100 min). The column was equilibrated with 60 mL of mobile phase between each sample.

Glucan within fractions was detected using iodine, based on an established method (Kaufman *et al*., 2015). 100 µL aliquots of each eluate were mixed with 100 µL of 3.04 g/L iodine in 90% (v/v) DMSO and slowly shaken for 2 min (using the slow setting of a Gyrotory® Shaker-Model G2 from New Brunswick Scientific Co., Inc. Edison, N.J. USA). 50 µL aliquots of eluate-iodine mixtures were mixed with 50 µL of water and shaken for another 2 min (dilutions were kept constant within each trial but slightly altered between separate trials to detect smaller glucan quantities in some experiments). The absorbance was immediately read at λ_{max} (510 nm for fractions following amylopectin and starch elutions or 620 nm for fractions following amylose elutions).

Glucan within fractions was quantified using the phenol sulfuric acid assay (Dubois *et al*., 1951). In the assay, polyglucans are converted to furan derivatives using sulfuric acid, and the derivatives are subsequently mixed with phenol, yielding yellow-orange condensates whose absorbance at 490 nm is directly related to the glucose content. 100 µL of each GPC fraction

was mixed with 50 µL of 80% (w/v) phenol in water and vortexed gently. Samples were then mixed with 2 mL of concentrated sulfuric acid (using glass pipettes and quick mixing for even colour formation). The samples were incubated at room temperature for 10 min before reading absorbance of each sample at 490 nm (using quartz cuvettes in the DU® 800 Spectrophotomer from Beckman Coulter). The standard curve used to calculate glucose content was generated using 0.1-0.8 mg/mL glucose in mobile phase (Figure 12). Cuvettes were not rinsed between samples. The phenol solution was stored for months in a glass bottle away from light and was shaken before each use to resuspend the phenol. A new standard curve was made for every phenol stock because phenol has a drastic effect on the colour formed in the assay.

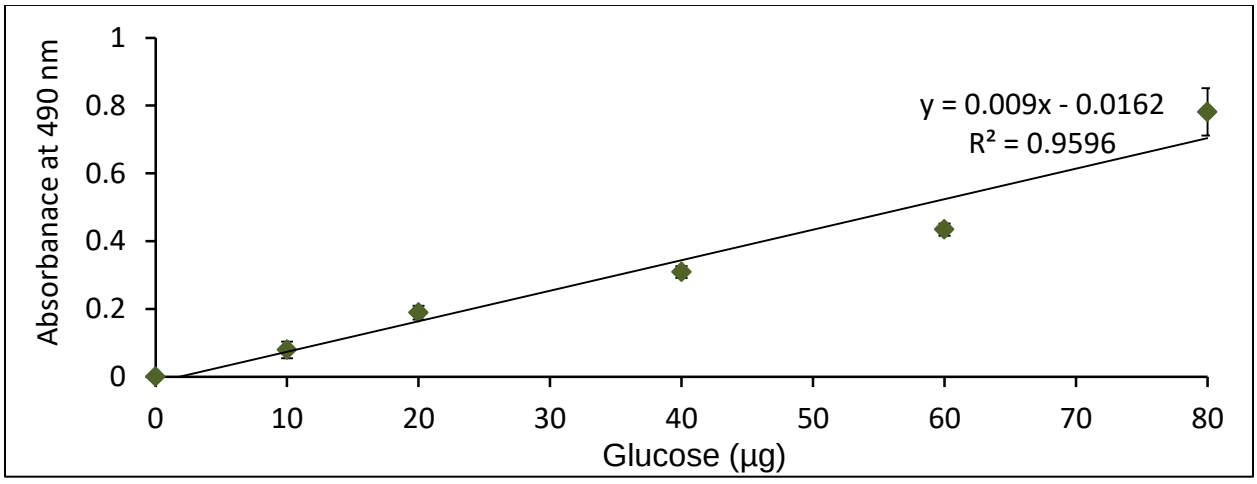

Figure 12: Standard curve for measurement of glucose using the phenol sulfuric acid assay. Values are averages from three replicates ± standard error of the mean.

CHAPTER 3: RESULTS

Design and Characterization of *Deinococcus radiodurans* Glycogen Branching Enzyme Mutants

Protein Structure Model

To identify potential substrate-interaction sites within DrGBE, a model for DrGBE residues 1-627 was threaded onto the template structure of *E. coli* GBE co-crystallized with β-cyclodextrin, and subsequently aligned to protein structures with distinct and relatively long co-crystallized substrates. The structures used shared 20-50% sequence identity and 72-98% coverage with the modelled region of DrGBE, with Expect values from $8x10^{-20}$-0, and had resolutions better than 2.9 Å (indicating that side chains could be accurately modelled) (Table 7).

Table 7: Properties of the structures used to model *Deinococcus radiodurans* glycogen branching enzyme.

Protein	Similarity to modelled region of DrGBE			Resolution (Å)	Co-crystallized substrate*
	Identity (%)	Coverage (%)	Expect value		
E. coli GBE (5e6z, Feng *et al*., 2016) Template for threading and used for alignment	50	98	0.0	1.88	β-cyclodextrin: 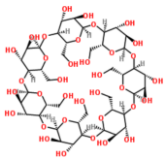
E. coli GBE (4lpc, Feng *et al*., 2015) Used for alignment	50	98	0.0	2.39	Maltoheptaose: 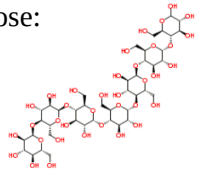
H. sapiens GBE (5clt, Krojer *et al*., to be published) Used for alignment	26	93	$1x10^{-57}$	2.79	Acarbose: 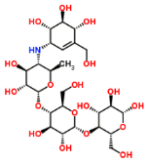
Sulfolobus solfataricus glycosyltrehalose trehalohydrolase (3vgf, Okazaki *et al*., 2012) Used for alignment	23	72	$8x10^{-20}$	2.3	Maltotriosyl-trehalose: 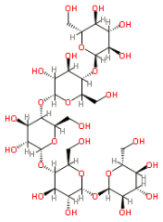

*Figures from Royal Society of Chemistry (2015).

DrGBE residues 628-705 were not modelled because this region was predicted to be disordered (PONDR scores using VSL2 analysis were above 0.5, shown in Figure 13), and residues 636-705 were previously shown to be unimportant in DrGBE activity (Palomo *et al.*, 2009). The DOPE scores (which approximate negative free energy of folding) for amino acids in the DrGBE model were nearly as low as those in the template except for the terminal regions, suggesting that the DrGBE model is reasonable, especially within the catalytic domain (scores were determined using MODELLER and are shown in Figure 14).

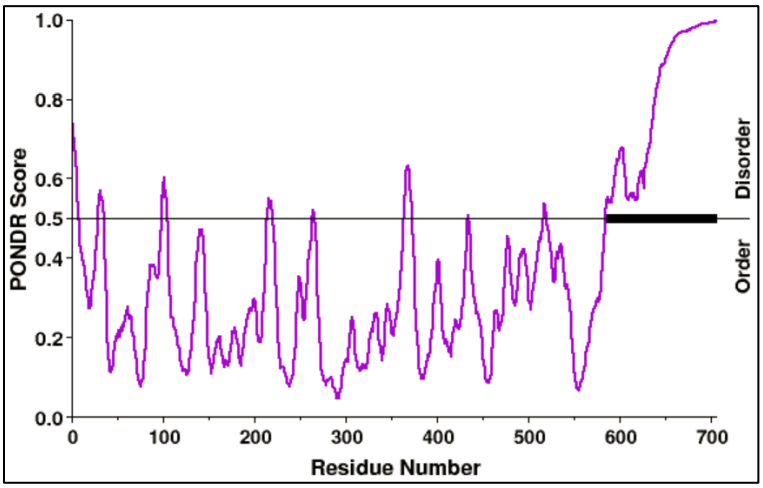

Figure 13: VSL2 prediction of disorder within *Deinococcus radiodurans* glycogen branching enzyme (performed using PONDR).

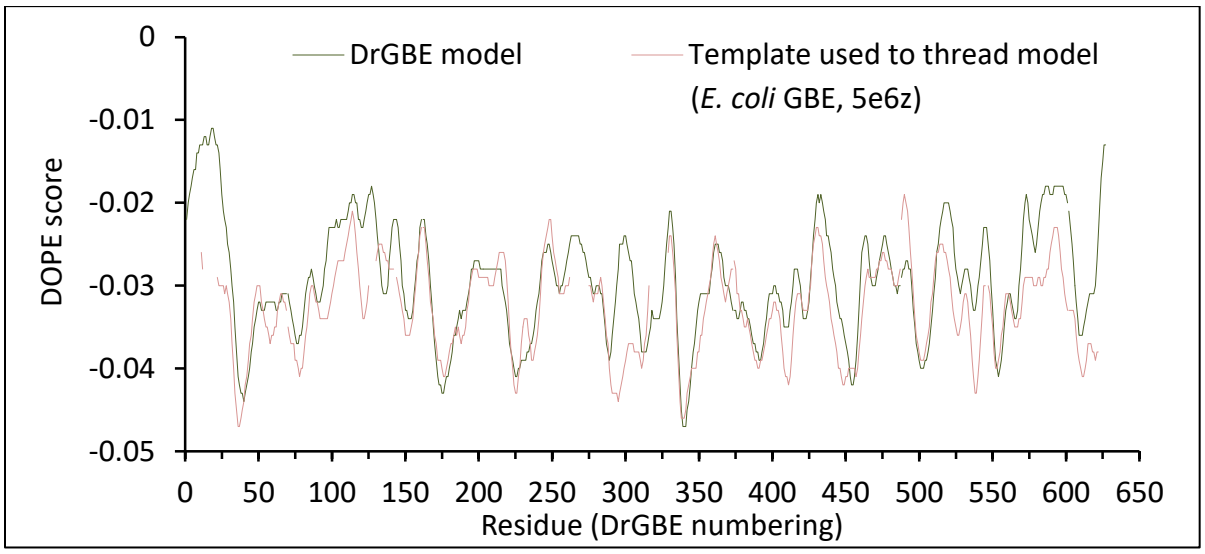

Figure 14: DOPE scores of residues within the *Deinococcus radiodurans* glycogen branching enzyme model and the template used to thread the model (calculated using MODELLER).

Rationale for Design of *Deinococcus radiodurans* Glycogen Branching Enzyme Mutations

Four site-directed DrGBE mutants were made. The mutated residues were in the catalytic domain, on the protein surface, or near a potential substrate-interaction site and the catalytic residues (Figure 15). One mutation, Q205H, was predicted to increase affinity for amylose for two reasons. Firstly, the mutation changed a residue that is conserved among GBEs to a residue that is conserved among SBEs, and SBEs prefer longer, less-branched substrates than GBEs (Figure 16). Secondly, the mutation increased the positive charge and aromaticity near a potential substrate-interaction site, both of which could facilitate interactions with glucan chains, possibly adding a binding site for long glucans such as amylose (Figure 15). One mutation changed the alanine at position 310, which is conserved among prokaryotic GBEs, to a glutamine (Figure 16). This mutation introduced a hydrophilic group near a potential substrate-interaction site, potentially adding an additional binding site for long glucans (Figure 15). One mutation changed the alanine at position 310 to a glycine. This mutation changed a residue that is conserved among prokaryotic GBEs to one that is conserved among eukaryotic BEs (Figure 16), and potentially increased protein flexibility in the catalytic cleft, possibly allowing catalysis with longer glucan chains (Figure 15). One mutation changed the alanine at position 312, which is conserved among prokaryotic GBEs, to a threonine, which is conserved among eukaryotic BEs (Figure 16). This mutation introduced into the catalytic region an additional nucleophile that could potentially assist the catalytic nucleophile D309 in branching longer glucans, and adds a potential glucan-interaction site (-OH group) (Figure 15). None of the residues that were mutated were required for catalysis according to the BRENDA database (BRENDA, 2016). The A310Q and A310G mutations had previously been made in *G. thermoglucosidans* GBE (Liu *et al*., 2017). The amino acid sequence location of the DrGBE mutations relative to previous BE mutations is shown in Table 8.

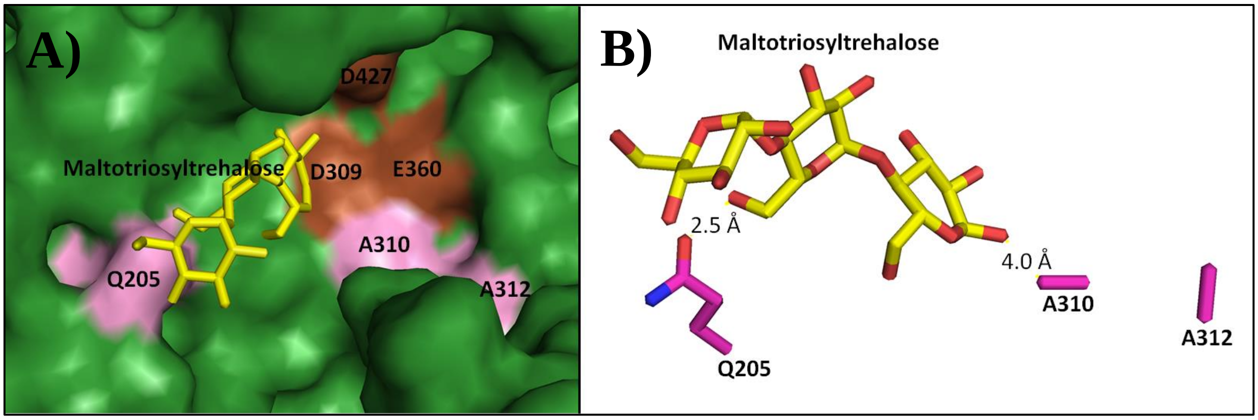

Figure 15: Mutation sites in a model of the *Deinococcus radiodurans* glycogen branching enzyme. A) Amino acid residues that were mutated (pink) relative to a potential α-glucan substrate (yellow) and the catalytic residues (brown). B) Distance between residues that were mutated (pink carbon atoms) and hydroxyl groups within a potential substrate (yellow carbon atoms). Note that hydrogen bonds are 2.6-3.2 Å. The model was made using MODELLER, PyMOL, the template 5e6z (*E. coli* GBE co-crystallized to β-cyclodextrin), and 3vgf (*S. solfataricus* glycosyltrehalose trehalohydrolase co-crystallized to maltotriosyltrehalose) for positioning the substrate. Other structures co-crystallized to glucans that were aligned to the DrGBE model positioned the substrate outside this region.

				Conserved region 2 / Putative catalytic nucleophile ↓
Prokaryotic GBEs				
Deinococcus radiodurans	201	S W G Y Q V	305	G L R V D A V A S
Deinococcus geothermalis	214	S W G Y Q V	318	G L R V D A V A S
Rhodothermus marinus	197	S W G Y Q V	301	G L R V D A V A S
Geobacillus thermoglucosidans	201	S W G Y Q G	305	G F R V D A V A N
Geobacillus stearothermophilus	215	S W G Y Q G	319	G F R V D A V A N
Escherichia coli	297	S W G Y Q P	401	A L R V D A V A S
Bacillus cereus	201	S W G Y Q G	305	G F R V D A V A N
Mycobacterium tuberculosis	303	S W G Y Q V	407	G L R V D A V A S
Mammalian GBE				
Homo sapiens	248	S F G Y Q I	353	G F R F D G V T S
Plant SBEs				
Zea mays IIb	277	S F G Y H V	382	G F R F D G V T S
Zea mays I	239	S F G Y H V	347	G F R F D G V T S
Oryza sativa I	232	S F G Y H V	340	G F R F D G V T S
Solanum tuberosum II	407	S F G Y H V	516	G F R F D G V T S
Arabidopsis thaliana 2.2	342	S F G Y H V	447	G F R F D G V T S

Figure 16: Partial sequence alignment of a diverse range of GH13 branching enzymes. Residues that are conserved among glycogen branching enzymes alone and plant starch branching enzymes alone are boxed in green, and those that are conserved among bacterial branching enzymes alone and eukaryotic branching enzymes alone are boxed in purple. The whole sequences were aligned using Clustal Omega.

Table 8: Site-directed mutagenesis experiments previously performed within branching enzymes.

Mutation*		Residue in DrGBE	Properties relative to wild-type			Reference
			Substrate-affinity	Catalytic activity	Thermo-stability	
1:	D15A,E (**bean SBEII**)	Absent	Similar	Decreased	Decreased	Hamada *et al.* (2007)
2:	H24A (**bean SBEII**)	Absent	Similar	Decreased	Decreased	
3:	R28A (**bean SBEII**)	Absent	Similar	Decreased	Decreased	
4:	S349F (**mSBEIIa**)	201	Similar	Eliminated	N/A	Li *et al.* (2015)
5:	Y235A (**rice SBEI**)	204	N/A	Decreased	N/A	Vu *et al.* (2008)
	Y300F (***E. coli* GBE**)		Similar		Decreased	Mikkelsen *et al.* (2001)
	Y352F (**mSBEIIa**)		Decreased		N/A	Li *et al.* (2015)
6:	R363K (**mSBEIIa**)	215	Decreased	Decreased	N/A	
7:	D270A (**rice SBEI**)	239	N/A	Decreased	N/A	Vu *et al.* (2008)
8:	H275A (**rice SBEI**)	244	N/A	Decreased	N/A	
	H320A (**mSBEIIb**)		Decreased		N/A	Funane *et al.* (1998)
9:	R342A (**rice SBEI**)	307	N/A	Decreased	N/A	Vu *et al.* (2008)
	R456K (**mSBEIIa**)		Decreased		N/A	Li *et al.* (2015)
	R384A,S,Q,E (**mSBEIIb**)		Similar		N/A	Libessart and Preiss (1998)
10:	D344A (**rice SBEI**)	309	N/A	Decreased	N/A	Vu *et al.* (2008)
	D386E, N (**mSBEIIb**)		N/A	Eliminated	N/A	Kuriki *et al.* (1996)
11:	A310G, N, I, E, Q (***G. thermoglucosidans* GBE**)	310	Increased**	Decreased	N/A	Liu *et al.* (2017)
12:	E408Q (**mSBEIIb**)	327	N/A	Similar	N/A	Kuriki *et al.* (1996)
13:	E435Q (**mSBEIIb**)	354	N/A	Similar	N/A	
14:	E441D, Q (**mSBEIIb**)	360	N/A	Eliminated	N/A	
	E399A (**rice SBEI**)		N/A	Decreased	N/A	Vu *et al.* (2008)
	E513D (**mSBEIIa**)		Decreased	Decreased	N/A	Li *et al.* (2015)
	E459A, K, Q (***E. coli* GBE**)	361	Decreased ***	Decreased	N/A	Binderup and Preiss (1998)
	E459D (***E. coli* GBE**)		Decreased	Increased	N/A	
15:	H467A (**rice SBEI**)	426	N/A	Decreased	N/A	Vu *et al.* (2008)
16:	H508A (**mSBEIIb**)		Decreased	Decreased	N/A	Funane *et al.* (1998)
17:	D509E, N (**mSBEIIb**)	427	N/A	Eliminated	N/A	Kuriki *et al.* (1996)

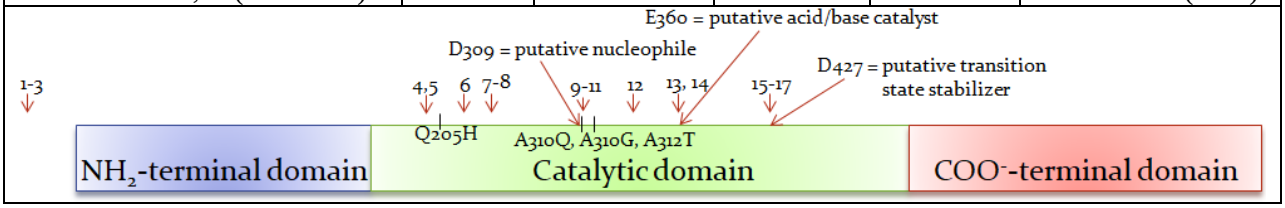

*Mutations (# 1-17) are shown at their respective locations within DrGBE, relative to the catalytic triad (D309, E360, and D427) and the mutations Q205H, A310Q, A310G, and A312T.
Multiple asterisks indicate substrate preference switched from amylopectin to amylose (**) or from amylose to amylopectin (***).
N/A – not analyzed.

Site-directed Mutagenesis

SDM of the gene encoding His-tagged DrGBE performed directly within the pET28a vector successfully produced the following mutants: Q205H, A310Q, A310G, and A312T. Sequencing showed that each DrGBE mutant contained the mutation of interest, a silent mutation (for each mutant, the CTG codon encoding leucine 167 in wild-type DrGBE was converted to CTT), and no parental DNA.

Protein Expression and Purification

Approximately 2.6-3.5 mg of His-tagged DrGBE and its variants were produced per liter of *E. coli* BL21(DE3). The mutations did not affect expression levels of the proteins (data not shown). Each purified DrGBE eluate showed two bands on SDS-PAGE analysis, one around 75 kDa and one slightly smaller (~71 kDa), both of which were denser after the addition of IPTG (DrGBE expression) (Figure 17).

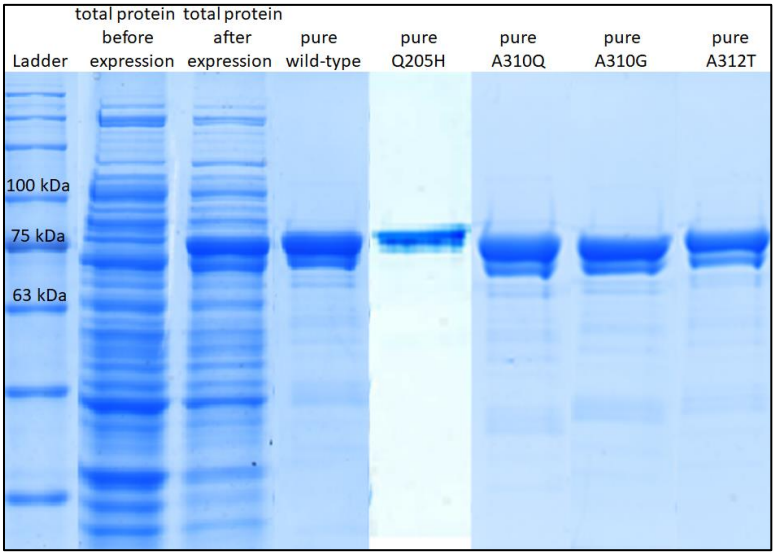

Figure 17: SDS-PAGE analysis of purified *Deinococcus radiodurans* glycogen branching enzyme and its variants. Lane 1: 5 µL of BLUeye prestained protein ladder. Lane 2: total protein content of 250 µL of *E. coli* cell culture before expression of recombinant wild-type DrGBE. Lane 3: total soluble protein content of 400 µL of *E. coli* cell culture after expression of recombinant wild-type DrGBE (unknown protein concentration). Lane 4: 5 µg of purified wild-type DrGBE. Lane 5: 5 µg of purified Q205H DrGBE. Lane 6: 5 µg of purified A310Q DrGBE. Lane 7: 5 µg of purified A310G DrGBE. Lane 8: 5 µg of purified A312T DrGBE. Note that DrGBE weighs ~80 kDa. The image for lane 5 was taken from a separate gel than that of the other lanes, after previously adjusting its size so that it corresponds with the ladder in this image.

Substrate Affinities

During affinity gel electrophoresis, DrGBE exhibited a smaller K_d with amylopectin than amylose, indicating that DrGBE has higher affinity for amylopectin, which is consistent with previous activity studies (Table 9) (Nasanovksy, 2017; Palomo *et al.*, 2009). Relative to wild-type, A312T DrGBE showed smaller K_d values with amylose and amylopectin, indicating increased substrate-affinity for both substrates (Table 9). Relative to wild-type, Q205H and A310Q DrGBE exhibited smaller K_d values with amylopectin but not amylose (Table 9). K_d values of A310G DrGBE with amylose and amylopectin were not altered relative to wild-type (Table 9). The migration of BSA through each affinity gel was unaffected by the presence or absence of glucan within the gel (confirmed using a protein ladder, Figure 18). BSA migration was thus used to calculate the relative mobility of each DrGBE variant, which was used to generate the reciprocal mobility plots from which the K_d values were derived (Figure 19).

Table 9: K_d values for *Deinococcus radiodurans* glycogen branching enzyme and its variants (Q205H, A310Q, A310G, and A312T) with amylose and amylopectin, calculated using affinity gel electrophoresis. Values are averages from three replicates ± standard error of the mean. Asterisks indicate that differences relative to wild-type are statistically significant ($p<0.05$).

Mutant	**K_d (mg/mL)**	
	Amylose	**Amylopectin**
Wild-type	0.58±0.03	0.12±0.01
Q205H	0.66±0.05	0.071±0.005*****
A310Q	0.58±0.04	0.040±0.004*****
A310G	0.69±0.02	0.11±0.02
A312T	0.20±0.01*****	0.079±0.007*****

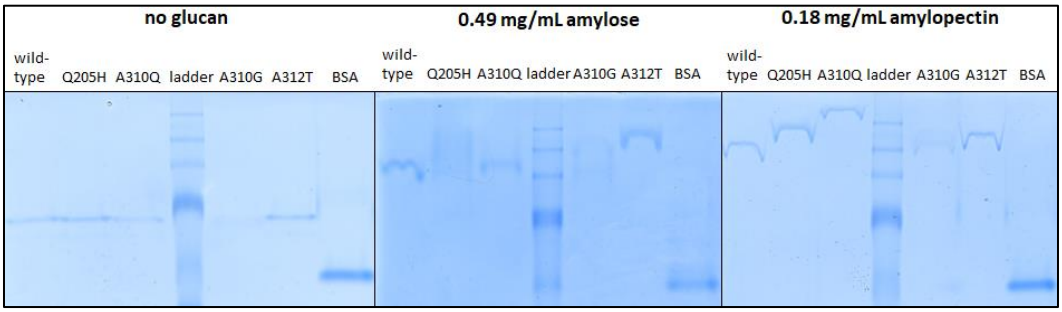

Figure 18: Example affinity gels for *Deinococcus radiodurans* glycogen branching enzyme and its variants (Q205H, A310Q, A310G, and A312T). 0.36 µg of each variant, 1 µg of BSA, and 3 µL of BLUeye ladder were electrophoresed through non-denaturing, 8% (w/v) acrylamide gels containing no glucan, amylose, or amylopectin (at 120 V and 4^{o}C for 2.5h before staining). Replicate gels (not shown) showed slight variations in enzyme migration, and were included when calculating K_d values and their standard errors.

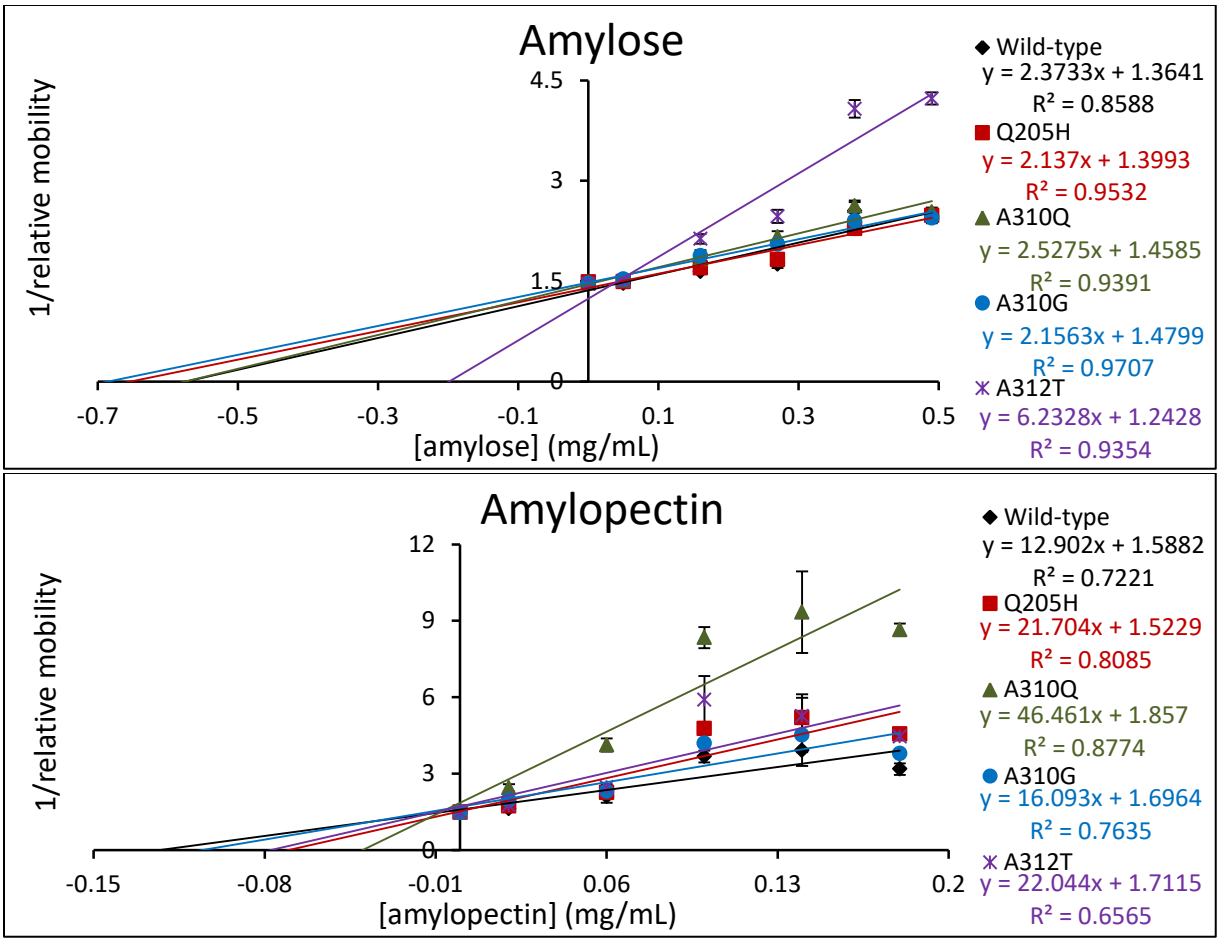

Figure 19: Reciprocal mobility plots of *Deinococcus radiodurans* glycogen branching enzyme and its variants (Q205H, A310Q, A310G, and A312T) electrophoresed through non-denaturing, 8% (w/v) acrylamide gels containing amylose or amylopectin (mobilities calculated relative to BSA). Values indicate averages of three replicates ± standard error of the mean.

Catalytic Activities

During the iodine-binding assay, wild-type DrGBE showed catalytic rates of 741±112 and 733±82 U/mg with amylose and amylopectin respectively. Note that units are not comparable between different substrates because glucan structure affects iodine staining in addition to BE activity. Relative to wild-type, A312T DrGBE exhibited increased activity with amylose and amylopectin, but the increase in activity with amylose was statistically insignificant due to high standard error (10,300±3,500 and 2,940±220 U/mg with amylose and amylopectin respectively) (Figure 20). The Q205H, A310Q, and A310G mutants showed decreased catalytic rates relative to wild-type DrGBE with both substrates (27.5±6.1, 19.8±1.1, and 34.8±28.3 U/mg respectively with amylose, and 6.73±34.45, 30.1±1.0, and 109±33 U/mg respectively with

amylopectin) (Figure 20). The units of activity were calculated using linear timecourses (see Figure 21 for the timecourses and enzyme and substrate concentrations used in the reactions).

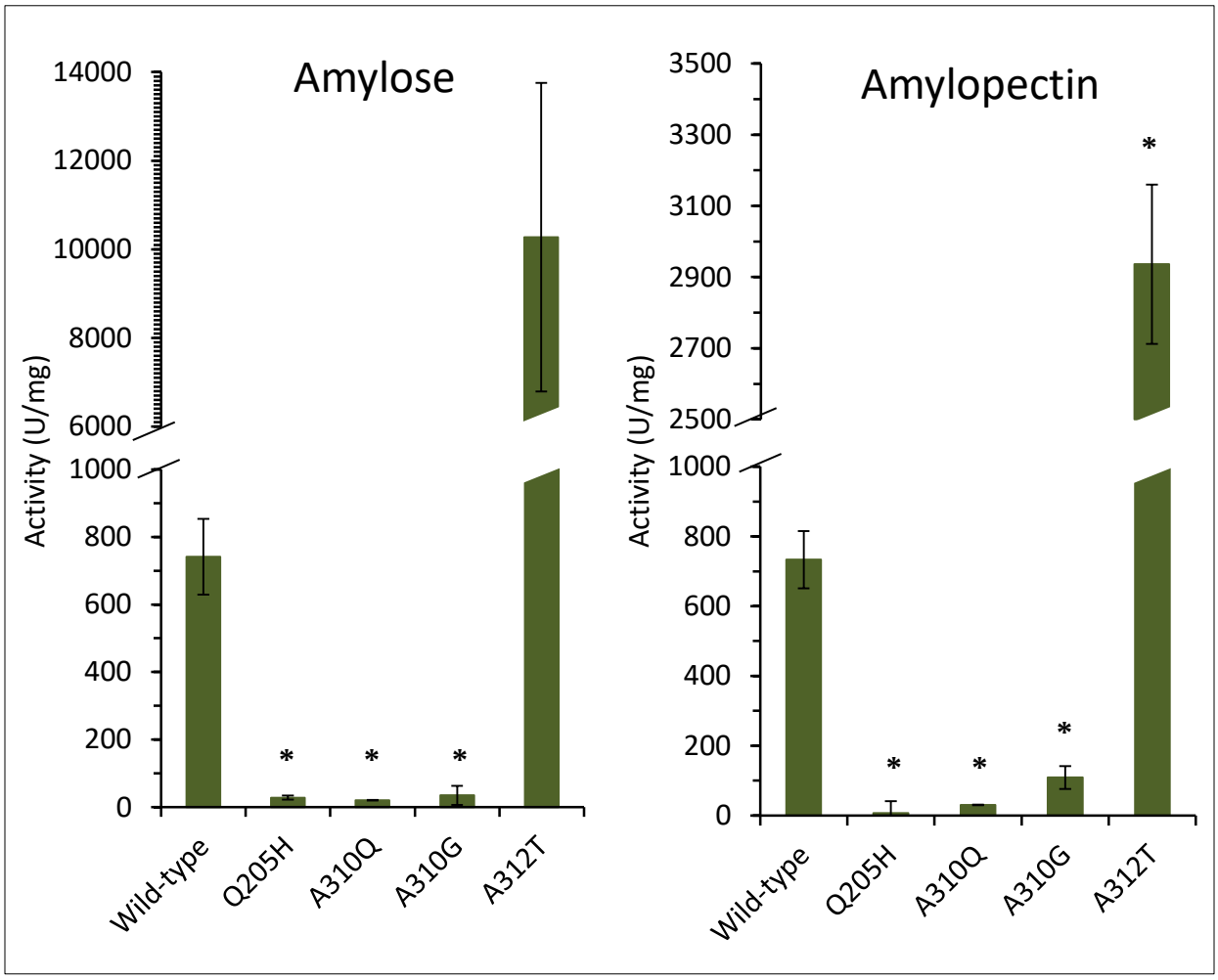

Figure 20: Catalytic rates of *Deinococcus radiodurans* glycogen branching enzyme and its variants (Q205H, A310Q, A310G, and A312T) with amylose and amylopectin, determined using the iodine-binding assay. Units are defined as a decrease in absorbance of the glucan-iodine complex at λ_{max} of 1 per min. Values are averages of three replicates ± standard error of the mean. Asterisks indicate that differences relative to wild-type are statistically significant ($p<0.05$).

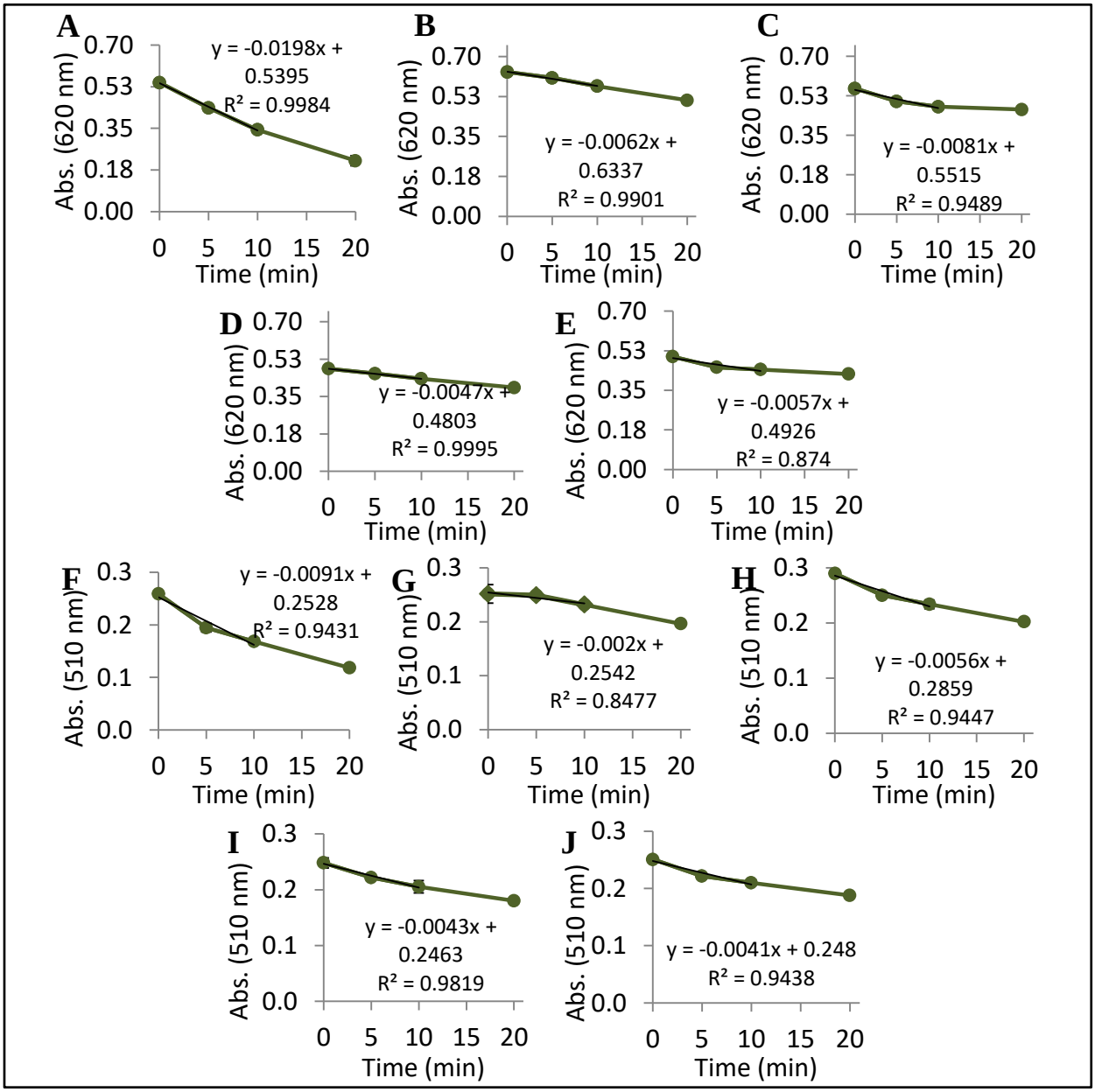

Figure 21: Catalytic activities of *Deinococcus radiodurans* glycogen branching enzyme or its variants, shown as timecourses. Reactions contained 0.89 mg/mL amylose in MOPS-NaOH pH7 and 1.3 µg/mL wild-type, 8.5 µg/mL Q205H, 26 µg/mL A310Q, 5.9 µg/mL A310G, or 0.042 µg/mL A312T DrGBE (parts A-E respectively), or 1 mg/mL amylopectin and 0.8 µg/mL wild-type, 3.6 µg/mL Q205H, 12 µg/mL A310Q, 2.2 µg/mL A310G, or 0.09 µg/mL A312T DrGBE (parts F-J respectively). Reactions were incubated at 34°C, and decreases in absorbance (Abs.) of the glucan-iodine complex were measured at λ_{max} (λ_{max} and y-axis values are different for amylose *versus* amylopectin). Different enzyme concentrations were required for each variant to observe linear decreases in absorbance (due to their distinct catalytic rates). Because catalytic rate is expressed per mg of enzyme, reactions with lower enzyme concentrations tend to yield higher calculated catalytic rates. Values are averages of three replicates ± standard error of the mean. Trendlines, equations, and R^2 values are shown for 10 min of reaction (used to calculate catalytic rates).

Gel Permeation Chromatography of Native and Enzyme-treated Polyglucans

Amylopectin migrated through the GPC column and eluted within the 12.5-25 min fractions ("amylopectin peak"), and chromatographed amylose eluted within the 35-62.5 min fractions ("amylose peak") (Figure 22). Chromatographed starch eluted within the 12.5-22.5 min fractions ("amylopectin peak") and the 30-70 min fractions ("amylose peak") (Figure 23). DrGBE-treated starch chromatographed through the GPC column showed no "amylopectin-like peak" and showed an "amylose-like peak" with increased area relative to native starch (Figure 23).

Several chromatograms showed contaminating peaks, such as "amylose-like peaks" in amylopectin samples, or "amylopectin-like peaks" in amylose samples. Quantification of the glucan content within these fractions using the phenol sulfuric acid assay (as opposed to semi-quantitative detection using iodine) showed that contamination composed up to a quarter (approximately) of the total glucan content (one example is shown in Figure 24).

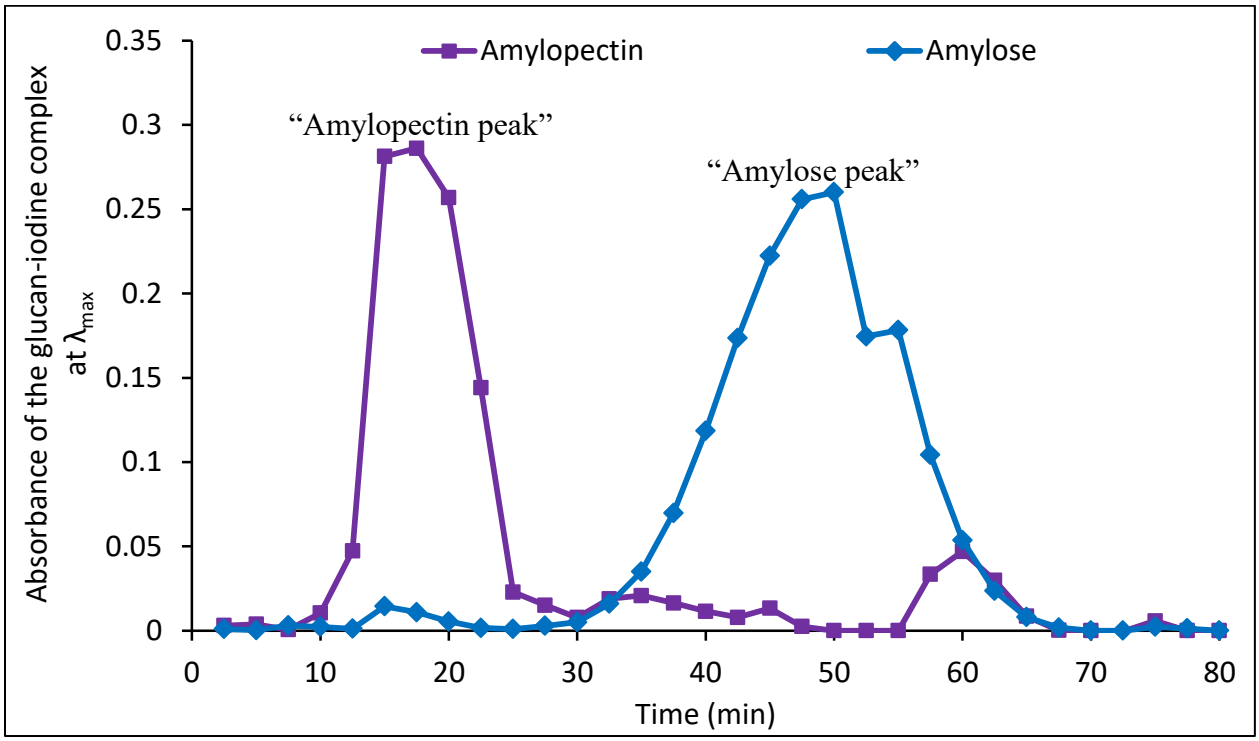

Figure 22: Elution profile of amylopectin and amylose chromatographed through Sepharose® CL-2B, detected using iodine. 200 µL of ~10 mg/mL potato amylose or corn amylopectin in MOPS-NaOH pH 7 was eluted using 0.01 M NaOH + 0.02 M NaCl at a rate of ~0.13 mL/min. Absorbance of the glucan-iodine complex within each fraction was measured at λ_{max} (510 nm for amylopectin or 620 nm for amylose).

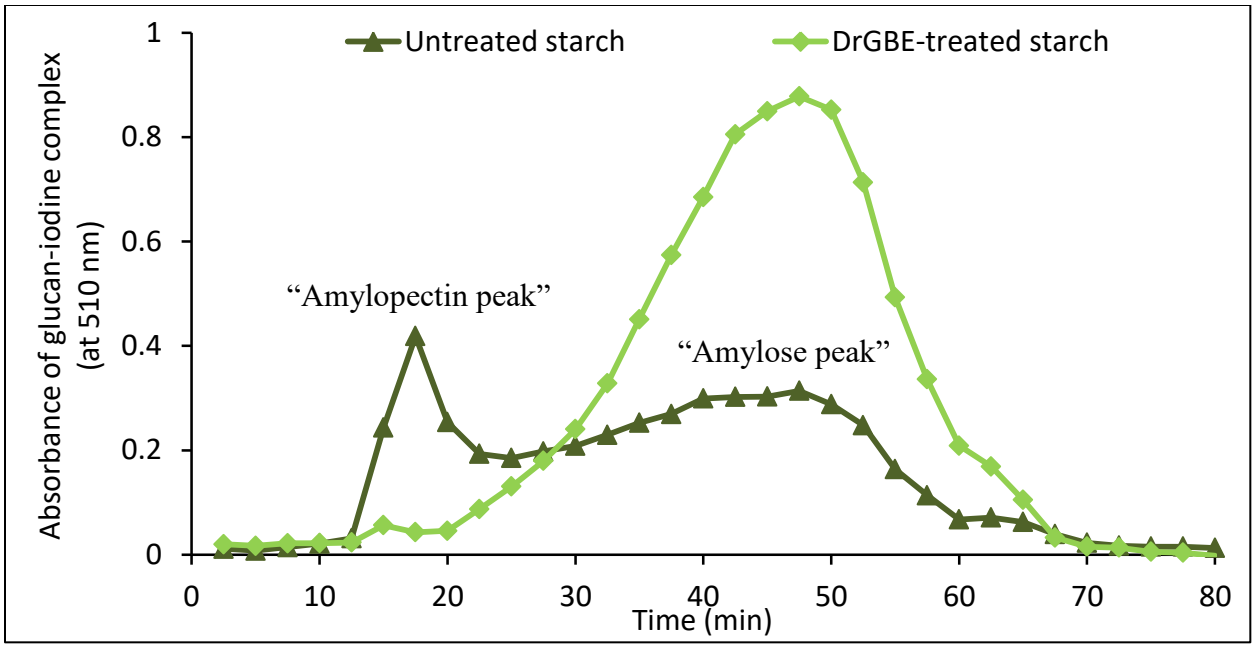

Figure 23: Elution profile of starch chromatographed through Sepharose® CL-2B before or after treatment with *Deinococcus radiodurans* glycogen branching enzyme, detected using iodine. 200 µL of 30-35 mg/mL starch in MOPS-NaOH pH 7 before or after enzyme treatment (1.95 µg/mL enzyme for 10 min at 35°C) was eluted with 0.01 M NaOH + 0.02 M NaCl at a flow rate of ~0.13 mL/min.

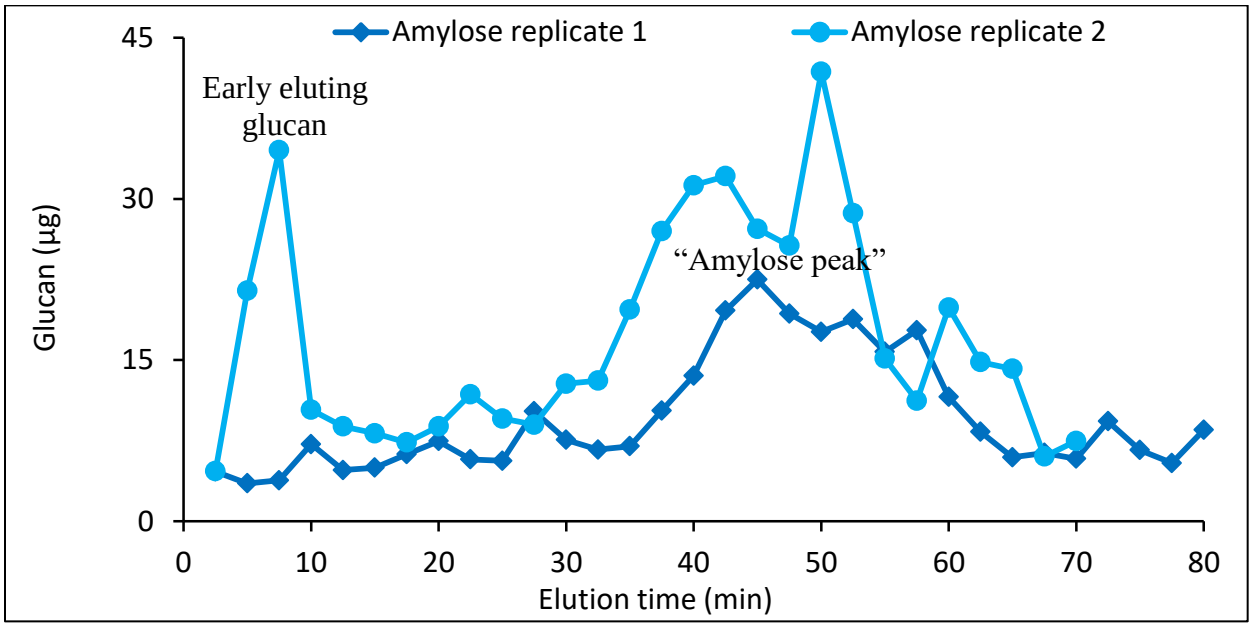

Figure 24: Elution profile of amylose replicate 1 and amylose replicate 2 chromatographed through Sepharose® CL-2B, quantified using the phenol sulfuric acid assay. 200 µL of ~10 mg/mL potato amylose in MOPS-NaOH pH 7 was eluted with 0.01 M NaOH + 0.02 M NaCl at a flow rate of ~0.13 mL/min.

Chimeric Branching Enzymes

Yields and activities of the chimeric enzymes $TtGBE_{cat}$-$mSBEI_{COO-}$ and $TtGBE_{cat}$-$mSBEI_{NH2}$ were low. A maximum of the equivalent of 0.7 mg of chimeric enzyme was purified per liter of *E. coli* culture, and enzyme yield and activity decreased when chimeric enzymes were expressed in cultures over ~300 mL. In comparison, around 6.3 mg of DrGBE was produced per liter of *E. coli* culture, and no decrease in DrGBE yield or activity was observed when DrGBE was expressed in cultures up to 2 L (data not shown). The chimeric enzymes exhibited catalytic rates below 5.5 U/mg with amylose or amylopectin (Table 10). These values are consistent with previous literature, which reported catalytic rates below 2.2 U/mg, and are lower those reported for mSBEI or TtGBE from which the chimeric enzymes were made (11.5 and 28.3 U/mg respectively) (Nasanovsky, 2017; Palomo *et al*., 2011; Takeda *et al*., 1993).

Table 10: Catalytic rates of chimeric enzymes made using domains from *Thermus thermophilus* and *Zea mays* branching enzymes, determined using the iodine-binding assay. Reactions contained 2.94 mg/mL amylose or amylopectin and ~37.4 or 230 µg/mL $TtGBE_{cat}$-$mSBEI_{COO-}$ or $TtGBE_{cat}$-$mSBEI_{NH2}$ respectively in MOPS-NaOH pH 7, and were incubated for 20 min. A unit of activity was defined as a decrease in absorbance of the glucan iodine-complex at λ_{max} of 1 per min.

Protein	Temperature (°C)	Activity (U/mg)	
		Amylose	Amylopectin
$TtGBE_{cat}$-$mSBEI_{COO-}$	34	2.59	0.426
	64	5.25	0
$TtGBE_{cat}$-$mSBEI_{NH2}$	34	1.18	0.0960
	64	0.691	0

SDS-PAGE analysis of purified $TtGBE_{cat}$-$mSBEI_{COO-}$ showed a denser band at the predicted weight for the tag-free enzyme (~77 kDa) than at the predicted weight for tagged enzyme (~105 kDa) (see Figure 25 on page 49), suggesting that most $TtGBE_{cat}$-$mSBEI_{COO-}$ was successfully cleaved from the intein tag during purification. However, SDS-PAGE analysis of the chitin resin after purification showed a dense band at the predicted weight for the tag-free enzyme (~77 kDa) (Figure 25), suggesting that high proportions of the enzyme remain bound to the chitin resin after purification, despite removal from the intein tag responsible for imparting affinity for chitin. SDS-PAGE analysis of eluate and chitin resin following purification $TtGBE_{cat}$-$mSBEI_{NH2}$ similarly suggested that $TtGBE_{cat}$-$mSBEI_{NH2}$ was successfully cleaved from

the intein tag during purification, but that high proportions of the enzyme remain bound to the chitin resin after elution.

Tag-free chimeric enzyme remaining bound to the chitin resin after purification suggested that protein insolubility might be responsible for the low enzyme yields and activities (New England Biolabs, 2017). Therefore, the more active chimeric enzyme, $TtGBE_{cat}$-$mSBEI_{COO-}$, was produced using altered expression or purification protocols or refolded in attempt to reduce protein aggregation that is often responsible for protein insolubility. Expression in the presence of arginine and glucose still resulted in $TtGBE_{cat}$-$mSBEI_{COO-}$ that remained bound to chitin after purification (Figure 25), and did not improve the catalytic activity. During protein purification, shortening the intein tag binding step to 4 h, or decreasing the time and temperature used for the intein tag cleavage step down to 36 h and 4^{o}C, had no detectable effect on chimeric enzyme yield or activity. Similarly, refolding of $TtGBE_{cat}$-$mSBEI_{COO-}$ from insoluble inclusion bodies failed to improve enzyme yield or activity, regardless of whether using low or high protein concentrations (undetectable up to 90 µg/mL protein), whether introducing the refolding buffer *via* dialysis or dilution, or whether including within the refolding buffer supplements previously shown to improve protein refolding (Figure 25).

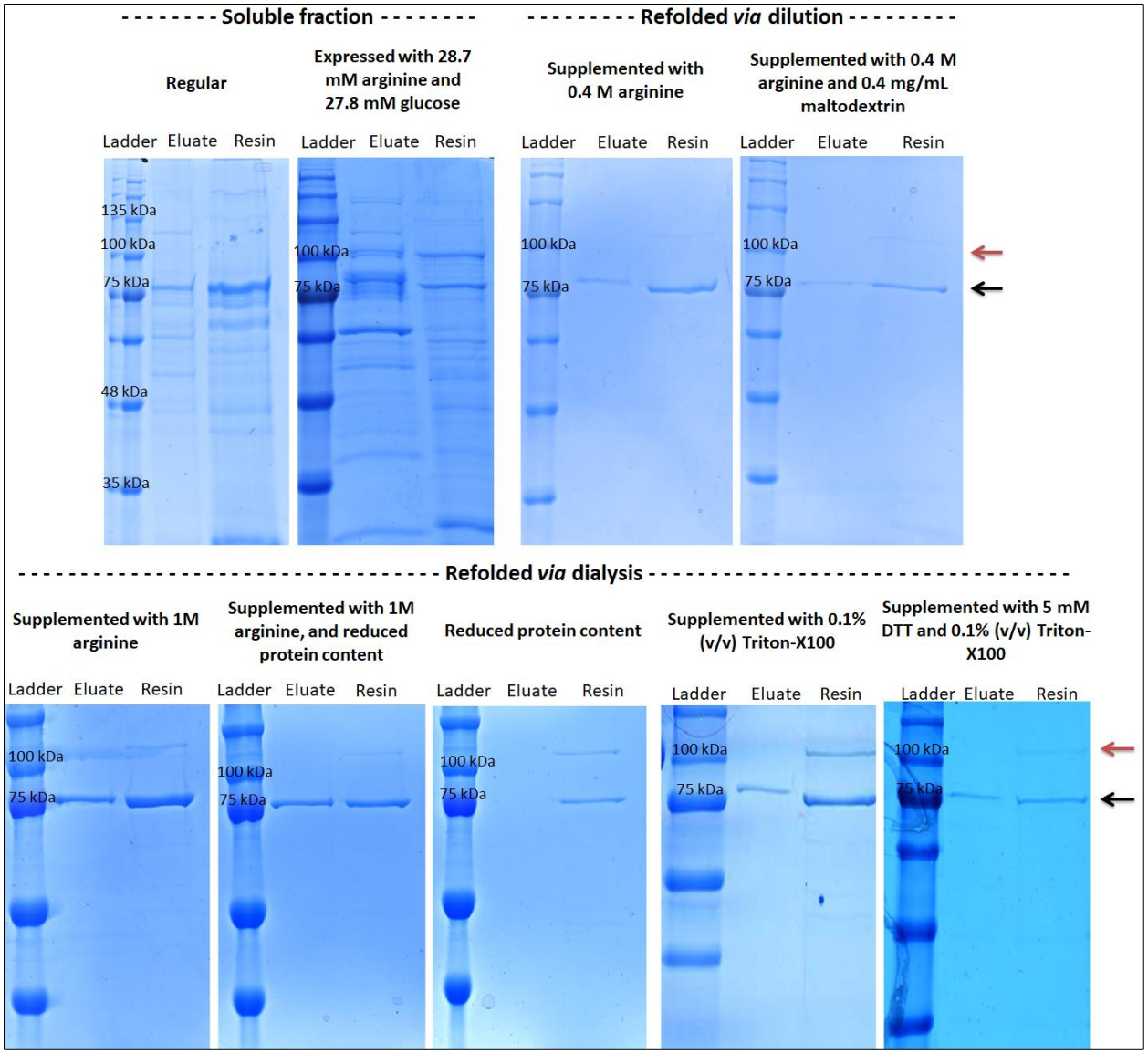

Figure 25: SDS-PAGE analysis of a chimeric enzyme made using domains from *Thermus thermophilus* and *Zea mays* branching enzymes after purification from soluble protein fractions of cell lysate or after purification from refolded inclusion bodies of cell lysate. Eluate lanes contain purified $TtGBE_{cat}$-$mSBEI_{COO-}$, and resin lanes contain chitin resin after $TtGBE_{cat}$-$mSBEI_{COO-}$ purification. Red arrows indicate intein-tagged $TtGBE_{cat}$-$mSBEI_{COO-}$ (~105 kDa), and black arrows represent tag-free $TtGBE_{cat}$-$mSBEI_{COO-}$ (~77 kDa). Supplements added to the cell culture during expression or to the buffer during refolding are indicated. Eluate lanes contain 1.1-2.5 µg of enzyme purified from soluble protein fractions or 16-50 µL of enzyme purified from refolded inclusion bodies (undetectable protein content). Resin lanes contained protein from ~28-36 µL of chitin. Ladder: 5 µL of BLUeye prestained or Precision Plus Protein^{TM} ladder.

CHAPTER 4: DISCUSSION

The goal of this M.Sc. project was to design and characterize BEs with the potential to reduce retrogradation of industrial starches. Four site-directed DrGBE mutants were made, and their substrate affinities and catalytic rates with amylose and amylopectin were measured. An attempt was also made to study their activities with amylose and amylopectin within starch. Additionally, several methods of protein expression, purification, and refolding were performed for chimeric enzymes (designed previously using domains from mSBEI and TtGBE) in an attempt to increase the chimeric enzyme yields and activities.

Design and Characterization of *Deinococcus radiodurans* Glycogen Branching Enzyme Mutants

SDM of DrGBE was performed in attempt to the increase the catalytic rate of DrGBE with amylose. SDM was favoured over directed evolution for making mutants, since directed evolution generates thousands of mutants and thus requires high-throughput screening methods (Arnold, 1996; Chen and Arnold, 1993; Hermes *et al*., 1990; Liao *et al*., 1986). Early attempts to develop high-throughput screening methods, including development of an *E. coli* strain without GBE (needed to study recombinant DrGBE within impure *E. coli* cell lysate) failed (data not shown). Furthermore, because amino acid sequences and 3D structural information are available for several BEs, sequence alignments and protein models could be made to assist in rational SDM design, eliminating the need for random mutagenesis (*e.g.* directed evolution).

To analyze potential glucan-interaction sites, a plausible 3D DrGBE model was made, and the model was subsequently aligned to structures with a diversity of co-crystallized glucans (using MODELLER and PyMOL, Table 7). The conformations of DrGBE residues 1-627 within the model were nearly as favourable as those within the template used for modelling except for the terminal regions (determined using DOPE score analysis, Figure 14). Residues 628-705 of DrGBE were not modelled because no appropriate template was available. This was not surprising, as the region was predicted to be disordered using VSL2 prediction within PONDR (Figure 13), and the region has been previously shown to be unimportant in affecting DrGBE catalytic rate, substrate preference, chain transfer properties, and thermostability using truncation of residues 636-705 (Palomo *et al*., 2009).

Sequence alignments showed that several amino acid residues are conserved among GBEs alone and plant SBEs alone, and that several other residues are conserved among prokaryotic BEs alone and eukaryotic BEs alone (Figure 16). The DrGBE model suggested that four of these residues are on the protein surface, near catalytic residues, or near a potential substrate-interaction site (Figure 15). This pattern of sequence conservation near the catalytic region suggested that the residues may be important in the variable properties between the different BE classes, and thus these residues were mutated.

The first mutation changed glutamine at position 205 to histidine (Q205H). Histidine was introduced because it possesses aromaticity and a positive charge. Aromaticity can facilitate nonpolar stacking interactions with glucans, and charge can strengthen polar interactions with glucan hydroxyl groups (Chaen *et al*., 2012; Matsui *et al*., 1994; Noguchi *et al*., 2011). Therefore, the Q205H mutation was predicted to add an interaction site for long-chain glucans and thus increase substrate-affinity and catalytic activity with amylose.

Indeed, the Q205H mutant showed an increase in substrate-affinity relative to wild-type DrGBE. However, Q205H DrGBE exhibited increased affinity for amylopectin and not amylose (Table 9), which is the opposite of the original goal. Substrate-affinity may have increased for only amylopectin due to the position of the introduced histidine residue. While the mutation had been made to potentially introduce a new interaction site for long-chained amylose, the close proximity of Q205H to the catalytic region/potential substrate-binding site may have caused introduction of a new interaction site (histidine) to instead strengthen a binding site that already existed for amylopectin, which is the preferred substrate for DrGBE (Figure 15). Previous studies also suggest that the effect of histidine residues on substrate-affinity depends on residue location. For example, histidine-to-alanine mutations within the catalytic domain of mSBEII, amino-terminal of or between the catalytic residues, decreased the substrate-affinity for amylose, whereas a histidine-to-alanine mutation within the amino-terminal domain of bean SBEII, in an amino-terminal extension not present within DrGBE, caused no observable effect on substrate-affinity (Funane *et al*., 1998; Hamada *et al*., 2007). When attempting to add binding sites for long-chain glucans in future SDM experiments, it may thus be useful to introduce histidine residues into different regions.

Despite the increased substrate-affinity of Q205H DrGBE, which had been predicted to increase catalytic rate, the mutant exhibited decreased catalytic rate with both amylose and

amylopectin relative to wild-type (Figure 20). It is possible that catalytic rate decreased due to an increase in steric hindrance within the catalytic cleft, which likely resulted from the introduction of the bulky and positively-charged histidine (Figure 15). Increased glucan-affinity may have also decreased the ability of the Q205H mutant to release the glucan product, hindering completion of catalysis (and thus catalytic rate). The results suggest that changes in catalytic activity do not always parallel changes in substrate-affinity, which has been reported previously. For example, the E459D mutant of *E. coli* GBE showed decreased substrate-affinity but increased catalytic rate relative to wild-type *E. coli* GBE (Binderup and Preiss, 1998). This indicates that increasing the affinity of a BE for a particular substrate may not necessarily increase the catalytic rate with that substrate, as had been the goal of the Q205H mutation.

The second mutation changed alanine at position 310 to glutamine (A310Q). As was the case with the Q205H mutation, the A310Q mutation was intended to increase substrate-affinity and catalytic rate with amylose by introducing an additional interaction site (a hydrophilic group). The equivalent mutation had already been performed within *G. thermoglucosidans* GBE (also at residue 310, Figure 16), resulting in increased substrate-affinity for amylose and amylopectin, and increased substrate preference for amylose (the ratio of affinity for amylose over the affinity for amylopectin increased) (Liu *et al*., 2017). However, similar to the Q205H mutant, A310Q DrGBE exhibited increased affinity for amylopectin but not amylose (relative to wild-type) (Table 9). The different effect of the A310Q mutation within DrGBE *versus G. thermoglucosidans* GBE may be due to differences between the two enzymes in their catalytic clefts. In the DrGBE model, the nucleophilic and acid/base residues required for catalysis are adjacent to A310 and each other, whereas in the *G. thermoglucosidans* GBE model, the catalytic nucleophile and acid/base appear to be separated by A310 (see Figure 15 in this report *versus* Figure 5 from Liu *et al*. (2017)). The more spacious arrangement of the residues within *G. thermoglucosidans* GBE may have allowed the addition of an interaction site to promote interactions with longer glucan chains (amylose), whereas the less spacious arrangement within DrGBE may allowed for only increased interactions with shorter glucan chains (amylopectin). Additionally, A310 in *G. thermoglucosidans* GBE may be further from an existing substrate-binding site than it is in DrGBE, so that introducing a glutamine at this location added a binding site for longer glucans in *G. thermoglucosidans* GBE but instead intensified a binding site already present for shorter glucan chains in DrGBE. Equivalent mutations often have different

effects for different enzymes. For example, changing the glutamic acid at position 459 in *E. coli* GBE to an aspartic acid increased catalytic activity, whereas the equivalent mutation in mSBEIIa (E513D) or mSBEIIb (E441D) decreased or eliminated catalytic activity respectively (Binderup and Preiss, 1998; Kuriki *et al*., 1996; Li *et al*., 2015) (Table 8).

The A310Q mutant of DrGBE exhibited decreased catalytic rate with amylose and amylopectin relative to wild-type, as was observed in the equivalent mutant of *G. thermoglucosidans* GBE (Figure 20) (Liu *et al*., 2017). The decrease in activity may have resulted due to increased steric hindrance caused by the introduction of a bulky residue near the catalytic residues, or due to increased glucan-affinity preventing product release during catalysis (Figure 15, Table 9).

The third mutation changed alanine at position 310 to glycine (A310G). Glycine can increase protein flexibility due to its small side chain, potentially increasing the ability of DrGBE to react with long-chained amylose (Neurath, 1943; Yan and Sun, 1997). However, A310G DrGBE exhibited decreased catalytic rate with amylose and amylopectin relative to wild-type (Figure 20), as was observed following the equivalent mutation in *G. thermoglucosidans* GBE (also at residue 310, Figure 16) (Liu *et al*., 2017). Perhaps the decrease in catalytic rate was due to improper protein folding within the catalytic region (caused by increased flexibility), which may have disfavoured BE activity.

The substrate-affinity of A310G DrGBE for amylose and amylopectin was not altered relative to wild-type (Table 9). While no change in substrate-affinity had been predicted, the opposite result was observed for the equivalent mutant of *G. thermoglucosidans* GBE (Liu *et al*., 2017). The A310G mutant of *G. thermoglucosidans* GBE, unlike that of DrGBE, exhibited increased substrate-affinity for both amylose and amylopectin. This may have been due to a more spacious catalytic cleft within *G. thermoglucosidans* GBE relative to DrGBE (Figure 5 from Liu *et al*. (2017) and Figure 15 in this report respectively), which may have allowed *G. thermoglucosidans* GBE to more easily interact with glucans or may have minimized the structural effects of altered protein flexibility caused by the introduced glycine.

The fourth mutation changed alanine at position 312 to threonine (A312T). This mutation was predicted to increase catalytic rate due to the addition of a nucleophile in the catalytic cleft, near the catalytic nucleophile D309, as nucleophilic attack is involved in the BE reaction (see Figure 15 and Figure 9 on page 14). As expected, A312T DrGBE exhibited

increased catalytic rates with amylose and amylopectin relative to wild-type (Figure 20). However, the increase in catalytic rate was only statistically significant with amylopectin, due to high standard error during the amylose studies. The high catalytic activity of A312T DrGBE may have been responsible for the high standard errors, as it caused small deviations in the time of the reaction (before inactivating the reaction) to greatly affect the calculated catalytic rates.

Of the four mutants produced in this study, all but A312T DrGBE exhibited decreased activity relative to wild-type, perhaps because the A312T mutation was the most subtle. Whereas the Q205H, A310Q, and A310G mutations altered amino acid aromaticity and charge, size (van der Waals volume), or flexibility respectively, the A312T mutation only altered reactivity and hydrophilicity with a minor change in size. Therefore, the A312T mutation likely caused only minor changes in DrGBE structure and steric hindrance relative to the other mutations. Additionally, the further distance of residue A312 from the catalytic residues, in comparison to residue A310, may have minimized effects of the mutation on hindering catalysis (Figure 15, Figure 16).

The A312T mutation was predicted to increase substrate-affinity for long-chain glucans due to the addition of an –OH group that could potentially add a glucan-interaction site. Indeed, A312T DrGBE exhibited increased affinity for amylose and amylopectin relative to wild-type (Table 9). The A312T mutation may have increased affinity for both amylose and amylopectin, as opposed to the Q205H and A310Q mutations, which increased affinity for only amylopectin, because the mutated residue in the A312T mutant was further from the substrate-interaction site (Figure 15). This may have allowed the altered residue at position 312 to add an additional glucan-binding site for long chains instead of only strengthening a binding site already present for short chains.

Overall, changes in substrate-affinity did not always parallel changes in catalytic rates, which is agreement with previous research (Table 9, Figure 20, and Table 8). For example, the A310G, N, I, E, and Q mutations in *G. thermoglucosidans* GBE increased substrate-affinity but decreased catalytic activity (Liu *et al.*, 2017), and the E459D mutation in *E. coli* (residue 361 in DrGBE) decreased substrate-affinity but increased catalytic activity (Binderup and Preiss, 1998). In some mutants, changes in substrate-affinity parallel changes in catalytic activity. For example, the Y352F, D363K, R456K, and E513D mutations in mSBEIIa (residues 204, 215, 307, and 310 in DrGBE respectively) decreased both substrate-affinity and catalytic activity (Li *et al.*, 2015).

Gel Permeation Chromatography of Native and Enzyme-treated Polyglucans

DrGBE activity with amylose and amylopectin within their natural milieu was studied using GPC to analyze whether DrGBE prefers amylose or amylopectin when both substrates are available, and to better represent what would occur if using the enzyme in industry. Other BE assays available, including but not limited to the iodine-binding assay, the branch-linkage assay, and NMR (described on page 57), only analyze changes in the overall glucan substrate, and not changes in each component of the substrate.

DrGBE treatment decreased the hydrodynamic volume of amylopectin within starch so that it eluted through the GPC column similarly to the smaller amylose component (DrGBE-treated starch exhibited a smaller "amylopectin peak" and a larger "amylose-like peak" than untreated starch, shown in Figure 23). The hydrodynamic volume of amylopectin may have decreased due to reductions in molecular weight and/or molecular linearity, both of which have been reported previously following DrGBE-treatment of polyglucan (Nasanovksy, 2017).

The elution of DrGBE-treated amylopectin within the fractions expected for amylose may have masked DrGBE-induced changes in amylose content (Figure 23). This negated the primary purpose of using GPC, which had been to detect changes in both starch components during BE activity, but primarily changes in amylose content (as the component most industries seek to reduce).

Additionally, the GPC system was unable to yield clear results due to contaminating peaks present in several of the glucan preparations (one example is shown in Figure 24). Contaminating peaks may have been due to glucan depolymerization (which can decrease amylopectin size, causing amylopectin to elute later, similar to amylose) and glucan aggregation (which can increase amylose size, causing amylose to elute earlier, similar to amylopectin). Glucan depolymerization and aggregation commonly occur during preparation of glucan stocks (Han and Lim, 2004a, 2004b; Han *et al*., 2003; Niemelä, 1990). Amylose-like peaks in amylopectin elutions may have also been caused by extra-long chain amylopectin, which can be difficult to distinguish from amylose, as observed previously in starches isolated from barley, rice, potato, sweet-potato, and cassava (Baba *et al*., 1987; Charoenkul *et al*., 2006; Hizukuri, 1986; Robin *et al*., 1974; Takeda *et al*., 1987, 1999). Other researchers who have used Sepharose CL-2B cross-linked beads for chromatographic separation of amylose and amylopectin did not report contamination, perhaps because they were using the chromatographs

solely to separate amylose and amylopectin from impure samples and not to quantify differences in amylose and amylopectin between samples (Bertoft *et al*., 2008; Forsyth *et al*., 2002). Due to the inability to detect changes in amylose content and the presence of contaminating peaks, GPC was not used for analyzing the DrGBE mutants.

Validity and Future Directions for Studying *Deinococcus radiodurans* Glycogen Branching Enzyme and its Variants

DrGBE and its variants contained no detectable protein contamination following His-tag purification. While SDS-PAGE analysis of each enzyme variant showed two bands near the size predicted for DrGBE (Figure 17), affinity gel electrophoresis detected only one band (or two similar bands) per sample (Figure 18). This indicated sample purity, as substrate-induced changes in mobility during affinity gel electrophoresis would unlikely be similar for contaminating protein as for the DrGBE variants, and thus contamination would have resulted in two dissimilar bands in the affinity gel lanes. The additional band in SDS-PAGE analysis may have been a truncation of DrGBE, which could be prevented in future experiments by using a more efficient protease inhibitor and/or working more quickly to reduce proteolysis.

DrGBE in this project exhibited 741 and 733 U/mg of activity with amylose and amylopectin respectively, which are similar to values previously reported for DrGBE of 404 and 538 U/mg of activity (Palomo *et al.*, 2009). It should be noted that DrGBE activity may have been underestimated if DrGBE aggregates had been present. Recombinant protein expressed in *E. coli* tends to aggregate into inactive oligomers (Baneyx, 1999; Marston, 1986). While insoluble oligomers were removed from samples using centrifugation, soluble oligomers were not removed from samples using GPC due to time limitations.

Affinity gel electrophoresis of DrGBE had not been performed prior to this project. However, during agarose gel electrophoresis, DrGBE exhibited a lower K_d with amylopectin than with amylose (Table 9), which is consistent with previous reports that showed DrGBE to prefer amylopectin over amylose (Nasanovsky, 2017; Palomo *et al*., 2009). Additionally, the K_d values for DrGBE and its variants were similar to those previously reported for other BEs (Tetlow *et al*., 2008).

Future studies should analyze the catalytic activities of the DrGBE variants at elevated temperatures to determine whether the enzymes are useful at the high temperatures required for processing starch in industry. Experiments should also analyze the efficiency of the DrGBE variants by analyzing their branching *versus* amylolytic activities, as amylolysis can reduce glucan molecular weight, potentially altering the properties of industrial polyglucans, such as binding behavior, transparency, and mechanical strength. Several industries seek to avoid glucan hydrolysis, as it can result in loss or browning of material, while other industries prefer at least partial hydrolysis because it can shorten glucan chains more than branching, which is useful in certain food and non-food applications (Ruben Lenz from Advanced Micro Polymers Inc. (Milton), unpublished communication).

The present experiments assumed DrGBE branching activity was efficient (no amylolysis) because previous branch-linkage assays and ^{1}H-NMR experiments indicated that around 98% of DrGBE activity is due to branching (Nasanovksy, 2017; Palomo *et al*., 2009). However, the mutations performed may have decreased DrGBE efficiency, and this should be analyzed. The branch-linkage assay can differentiate branching from amylolysis using a colorimetric reducing sugar assay, because amylolysis directly introduces reducing ends (free aldehyde groups), whereas branching only introduces reducing ends if the branches are subsequently cleaved (*e.g.* using isoamylase) (Borovsky *et al*., 1975; Park and Johnson, 1949; Takeda *et al*., 1993; Utsumi *et al*., 2009; Waffenschmidt and Jaenicke, 1987). ^{1}H-NMR can differentiate branching from amylolysis because the differing ^{1}H resonance frequencies attached to the different carbon atoms (Gidley, 1985; Usui *et al*., 1974).

Chimeric Branching Enzymes

Attempts were made to refold and/or modify the expression and/or purification of $TtGBE_{cat}$-$mSBEI_{COO-}$ and $TtGBE_{cat}$-$mSBEI_{NH2}$ to increase their yields and catalytic activities, as low yields and activities had previously hindered characterization of the chimeric enzymes (Nasanovsky, 2017). The catalytic activities of the chimeric enzymes were lower than their native counterparts, and chimeric enzyme yields and activities decreased following expression from large volumes of culture, making it difficult to produce the amount of enzyme required for

characterization (Results described on page 47; Table 10; Nasanovsky, 2017; Palomo *et al*., 2011; Takeda *et al*., 1993).

During chimeric enzyme purification, high proportions of tag-free, chimeric enzyme remained bound to chitin resin, even after cleavage from the intein tag that is responsible for imparting affinity for chitin (examples for $TtGBE_{cat}$-$mSBEI_{COO-}$ are shown in Figure 25). As this can indicate protein insolubility (New England Biolabs, 2017), attempts were made to reduce enzyme aggregation (which can cause insolubility).

Chimeric proteins commonly misfold since they are composed of domains from different enzymes that may not fit well together. For example, of the eight chimeric enzymes made by Kuriki *et al*. in 1997, using domains from mSBEI and mSBEII, only two were active, one of which exhibited low catalytic activity relative to its native counterpart and was only partially characterized. The probability that $TtGBE_{cat}$-$mSBEI_{COO-}$ and $TtGBE_{cat}$-$mSBEI_{NH2}$ were improperly folded was high, as they were composed of domains from dissimilar enzymes that therefore may not have fit well together (TtGBE is a GH57, bacterial, glycogen branching enzyme, whereas mSBEI is a GH13, plant, starch branching enzyme). Furthermore, $TtGBE_{cat}$-$mSBEI_{NH2}$ contained the amino terminal domain of TtGBE, the amino terminal domain from mSBEI (at the carboxyl-terminal end of the enzyme), and no classical "carboxyl-terminal domain" from either enzyme (see Figure 11), perhaps abolishing domain interactions between the amino-terminal and "carboxyl-terminal" domains that are necessary for proper folding.

Prior to this project, attempts were made to lower $TtGBE_{cat}$-$mSBEI_{COO-}$ and $TtGBE_{cat}$-$mSBEI_{NH2}$ expression rates within *E. coli* by varying culture size and temperature, as researchers have previously used this technique to reduce unfavourable hydrophobic interactions between proteins in the process of folding (reviewed by Rosano and Ceccarelli (2014)). However, these attempts were not successful (Nasanovsky, unpublished results).

Attempts were made in the current project to increase the solubility of $TtGBE_{cat}$-$mSBEI_{COO-}$ (the more active chimeric enzyme; Table 10) using protein refolding (from insoluble inclusion bodies) and/or altered protein expression and/or purification. All attempts were unsuccessful, even when including additives previously shown to suppress protein aggregation (additives were included within the growth cultures or purification and/or refolding buffers). These additives included arginine, maltodextrin (as a possible ligand), DTT, and Triton X-100 (see Figure 25 and page 48) (Arora and Khanna, 1996; Buchner *et al*., 1992; London and

Khorana, 1982; Matsuzaki *et al*., 1996; Matulis *et al*., 2005; Niesen *et al*., 2007; Umetsu *et al*., 2003; Vedadi *et al*., 2006; Wang and Li, 2014). During refolding, use of low temperatures (4-10^{o}C to reduce the hydrophobic interaction between intermediately- and unfolded proteins) and use of dialysis or dilution (to reduce protein concentration and thus hydrophobic interactions between proteins) both failed to improve $TtGBE_{cat}$-$mSBEI_{COO-}$ yield or activity (Figure 25 and page 48) (Buchner *et al*., 1992; Vallejo and Rinas, 2004a, 2004b). Protein concentrations during refolding were kept below those previously used to successfully refold proteins: 13 and 90 µg/mL protein used during direct dilution and dialysis respectively (successful protein refolding with 1-30 and 10 mg/mL protein respectively has been previously reported (Buchner *et al*., 1992; Weir and Sparks, 1987; Maeda *et al*.,1995; Yoshii *et al*., 2000).

It is possible that the techniques described above did not improve $TtGBE_{cat}$-$mSBEI_{COO-}$ solubility due to differences in the enzymes studied. For example, refolding of $TtGBE_{cat}$-$mSBEI_{COO-}$ in the presence of arginine (within the protein refolding buffer) may have failed to improve chimeric enzyme solubility because $TtGBE_{cat}$-$mSBEI_{COO-}$ contains cysteine residues, and arginine may have promoted improper disulfide bond formation due to its tendency to slow protein folding (Chen et al., 2008). The inability of the possible ligand maltodextrin to increase $TtGBE_{cat}$-$mSBEI_{COO-}$ solubility may have been due to using too short a glucan for the chimeric enzyme to bind (maltodextrin contains 2-20 glucose residues, whereas amylose contains 100-10,000 glucose residues) (Blennow *et al*., 2013). Alternatively, the maltodextrin concentration may have been too low, or arginine present in the buffer may have prevented hydrophobic interactions necessary for the chimeric enzyme to bind to maltodextrin.

Future Directions for Studying Chimeric Branching Enzymes

It is possible $TtGBE_{cat}$-$mSBEI_{COO-}$ yield and activity cannot be improved using protein refolding or altered protein expression and purification. For example, monomeric $TtGBE_{cat}$-$mSBEI_{COO-}$ may be inactive. This could be tested by separating monomeric and oligomeric $TtGBE_{cat}$-$mSBEI_{COO-}$ (using GPC) before analyzing enzyme activity. Folding of $TtGBE_{cat}$-$mSBEI_{COO-}$ could also be analyzed using circular dichroism. It is also possible that the chimeric enzymes observed using SDS-PAGE analysis were misidentified (contaminating proteins), which could be tested using mass spectroscopy.

Analyzing chimeric enzyme activities using more sensitive assays, such as the quantitative branch-linkage assay (unlike the insensitive, semi-quantitative iodine-binding assay) would be advantageous. Amylopectin chain-length distribution analysis has previously been used to characterize $TtGBE_{cat}$-$mSBEI_{COO-}$ (Nasanovsky, 2017). Affinity gel electrophoresis may also be useful for analyzing proteins with low catalytic activities and yields, as it analyzes substrate-affinity independently of BE activity or BE-induced changes in glucan structure, and silver staining can be used to visualize low quantities of enzyme. Affinity gel electrophoresis of the chimeric enzymes relative to their native counterparts could reveal new information regarding the domains from mSBEI or TtGBE.

CONCLUSIONS

My M.Sc. thesis produced four site-directed mutants of *Deinococcus radiodurans* glycogen branching enzyme (Q205H, A310Q, A310G, and A312T) with novel characteristics relative to wild-type DrGBE. The A312T mutant exhibited increased substrate-affinity for amylose and amylopectin and increased catalytic rate with amylopectin relative to wild-type DrGBE. A312T DrGBE thus shows potential for reducing the molecular linearity (and thus retrogradation) of industrial starches, as it has higher catalytic activity than its wild-type counterpart, which could reduce enzyme production costs associated with modifying starches. The Q205H and A310Q mutants exhibited increased substrate-affinity for amylopectin relative to wild-type DrGBE. However, the Q205H, A310Q, and A310G mutants exhibited decreased catalytic activity with amylose and amylopectin relative to wild-type DrGBE, and thus show less potential for industrial use. Measuring the activities of the mutated enzymes towards amylose or amylopectin using gel permeation chromatography was unsuccessful because DrGBE-induced changes in the amylopectin masked changes in the amylose content. Attempts were made to improve the yields and activities of the chimeric enzymes $TtGBE_{cat}$-$mSBEI_{COO-}$ and $TtGBE_{cat}$-$mSBEI_{NH2}$ by deceasing protein aggregation, but were not successful, perhaps because aggregation was not responsible for the low chimeric enzyme yields and activities. Follow-up studies should analyze the thermotolerance and branching efficiency of the A312T DrGBE variant, as this enzyme showed the most industrial potential.

REFERENCES

Abad, M.C., Binderup, K., Rios-Steiner, J., Arni, R.K., Preiss, J., and Geiger, J.H. (2002). The X-ray crystallographic structure of *Escherichia coli* branching enzyme. The Journal of Biological Chemistry 277, 42164–42170.

Abbas, K.A., Khalil, S.K., and Hussin, A.S.M. (2010). Modified starches and their usages in selected food products: A review study. Journal of Agricultural Science 2, 90–100.

Ačkar, D., Babić, J., Jozinović, A., Miličević, B., Jokić, S., Miličević, R., Rajič, M., and Šubarić, D. (2015). Starch modification by organic acids and their derivatives: A review. Molecules 20, 19554–19570.

Alcázar-Alay, S.C., and Meireles, M.A.A. (2015). Physicochemical properties, modifications and applications of starches from different botanical sources. Food Science and Technology 35, 215–236.

Alting, A.C., van der Velde, F., Kanning, M.W., Burgering, M., Mulleners, L., Sein, A., and Buwalda, P. (2009). Improved creaminess of low-fat yoghurt: The impact of amylomaltase-treated starch domains. Food Hydrocolloids 23, 980–987.

Anderson, B.A., and Singh, R.P. (2003). Use of phytoglycogen extracted from corn to increase the bowl-life of breakfast cereal. Journal of Food Process Engineering 26, 315–322.

Archibald, A.R., Fleming, I.D., Liddle, A.M., Manners, D.J., Mercer, G.A., and Wright, A. (1961). α-1,4-Glucosans. Part XI. The absorption spectra of glycogen- and amylopectin-iodine complexes. Journal of the Chemical Society 0, 1183–1190.

Arnold, F.H. (1996). Directed evolution: creating biocatalysts for the future. Chemical Engineering Science 51, 5091–5102.

Arora, D., and Khanna, N. (1996). Method for increasing the yield of properly folded recombinant human gamma interferon from inclusion bodies. Journal of Biotechnology 52, 127–133.

Auh, J., Chae, H.Y., Kim, Y., Shim, K., Yoo, S., and Park, K. (2006). Modification of rice starch by selective degradation of amylose using alkalophilic *Bacillus* cyclomaltodextrinase. Journal of Agricultural and Food Chemistry 54, 2314–2319.

Baba, T., Yoshii, M., and Kainuma, K. (1987). Acceptor molecule of granular-bound starch synthase from sweet-potato roots. Starch/Stärke 39, 52–56.

Baba, T., Kimura, K., Mizuno, K., Etoh, H., Ishida, Y., Shida, O., and Arai, Y. (1991). Sequence conservation of the catalytic regions of amylolytic enzymes in maize branching enzyme-I. Biochemical and Biophysical Research Communications 181, 87–94.

Bailey, J.M., and Whelan, W.J. (1961). Physical properties of starch. The Journal of Biological Chemistry 236, 969–973.

Ball, S.G., and Morell, M.K. (2003). From bacterial glycogen to starch: understanding the biogenesis of the plant starch granule. Annual Review of Plant Biology 54, 207–233.

Ball, S.G., Guan, H.P., James, M., Myers, A., Keeling, P., Mouille, G., Buléon, A., Colonna, P., and Preiss, J. (1996). From glycogen to amylopectin: A model for the biogenesis of the plant starch granule. Cell 86, 349–352.

Ball, S.G., van de Wal, M.H.B.J., and Visser, R.G.F. (1998). Progress in understanding the biosynthesis of amylose. Trends in Plant Science 3, 462–467.

Baneyx, F. (1999). Recombinant protein expression in *Escherichia coli*. Current Opinion in Biotechnology 10, 411–421.

Baum, B.R., and Bailey, L.G. (1987). A survey of endosperm starch granules in the genus *Hordeum*: A study using image analytic and numerical taxonomic techniques. Canadian Journal of Botany 65, 1563–1569.

Baunsgaard, L., Lütken, H., Mikkelsen, R., Glaring, M.A., Pham, T.T., and Blennow, A. (2005). A novel isoform of glucan, water dikinase phosphorylates pre-phosphorylated α-glucans and is involved in starch degradation in Arabidopsis. Plant Journal 41, 595–605.

Beck, E., and Ziegler, P. (1989). Biosynthesis and degradation of starch in higher plants. Annual Review of Plant Physiology and Plant Molecular Biology 40, 95–117.

Bertoft, E. (2004). On the nature of categories of chains in amylopectin and their connection to the super helix model. Carbohydrate Polymers 57, 211–224.

Bertoft, E., Piyachomkwan, K., Chatakanonda, P., and Sriroth, K. (2008). Internal unit chain composition in amylopectins. Carbohydrate Polymers 74, 527–543.

Bertoft, E., Laohaphatanalert, K., Piyachomkwan, K., and Sriroth, K. (2010). The fine structure of cassava starch amylopectin. Part 2: building block structure of clusters. International Journal of Biological Macromolecules 47, 325–335.

Bertoft, E., Källman, A., Koch, K., Andersson, R., and Åman, P. (2011). The building block structure of barley amylopectin. International Journal of Biological Macromolecules 49, 900–909.

Bertoft, E. (2017). Understanding starch structure: Recent progress. Agronomy 7, 1-29.

Bhandari, P.N., and Singhal, R.S. (2002). Effect of succinylation on the corn and amaranth starch pastes. Carbohydrate Polymers 48, 233–240.

Bi, L., Yang, L., Bhunia, A.K., and Yao, Y. (2011a). Carbohydrate nanoparticle-mediated colloidal assembly for prolonged efficacy of bacteriocin against food pathogen. Biotechnology and Bioengineering 108, 1529–1536.

Bi, L., Yang, L., Narsimhan, G., Bhunia, A.K., and Yao, Y. (2011b). Designing carbohydrate nanoparticles for prolonged efficacy of antimicrobial peptide. Journal of Controlled Release 150, 150–156.

Binderup, K., and Preiss, J. (1998). Glutamate-459 is important for *Escherichia coli* branching enzyme activity. Biochemistry 37, 9033–9037.

Binderup, K., Mikkelsen, R., and Preiss, J. (2002). Truncation of the amino terminus of branching enzyme changes its chain transfer pattern. Archives of Biochemistry and Biophysics 397, 279–285.

Blennow, A., Engelsen, S.B., Nielsen, T.H., Baunsgaard, L., and Mikkelsen, R. (2002). Starch phosphorylation: A new front line in starch research. Trends in Plant Science 7, 445–450.

Blennow, A., Jensen, S.L., Shaik, S.S., Skryhan, K., Carciofi, M., Holm, P.B., Hebelstrup, K.H., and Tanackovic, V. (2013). Future cereal starch bioengineering: Cereal ancestors encounter gene technology and designer enzymes. Cereal Chemistry 90, 274–287.

Borovsky, D., Smith, E.E., and Whelan, W.J. (1975). Temperature-dependence of the action of Q-enzyme and the nature of the substrate for Q-enzyme. FEBS Letters 54, 201–205.

Borovsky, D., Smith, E.E., and Whelan, W.J. (1976). On the mechanism of amylose branching by potato Q-enzyme. European Journal of Biochemistry 62, 307–312.

Bourne, E.J., Macey, A., and Peat, S. (1945). The enzymatic synthesis and degradation of starch. Part II. The amylolytic function of the Q-enzyme of the potato. Journal of the Chemical Society 0, 882–888.

Boyer, C.D., and Preiss, J. (1978). Multiple forms of (1-4)-α-D-glucan, (1-4)-α-D-glucan-6-glycosyl transferase from developing *Zea mays* L. kernels. Carbohydrate Research 61, 321–334.

Bradford, M.M. (1976). A rapid and sensitive method for the quantitation of microgram quantities of protein utilizing the principle of protein-dye binding. Analytical Biochemistry 72, 248–254.

BRENDA (2016). BRENDA: The Comprehensive Enzyme Information System. Retrieved from https://www.brenda-enzymes.org/ in Fall, 2016.

Brumm, P.J. (1997). Process for the non-random cleavage of starch and the low D.E. starch conversion products produced thereby (United States of America patent number US5612202 A).

Buchner, J., Pastan, I., and Brinkmann, U. (1992). A method for increasing the yield of properly folded recombinant fusion proteins: Single-chain immunotoxins from renaturation of bacterial inclusion bodies. Analytical Biochemistry 205, 263–270.

Buisson, G., Duée, E., Haser, R., and Payan, F. (1987). Three dimensional structure of porcine pancreatic α-amylase at 2.9 Å resolution. Role of calcium in structure and activity. The EMBO Journal 6, 3909–3916.

Buléon, A., Colonna, P., Planchot, V., and Ball, S.G. (1998). Starch granules: Structure and biosynthesis. International Journal of Biological Macromolecules 23, 85–112.

Burrell, M. (2012). Industrial use of starch. In Starch: Origins, Structure and Metabolism, I. J. Tetlow, ed. (London, United Kingdom, Society for Experimental Biology), pp. 375–388.

Burrell, M.M. (2003). Starch: The need for improved quality or quantity - An overview. Journal of Experimental Botany 54, 451–456.

Burton, R.A., Jenner, H., Carrangis, L., Fahy, B., Fincher, G.B., Hylton, C., Laurie, D.A., Parker, M., Waite, D., van Wegen, S., Verhoeven, T., Denyer, K. (2002). Starch granule initiation and growth are altered in barley mutants that lack isoamylase activity. The Plant Journal 31, 97–112.

Chaen, K., Noguchi, J., Omori, T., Kakuta, Y., and Kimura, M. (2012). Crystal structure of the rice branching enzyme I (BEI) in complex with maltopentaose. Biochemical and Biophysical Research Communications 424, 508–511.

Charoenkul, N., Uttapap, D., Pathipanawat, W., and Takeda, Y. (2006). Simultaneous determination of amylose content & unit chain distribution of amylopectins of cassava starches by fluorescent labeling/HPSEC. Carbohydrate Polymers 65, 102–108.

Chen, K., and Arnold, F.H. (1993). Tuning the activity of an enzyme for unusual environments: Sequential random mutagenesis of subtilisin E for catalysis in dimethylformamide. Proceedings of the National Academy of Sciences 90, 5618–5622.

Chen, J., Liu, Y., Wang, Y., Ding, H., and Su, Z. (2008). Different effects of L-arginine on protein refolding: Suppressing aggregates of hydrophobic interaction, not covalent binding. Biotechnology Progress 24, 1365–1372.

Chong, S., Shao, Y., Paulus, H., Benner, J., Perler, F.B., and Xu, M. (1996). Protein splicing involving the *Saccharomyces cerevisiae* VMA intein. The Journal of Biological Chemistry 271, 22159–22168.

Chong, S., Mersha, F.B., Comb, D.G., Scott, M.E., Landry, D., Vence, L.M., Perler, F.B., Benner, J., Kucera, R.B., Hirvonen, C.A., Pelletier, J.J., Paulus, H., Xu, M. (1997). Single-column purification of free recombinant proteins using a self-cleavable affinity tag derived from a protein splicing element. Gene 192, 271–281.

Colleoni, C., Dauvillée, D., Mouille, G., Morell, M., Samuel, M., Slomiany, M.C., Liénard, L., Wattebled, F., D'Hulst, C., and Ball, S. (1999). Biochemical characterization of the *Chlamydomonas reinhardtii* α-1,4 glucanotransferase supports a direct function in amylopectin biosynthesis. Plant Physiology 120, 1005–1014.

Colonna, P., Doublier, J.L., Melcioin, J.P., Mondredon, F., and Mercier, C. (1984). Extrusion cooking and drum drying of wheat starch. I. Physical and macromolecular modifications. Cereal Chemistry 61, 538–543.

Copeland, L., Blazek, J., Salman, H., and Tang, M.C. (2009). Form and functionality of starch. Food Hydrocolloids 23, 1527–1534.

Dang, P.L., and Boyer, C.D. (1988). Maize leaf and kernel starch synthases and starch branching enzymes. Phytochemistry 27, 1255–1259.

Delatte, T., Trevisan, M., Parker, M.L., and Zeeman, S.C. (2005). Arabidopsis mutants *Atisa1* and *Atisa2* have identical phenotypes and lack the same multimeric isoamylase, which influences the branch point distribution of amylopectin during starch synthesis. The Plant Journal 41, 815–830.

Denyer, K., Sidebottom, C., Hylton, C.M., and Smith, A.M. (1993). Soluble isoforms of starch synthase and starch-branching enzyme also occur within starch granules in developing pea embryos. Plant Journal 4, 191–198.

Doublier, J.L., Colonna, P., and Mercier, C. (1986). Extrusion cooking and drum drying of wheat starch. II. Rheological characterization of starch pastes. Cereal Chemistry 63, 240–246.

Dubois, M., Gilles, K., Hamilton, J.K., Rebers, P.A., and Smith, F. (1951). A colorimetric method for determination of sugars. Nature 168, 167.

El-Sheikh, M.A., Ramadan, M.A., and El-Shafie, A. (2009). Photo oxidation of rice starch II. Using a water soluble photo initiator. Carbohydrate Polymers 78, 235–239.

EMBL-EBI (2016). Clustal Omega. Retrieved from http://www.ebi.ac.uk/Tools/msa/clustalo/ in Fall, 2016.

Fan, Q., Xie, Z., Zhan, J., Chen, H., and Tian, Y. (2016). A glycogen branching enzyme from *Thermomonospora curvata*: Characterization and its action on maize starch. Starch/Stärke 68, 355–364.

Farkass, I., Hardy, T.A., Goebl, M.G., and Roach, P.J. (1991). Two glycogen synthase isoforms in *Saccharomyces cerevisiae* are coded by distinct genes that are differentially controlled. The Journal of Biological Chemistry 266, 15602–15607.

Feng, L., Fawaz, R., Hovde, S., Gilbert, L., Choi, J., and Geiger, J.H. (2015). Crystal Structures of *Escherichia coli* branching enzyme in complex with linear oligosaccharides. Biochemistry 54, 6207–6218.

Feng, L., Fawaz, R., Hovde, S., Sheng, F., Nosrati, M., and Geiger, J.H. (2016). Crystal structures of *Escherichia coli* branching enzyme in complex with cyclodextrins. Acta Crystallographica 72, 641–647.

Fiser, A., Do, R.K., and Sali, A. (2000). Modeling of loops in protein structures, Protein Science 9, 1753-1773.

Flach, B., Bendz, K., Krautgartner, R., Lieberz, S., and Smith, M.E. (2013). EU-27 Biofuels Annual. EU Biofuels Annual 2013. GAIN report number NL3034. Washington, D.C.: United States Department of Agriculture.

Forsyth, J.L., Ring, S.G., Noel, T.R., Parker, R., Cairns, P., Findlay, K., and Shewry, P.R. (2002). Characterization of starch from tubers of yam bean (*Pachyrhizus ahipa*). Journal of Agricultural and Food Chemistry 50, 361–367.

François, J., and Parrou, J.L. (2001). Reserve carbohydrates metabolism in the yeast *Saccharomyces cerevisiae*. FEMS Microbiology Reviews 25, 125–145.

Funane, K., Libessart, N., Stewart, D., Michishita, T., and Preiss, J. (1998). Analysis of essential histidine residues of maize branching enzymes by chemical modification and site-directed mutagenesis. Journal of Protein Chemistry 17, 579–590.

Gallant, D.J., Bouchet, B., and Baldwin, P.M. (1997). Microscopy of starch: Evidence of a new level of granule organization. Carbohydrate Polymers 32, 177–191.

Ghosh, H.P., and Preiss, J. (1966). Adenosine diphosphate glucose pyrophosphorylase. The Journal of Biological Chemistry 241, 4491–4504.

Gidley, M.J. (1985). Quantification of the structural features of starch polysaccharides by N.M.R. spectroscopy. Carbohydrate Research 139, 85–93.

Gidley, M.J., and Bulpin, P.V. (1987). Crystallisation of malto-oligosaccharides as models of the crystalline forms of starch: Minimum chain-length requirement for the formation of double helices. Carbohydrate Research 161, 291–300.

Guan, H.P., and Preiss, J. (1993). Differentiation of the properties of the branching isozymes from maize (*Zea mays*). Plant Physiology 102, 1269–1273.

Guan, H., Li, P., Imparl-Radosevich, J., Preiss, J., and Keeling, P. (1997). Comparing the properties of *Escherichia coli* branching enzyme and maize branching enzyme. Archives of Biochemistry and Biophysics 342, 92–98.

Hajji, F. (2011). Engineering renewable cellulosic thermoplastics. Reviews in Environmental Science and Biotechnology 10, 25–30.

Hamada, S., Ito, H., Ueno, H., Takeda, Y., and Matsui, H. (2007). The N-terminal region of the starch-branching enzyme from *Phaseolus vulgaris* L. is essential for optimal catalysis and structural stability. Phytochemistry 68, 1367–1375.

Han, J., and Lim, S. (2004a). Structural changes in corn starches during alkaline dissolution by vortexing. Carbohydrate Polymers 55, 193–199.

Han, J., and Lim, S. (2004b). Structural changes of corn starches by heating and stirring in DMSO measured by SEC-MALLS-RI system. Carbohydrate Polymers 55, 265–272.

Han, J., BeMiller, J.N., Hamaker, B., and Lim, S.T. (2003). Structural changes of debranched corn starch by aqueous heating and stirring. Cereal Chemistry 80, 323–328.

Hanes, C.S. (1937). The action of amylases in relation to the structure of starch and its metabolism in the plant. Parts I-III. The New Phytologist 36, 101–141.

Hansen, M.R., Blennow, A., Pedersen, S., Nørgaard, L., and Engelsen, S.B. (2008). Gel texture and chain structure of amylomaltase-modified starches compared to gelatin. Food Hydrocolloids 22, 1551–1566.

Henrissat, B. (1991). A classification of glycosyl hydrolases based on amino acid sequence similarities. Biochemical Journal 280, 309–316.

Henrissat, B., and Bairoch, A. (1996). Updating the sequence-based classification of glycosyl hydrolases. Biochemical Journal Letters 316, 695–696.

Hermes, J.D., Blacklow, S.C., and Knowles, J.R. (1990). Searching sequence space by definably random mutagenesis: Improving the catalytic potency of an enzyme. Proceedings of the National Academy of Sciences of the United States of America 87, 696–700.

Hizukuri, S. (1986). Polymodal distribution of the chain lengths of amylopectins, and its significance. Carbohydrate Research 147, 342–347.

Hizukuri, S., Tabata, S., and Nikuni, Z. (1970). Studies on starch phosphate. Part 1. Estimation of glucose-6-phosphate residues in starch and the presence of other bound phosphate(s). Die Stärke 22, 338–343.

Hizukuri, S., Takeda, Y., and Yasuda, H. (1981). Multi-branched nature of amylose and the action of de-branching enzymes. Carbohydrate Research 94, 205–213.

Hofreiter, B.T., Smiley, K.L., and Boundy, J.A. (1978). Preparation of retrogradation-resistant starches with immobilized amylases (United States of America patent number US 4121974 A).

Hong, S., Preiss, J. (2000). Localization of C-terminal domains required for the maximal activity or for determining substrate preference of maize branching enzymes. Archives of Biochemistry and Biophysics 378, 349-355.

Hovenkamp-Hermelink, J.H.M., Jacobsen, E., Ponstein, A.S., Visser, R.G.F., Vos-Scheperkeuter, G.H., Bijmolt, E.W., de Vries, J.N., Witholt, B., and Feenstra, W.J. (1987). Isolation of an amylose-free starch mutant of the potato (*Solanum tuberosum* L.). Theoretical and Applied Genetics 75, 217–221.

Imamura, H., Fushinobu, S., Jeon, B., Wakagi, T., and Matsuzawa, H. (2001). Identification of the catalytic residue of *Thermococcus litoralis* 4-α-glucanotransferase through mechanism-based labeling. Biochemistry 40, 12400–12406.

Imamura, H., Fushinobu, S., Yamamoto, M., Kumasaka, T., Jeon, B., Wakagi, T., and Matsuzawa, H. (2003). Crystal structures of 4-α-glucanotransferase from *Thermococcus litoralis* and its complex with an inhibitor. The Journal of Biological Chemistry 278, 19378–19386.

Ito, H., Hamada, S., Isono, N., Yoshizaki, T., Ueno, H., Yoshimoto, Y., Takeda, Y., and Matsui, H. (2004). Functional characteristics of C-terminal regions of starch-branching enzymes from developing seeds of kidney bean (*Phaseolus vulgaris* L.). Plant Science 166, 1149–1158.

James, M.G., Robertson, D.S., and Myers, A.M. (1995). Characterization of the maize gene *sugary1*, a determinant of starch composition in kernels. The Plant Cell 7, 417–429.

Jane, J. (2009). Structural Features of Starch Granules II. In Starch Chemistry and Technology, J. BeMiller and R. Whistler, ed. (Oxford, United Kingdom: Academic Press), pp. 193–236.

Jane, J., Kasemsuwan, T., Leas, S., Zobel, H., and Robyt, J.F. (1994). Anthology of starch granule morphology by scanning electron microscopy. Stach/Stärke 46, 121–129.

Janeček, Š. (1994). Parallel β/α-barrels of α-amylase, cyclodextrin glycosyltransferase and oligo-1,6-glucosidase *versus* the barrel of β-amylase: Evolutionary distance is a reflection of unrelated sequences. FEBS Letters 353, 119–123.

Jenkins, P.J., Cameron, R.E., and Donald, A.M. (1993). A universal feature in the structure of starch granules from different botanical sources. Starch/Stärke 45, 417–420.

Jensen, S.L., Larsen, F.H., Bandsholm, O., and Blennow, A. (2013). Stabilization of semi-solid-state starch by branching enzyme-assisted chain-transfer catalysis at extreme substrate concentration. Biochemical Engineering Journal 72, 1–10.

Jia, Y., Fei, J., Cui, Y., Yang, Y., Gao, L., and Li, J. (2011). pH-responsive polysaccharide microcapsules through covalent bonding assembly. Chemical Communications 47, 1175–1177.

Jobling, S. (2004). Improving starch for food and industrial applications. Current Opinion in Plant Biology 7, 210–218.

John, M., Schmidt, J., and Kneifel, H. (1983). Iodine-matlosaccharide complexes: Relation between chain-length and colour. Carbohydrate Research 119, 254–257.

Jyothi, A.N., Sajeev, M.S., and Sreekumar, J.N. (2010). Hydrothermal modifications of tropical tuber starches. 1. Effect of heat-moisture treatment on the physicochemical, rheological and gelatinization characteristics. Starch/Stärke 62, 28–40.

Katsuya, Y., Mezaki, Y., Kubota, M., and Matuura, Y. (1998). Three-dimensional structure of *Pseudomonas* isoamylase at 2.2 Å Resolution. Journal of Molecular Biology 281, 885–897.

Kaufman, R.C., Wilson, J.D., Bean, S.R., Herald, T.J., and Shi, Y. (2015). Development of a 96-well plate iodine binding assay for amylose content determination. Carbohydrate Polymers 115, 444–447.

Kim, E., Ryu, S., Bae, H., Huong, N.T., and Lee, S. (2008). Biochemical characterisation of a glycogen branching enzyme from *Streptococcus mutans*: Enzymatic modification of starch. Food Chemistry 110, 979–984.

Koay, A., Rimmer, K.A., Mertens, H.D.T., Gooley, P.R., and Stapleton, D. (2007). Oligosaccharide recognition and binding to the carbohydrate binding module of AMP-activated protein kinase. FEBS Letters 581, 5055–5059.

Komulainen, S., Verlackt, C., Pursiainen, J., and Lajunen, M. (2013). Oxidation and degradation of native wheat starch by acidic bromate in water at room temperature. Carbohydrate Polymers 93, 73–80.

Korma, S.A., Kamal-Alahmad, Niazi, S., Ammar, A., Zaaboul, F., and Zhang, T. (2016). Chemically modified starch and utilization in food stuffs. International Journal of Nutrition and Food Sciences 5, 264–272.

Krojer, T., Froese, D.S., Goubin, S., Strain-Damerelle, C., Mahajan, P., Burgess-Brown, N., von Delft, F., Arrowsmith, C.H., Edwards, A., and Yue, W. Crystal structure of human glycogen branching enzyme (GBE1) in complex with acarbose - to be published.

Kümmerer, K., Menz, J., Schubert, T., and Thielemans, W. (2011). Biodegradability of organic nanoparticles in the aqueous environment. Chemosphere 82, 1387–1392.

Kuriki, T., Takata, H., Okada, S., and Imanaka, T. (1991). Analysis of the active center of *Bacillus stearothermophilus* neopullulanase. Journal of Bacteriology 173, 6147–6152.

Kuriki, T., Guan, H., Sivak, M., and Preiss, J. (1996). Analysis of the active center of branching enzyme II from maize endosperm. Journal of Protein Chemistry 15, 305–313.

Kuriki, T., Stewart, D.C., Preiss, J (1997). Construction of chimeric enzymes out of maize endosperm branching enzymes I and II: Activity and properties. The Journal of Biological Chemistry 272: 28999-29004.

Laemmli, U.K. (1970). Cleavage of structural proteins during the assembly of the head of bacteriophage T4. Nature 227, 680–685.

Lampitt, L.H., Fuller, C.H.F., and Goldenburg, N. (1948). The fractionation of potato starch. Part V. The phosphorus of potato starch. Journal of the Society of Chemical Industry 67, 121–125.

Langer, L.J., and Engel, L.L. (1958). Human placental estradiol-17β dehydrogenase. Journal of Biological Chemistry 233, 583–588.

Langer Instruments (2016). Low Flow Rate Peristaltic Pump. Retrieved from www.langerinstruments.com/lowflowrateperistalticpump-p-2.html in Summer, 2016.

Lawal, O.S. (2004). Succinyl and acetyl starch derivatives of a hybrid maize: Physicochemical characteristics and retrogradation properties monitored by differential scanning calorimetry. Carbohydrate Research 339, 2673–2682.

Le, Q., Lee, C., Kim, Y., Lee, S., Zhang, R., Withers, S.G., Kim, Y., Auh, J., and Park, K. (2009). Amylolytically-resistant tapioca starch modified by combined treatment of branching enzyme and maltogenic amylase. Carbohydrate Polymers 75, 9–14.

Leloir, L.F., Olavarria, J.M., and Carminatti, H. (1959). Biosynthesis of glycogen from uridine diphosphate glucose. Archives of Biochemistry and Biophysics 81, 508–520.

Leloir, L.F., De Fekete, M.A.R., and Cardini, C.E. (1961). Starch and oligosaccharide synthesis from uridine diphosphate glucose. The Journal of Biological Chemistry 236, 636–641.

Lewicka, K., Siemion, P., and Kurcok, P. (2015). Chemical modifications of starch: Microwave effect. International Journal of Polymer Science 2015, 1–10.

Li, C., Wu, A.C., Go, R.M., Malouf, J., Turner, M.S., Malde, A.K., Mark, A.E., and Gilbert, R.G. (2015). The characterization of modified starch branching enzymes: Toward the control of starch chain-length distributions. Plos One 10, e0125507.

Li, W., Li, C., Gu, Z., Qiu, Y., Cheng, L., Hong, Y., Li, Z. (2016). Retrogradation behavior of corn starch treated with 1,4-α-glucan branching enzyme. Food Chemistry 203, 308-313.

Li, X., Miao, M., Jiang, H., Xue, J., Jiang, B., Zhang, T., Gao, Y., and Jia, Y. (2014). Partial branching enzyme treatment increases the low glycaemic property and α-1,6 branching ratio of maize starch. Food Chemistry 164, 502–509.

Liao, H., McKenzie, T., and Hageman, R. (1986). Isolation of a thermostable enzyme variant by cloning and selection in a thermophile. Proceedings of the National Academy of Sciences of the United States of America 83, 576–580.

Libessart, N., and Preiss, J. (1998). Arginine residue 384 at the catalytic center is important for branching enzyme II from maize endosperm. Archives of Biochemistry and Biophysics 360, 135–141.

Lim, S., Kasemuwan, T., and Jane, J. (1994). Characterization of phosphorus in starch by ^{31}P-nuclear magnetic resonance spectroscopy. Cereal Chemistry 71, 488–492.

Liu, Y., Li, C., Gu, Z., Xin, C., Cheng, L., Hong, Y., and Li, Z. (2017). Alanine 310 is important for the activity of 1,4-α-glucan branching enzyme from *Geobacillus thermoglucosidans* STB02. International Journal of Biological Macromolecules 97, 156–163.

London, E., and Khorana, H.G. (1982). Denaturation and renaturation of bacteriorhodopsin in detergents and lipid-detergent mixtures. The Journal of Biological Chemistry 257, 7003–7011.

Lorberth, R., Ritte, G., Willmitzer, L., and Kossmann, J. (1998). Inhibition of a starch-granule-bound protein leads to modified starch and repression of cold sweetening. Nature 16, 473–477.

van der Maarel, M.J.E.C., van der Veen, B., Uitdehaag, J.C.M., Leemhuis, H., and Dijkhuizen, L. (2002). Properties and applications of starch-converting enzymes of the α-amylase family. Journal of Biotechnology 94, 137–155.

van der Maarel, M.J.E.C., Vos, A., Sanders, P., and Dijkhuizen, L. (2003). Properties of the glucan branching enzyme of the hyperthermophilic bacterium *Aquifex aeolicus*. Biocatalysis and Biotransformation 21, 199–207.

van der Maarel, M.J.E.C., Capron, I., Euverink, G., Bos, H.T., Kaper, T., Binnema, D.J., and Steeneken, P.A.M. (2005). A novel thermoreversible gelling product made by enzymatic modification of starch. Starch/Stärke 57, 465–472.

MacGregor, E.A., Janeček, Š., and Svensson, B. (2001). Relationship of sequence and structure to specificity in the α-amylase family of enzymes. Biochimica et Biophysica Acta 1546, 1–20.

Maeda, Y., Koga, H., Yamada, H., Ueda, T., and Imoto, T. (1995). Effective renaturation of reduced lysozyme by gentle removal of urea. Protein Engineering 8, 201–205.

Malmsjo, M., Thordarson, E., Apell, S.P., and Fyhr, P. (2012). Microspheres of hydrolysed starch with endogenous, charged ligands (United States of America patent number US 2012/0244198 A1).

Malvern Instruments Limited (2013). Static Light Scattering Technologies For GPC/SEC Explained: Inform White Paper. Worcestershire, United Kingdom: Malvern Instruments Limited.

Manners, D.J. (1989). Recent developments in our understanding of amylopectin structure. Carbohydrate Polymers 11, 87–112.

Marston, F.A. (1986). The purification of eukaryotic polypeptides synthesized in *Escherichia coli*. Biochemical Journal 240, 1–12.

Marti-Renom, M.A., Stuart, A., Fiser, A., Sánchez, R., Melo, F. Sali, A. (2000). Comparative protein structure modeling of genes and genomes. Annual Review of Biophysics and Biomolecular Structure 29, 291-325.

Martin, C., and Smith, A.M. (1995). Starch biosynthesis. The Plant Cell 7, 971–985.

Mathupala, S.P., Lowe, S.E., Podkovyrov, S.M., and Zeikus, J.G. (1993). Sequencing of the amylopullulanase (*apu*) gene of *Thermoanaerobacter ethanolicus* 39E, and identification of the active site by site-directed mutagenesis. Journal of Biological Chemistry 268, 16332–16344.

Matsui, I., Yondeda, S., Ishikawa, K., Miyairi, S., Fukui, S., Umeyama, H., and Honda, K. (1994). Roles of the aromatic residues conserved in the active center of *Saccharomycopsis* α-amylase for transglycosylation and hydrolysis activity. Biochemistry 33, 451–458.

Matsumoto, A., Nakajima, T., and Matsuda, K. (1990). A kinetic study of the interaction between glycogen and *Neurospora crassa* branching enzyme. Journal of Biochemistry 107, 123–126.

Matsuura, Y., Kusunoki, M., Harada, W., and Kakudo, M. (1984). Structure and possible catalytic residues of Taka-amylase A. Journal of Biochemistry 95, 697–702.

Matsuzaki, M., Yamaguchi, Y., Masui, H., and Satoh, T. (1996). Stabilization by GroEL, a molecular chaperone, and a periplasmic fraction, as well as refolding in the presence of dithiothreitol, of acid-unfolded dimethyl sulfoxide reductase, a periplasmic protein of *Rhodobacter sphaeroides* f. sp. *denitrificans*. Plant Cell Physiology 37, 333–339.

Matulis, D., Kranz, J.K., Salemme, F.R., and Todd, M.J. (2005). Thermodynamic stability of carbonic anhydrase: Measurements of binding affinity and stoichiometry using ThermoFluor. Biochemistry 44, 5258–5266.

Mikkelsen, R., Binderup, K., and Preiss, J. (2001). Tyrosine residue 300 is important for activity and stability of branching enzyme from *Escherichia coli*. Archives of Biochemistry and Biophysics 385, 372–377.

Molecular Kinetics Incorporation (2003). PONDR Predictor of Natural Disordered Regions. Retrieved from http://www.pondr.com/ on 2016-11-01.

Mosi, R., He, S., Uitdehaag, J., Dijkstra, B.W., and Withers, S.G. (1997). Trapping and characterization of the reaction intermediate in cyclodextrin glycosyltransferase by use of activated substrates and a mutant enzyme. Biochemistry 36, 9927–9934.

Mouille, G., Maddelein, M., Libessart, N., Talaga, P., Decq, A., Delrue, B., and Ball, S.G. (1996). Preamylopectin processing: A mandatory step for starch biosynthesis in plants. The Plant Cell 8, 1353–1366.

Muhamedbegović, B., Šubarić, D., Babić, J., Ačkar, Đ., Jašić, M., Keran, H., Budimlić, A., and Matas, I. (2012). Modification of potato starch. Technologica Acta 5, 1–6.

Murakami, T., Kanai, T., Takata, H., Kuriki, T., and Imanaka, T. (2006). A novel branching enzyme of the GH-57 family in the hyperthermophilic archaeon *Thermococcus kodakaraensis* KOD1. Journal of Bacteriology 188, 5915–5924.

Nagashima, T., Tada, S., Kitamota, K., Gomi, K., Kumagai, C., and Toda, H. (1992). Site-directed mutagenesis of catalytic active-site residues of Taka-amylase A. Bioscience, Biotechnology, and Biochemistry 56, 207–210.

Nakajima, R., Imanaka, T., and Aiba, S. (1986). Comparison of amino acid sequences of eleven different α-amylases. Applied Microbiology and Biotechnology 23, 355–360.

Nakamura, T., Vrinten, P., Hayakawa, K., and Ikeda, J. (1998). Characterization of a granule-bound starch synthase isoform found in the pericarp of wheat. Plant Physiology 118, 451–459.

Nasanovsky, L. (2017). Bacterial branching enzymes as agents for modifying glucan structure in industrial processing (doctoral dissertation). Retrieved from University of Guelph Atrium.

Neurath, H. (1943). The role of glycine in protein structure. Journal of the American Chemical Society 65, 2039–2041.

New England Biolabs (2017). Impact^{TM} Kit: Instruction Manual. Ipswich, Massachusetts: New England Biolabs.

Nichols, S.E. (2002). Glucan-containing compositions and paper (United States of America patent number US 6,465,203 B2).

Niemelä, K. (1990). Conversion of xylan, starch, and chitin into carboxylic acids by treatment with alkali. Carbohydrate Research 204, 37–49.

Niesen, F.H., Berglund, H., and Vedadi, M. (2007). The use of differential scanning fluorimetry to detect ligand interactions that promote protein stability. Nature Protocols 2, 2212–2221.

Noguchi, J., Chaen, K., Vu, N.T., Akasaka, T., Shimada, H., Nakashima, T., Nishi, A., Satoh, H., Omori, T., Kakuta, Y., Kimura, M. (2011). Crystal structure of the branching enzyme I (BEI) from *Oryza sativa* L. with implications for catalysis and substrate binding. Glycobiology 21, 1108–1116.

Ochubiojo, E.M., and Rodrigues, A. (2012). Starch: From food to medicine. In Scientic, Health and Social Aspects of the Food Industry. B. Valdez, ed. (Rijeka, Croatia: InTech Europe), pp. 355–380.

Oh, E.J., Choi, S.J., Lee, S.L., Kim, C.H., and Moon, T.W. (2008). Modification of granular corn starch with 4-α-glucanotransferase from *Thermotoga maritima*: Effects on structural and physical properties. Journal of Food Science 73, C158–C166.

Okazaki, N., Tamada, T., Feese, M.D., Kato, M., Miura, Y., Komeda, T., Kobayashi, K., Kondo, K., Blaber, M., and Kuroki, R. (2012). Substrate recognition mechanism of a glycosyltrehalose trehalohydrolase from *Sulfolobus solfataricus* KM1. Protein Science 21, 539–552.

Olayinka, O.O., Olu-Owolabi, B.I., and Adebowale, K.O. (2011). Effect of succinylation on the physicochemical, rheological, thermal and retrogradation properties of red and white sorghum starches. Food Hydrocolloids 25, 515–520.

Otegbayo, B., Oguniyan, D., and Akinwumi, O. (2014). Physicochemical and functional characterization of yam starch for potential industrial applications. Starch/Stärke 66, 235–250.

Pal, K., Kumar, S., Sharma, S., Garg, S.K., Alam, M.S., Xu, H.E., Agrawal, P., and Swaminathan, K. (2010). Crystal structure of full-length *Mycobacterium tuberculosis* H37Rv glycogen branching enzyme: Insights of N-terminal β-sandwich in substrate specificity and enzymatic activity. Journal of Biological Chemistry 285, 20897–20903.

Palomo, M., Kralj, S., van der Maarel, M.J.E.C., and Dijkhuizen, L. (2009). The unique branching patterns of *Deinococcus* glycogen branching enzymes are determined by their N-terminal domains. Applied and Environmental Microbiology 75, 1355–1362.

Palomo, M., Pijning, T., Booiman, T., Dobruchowska, J.M., van der Vlist, J., Kralj, S., Planas, A., Loos, K., Kamerling, J.P., Dijkstra, B.W., van der Maarel, M.E.C., Dijkhuizen, L., Leemhuis, H. (2011). *Thermus thermophilus* glycoside gydrolase family 57 branching enzyme. Crystal structure, mechanism of action, and products formed. Journal of Biological Chemistry 286, 3520–3530.

Pan, D., and Nelson, O.E. (1984). A debranching enzyme deficiency in endosperms of the *sugary-1* mutants of maize. Plant Physiology 74, 324–328.

Park, J.T., and Johnson, M.J. (1949). A submicrodetermination of glucose. The Journal of Biological Chemistry 181, 149–151.

Park, S., Chung, O.K., and Seib, P.A. (2005). Effects of varying weight ratios of large and small wheat starch granules on experimental straight-dough bread. Cereal Chemistry 82, 166–172.

Pauley, E., Markland, F., Page, R., and Rooff, L. (2000). Improved enzyme thinned starches (Canada patent number WO2000012746 A1).

Peng, K., Radivojac, P., Vucetic, S., Dunker, A.K., Obradovic, Z. (2006). Length-dependent prediction of protein intrinsic disorder. BMC Bioinformatics 7, 208.

Pilling, E., and Smith, A.M. (2003). Growth ring formation in the starch granules of potato tubers. Plant Physiology 132, 365–371.

Recondo, E., and Leloir, L.F. (1961). Adenosine diphosphate glucose and starch synthesis. Biochemical and Biophysical Research Communications 6, 85–88.

Ritte, G., Lloyd, J.R., Eckermann, N., Rottmann, A., Kossmann, J., and Steup, M. (2002). The starch-related R1 protein is an α-glucan, water dikinase. Proceedings of the National Academy of Sciences 99, 7166–7171.

Roach, P.J., Depaoli-Roach, A.A., Hurley, T.D., and Tagliabracci, V.S. (2012). Glycogen and its metabolism: Some new developments and old themes. Biochemical Journal 441, 763–787.

Robin, J.P., Mercier, C., Charbonniere, R., and Guilbot, A. (1974). Lintnerized starches. Gel filtration and enzymatic studies of insoluble residues from prolonged acid treatment of potato starch. Cereal Chemistry 51, 389–406.

Rosano, G.L., and Ceccarelli, E.A. (2014). Recombinant protein expression in *Escherichia coli*: Advances and challenges. Frontiers in Microbiology 5, 1–17.

Royal Society of Chemistry (2015). ChemSpider. Retrieved from http://www.chemspider.com/ on 2017-09-01.

Rundle, R.E., and Baldwin, R.R. (1943). The configuration of starch and the starch-iodine complex. I. The dichroism of flow of starch-iodine solutions. Journal of the American Chemical Society 65, 554–558.

Rundle, R.E., and French, D. (1943). The configuration of starch in the starch-iodine complex. 111. X-ray diffraction studies of the starch-iodine complex. Journal of the American Chemical Society 65, 1707–1710.

Sali, A., and Blundell T.L. (1993). Comparative protein modelling by satisfaction of spatial restraints. Journal of Molecular Biology 234, 779-815.

Sarko, A., and Wu, H.H. (1978). The crystal structures of A-, B- and C-polymorphs of amylose and starch. Starch/Stärke 30, 73–78.

Schoch, T.J. (1942). Fractionation of starch by selective precipitation with butanol. Journal of the American Chemical Society 64, 2957–2961.

Schrödinger (2016). The PyMOL Molecular Graphics System, Version 1.8. Retrieved from https://pymol.org/2/ in 2016.

Shinohara, M.L., Ihara, M., Abo, M., Hashida, M., Takagi, S., and Beck, T.C. (2001). A novel thermostable branching enzyme from an extremely thermophilic bacterial species, *Rhodothermus obamensis*. Applied Microbiology and Biotechnology 57, 653–659.

Shure, M., Wessler, S., and Fedoroff, N. (1983). Molecular identification and isolation of the *Waxy* locus in maize. Cell 35, 225–233.

Singh, N., and Kaur, L. (2004). Morphological, thermal, rheological and retrogradation properties of potato starch fractions varying in granule size. Journal of the Science of Food and Agriculture 84, 1241–1252.

Skuratowicz, R., Rice, M., Stubberfield, A., and Strong, P. (2009). Method for producing high molecular weight reduced viscosity starch pastes (United States of America patent number US 20090142812 A1).

Sodhi, N.S., and Singh, N. (2005). Characteristics of acetylated starches prepared using starches separated from different rice cultivars. Journal of Food Engineering 70, 117–127.

Soh, H.N., Sissons, M.J., and Turner, M.A. (2006). Effect of starch granule size distribution and elevated amylose content on dorum dough rheology and spaghetti cooking quality. Cereal Chemistry 83, 513–519.

Soni, P.L., Sharma, H., Srivastava, H.C., and Gharia, M.M. (1990). Physicochemical properties of *Canna edulis* starch - comparison with maize starch. Starch/Stärke 42, 460–464.

Stagner, J., Alves, V.D., Narayan, R., and Beleia, A. (2011). Thermoplasticization of high amylose starch by chemical modification using reactive extrusion. Journal of Polymers and the Environment 19, 589–597.

Svensson, B. (1988). Regional distant sequence homology between amylases, α-glucosidases and transglucanosylases. FEBS Letters 230, 72–76.

Swanson, M.A. (1948). Studies on the structure of polysaccharides. IV. Relation of the iodine colour to the structure. Journal of Biological Chemistry 172, 825–837.

Tabata, S., and Hizukuri, S. (1971). Studies on starch phosphate. Part 2. Isolation of glucose 3-phosphate and maltose phosphate by acid hydrolysis of potato starch. Die Stärke 23, 267–272.

Takahashi, R., and Ojima, T. (1969). Pregelatinization of wheat starch in a drum drier. Die Stärke 12, 318–321.

Takata, H., Kuriki, T., Okada, S., Takesada, Y., Iizuka, M., Minamiura, N., and Imanaka, T. (1992). Action of neopullulanase. Journal of Biological Chemistry 267, 18447–18452.

Takata, H., Ohdan, K., Takaha, T., Kuriki, T., and Okada, S. (2003). Properties of branching enzyme from hyperthermophilic bacterium, *Aquifex aeolicus*, and its potential for production of highly-branched cyclic dextrin. Journal of Applied Glycoscience 50, 15–20.

Takeda, Y., and Hizukuri, S. (1982). Location of phosphate groups in potato amylopectin. Carbohydrate Research 102, 321–327.

Takeda, Y., Hizukuri, S., and Juliano, B.O. (1987). Structures of rice amylopectins with low and high affinities for iodine. Carbohydrate Research 168, 79–88.

Takeda, Y., Guan, H., and Preiss, J. (1993). Branching of amylose by the branching isoenzymes of maize endosperm. Carbohydrate Research 240, 253–263.

Takeda, Y., Takeda, C., Mizukami, H., and Hanashiro, I. (1999). Structures of large, medium and small starch granules of barley grain. Carbohydrate Polymers 38, 109–114.

Takeo, K., and Nakamura, S. (1972). Dissociation constants of glucan phosphorylases of rabbit tissues studied by polyacrylamide disc electrophoresis. Archives of Biochemistry and Biophysics 153, 1–7.

Tetlow, I.J., Beisel, K.G., Cameron, S., Makhmoudova, A., Liu, F., Bresolin, N.S., Wait, R., Morell, M.K., and Emes, M.J. (2008). Analysis of protein complexes in wheat amyloplasts reveals functional interactions among starch biosynthetic enzymes. Plant Physiology 146, 1878–1891.

Tetlow, I.J., Emes, M.J. (2017). Starch Biosynthesis in the Developing Endosperms of Grasses and Cereals. Agronomy 7, 1-43.

Tharanathan, R.N. (2005). Starch - value addition by modification. Critical Reviews in Food Science and Nutrition 45, 371–384.

Trethewey, R.N., and Rees, T.A. (1994a). The role of the hexose transporter in the chloroplasts of *Arabidopsis thaliana* L. Planta 195, 168–174.

Trethewey, R.N., and Rees, T.A. (1994b). A mutant of *Arabidopsis thaliana* lacking the ability to transport glucose across the chloroplast envelope. The Biochemical Journal 301, 449–454.

U.S. Grains Council (2006). Value Enhanced Corn Report 2005/06. Washington, D.C.: United States Department of Agriculture.

Uitdehaag, J.C.M., Mosi, R., Kalk, K.H., van der Veen, B.A., Dijkhuizen, L., Withers, S.G., and Dijkstra, B.W. (1999). X-ray structures along the reaction pathway of cyclodextrin glycosyltransferase elucidate catalysis in the α-amylase family. Nature Structural Biology 6, 432–436.

Umetsu, M., Tsumoto, K., Hara, M., Ashish, K., Goda, S., Adschiri, T., and Kumagai, I. (2003). How additives influence the refolding of immunoglobulin-folded proteins in a stepwise dialysis system. The Journal of Biological Chemistry 278, 8979–8987.

Usui, T., Yokoyama, M., Yamaoka, N., Matuda, K., Tuzimura, K., Sugiyama, H., and Seto, S. (1974). Proton magentic resonance spectra of D-gluco-oligosaccharides and D-glucans. Carbohydrate Research 33, 105–116.

Utrilla-Coello, R.G., Agama-Acevedo, E., de la Rosa, A.P.B., Rodríguez-Ambriz, S.L., and Bello-Pérez, L.A. (2010). Physicochemical and enzyme characterization of small and large starch granules isolated from two maize cultivars. Cereal Chemistry 87, 50–56.

Utsumi, Y., Yoshida, M., Francisco, Jr., P.B., Sawada, T., Kitamura, S., and Nakamura, Y. (2009). Quantitative assay method for starch branching enzyme with bicinchoninic acid by measuring the reducing terminals of glucans. Journal of Applied Glycoscience 56, 215–222.

Vallejo, L.F., and Rinas, U. (2004a). Optimized procedure for renaturation of recombinant human bone morphogenetic protein-2 at high protein concentration. Biotechnology and Bioengineering 85, 601–609.

Vallejo, L.F., and Rinas, U. (2004b). Strategies for the recovery of active proteins through refolding of bacterial inclusion body proteins. Microbial Cell Factories 3, 1–12.

Vedadi, M., Niesen, F.H., Allali-Hassani, A., Fedorov, O.Y., Finerty, P.J.J., Wasney, G.A., Yeung, R., Arrowsmith, C., Ball, L.J., Berglund, H., Hui, R. Marsden, D., Nordlund, P., Sundstrom, M., Weigelt, J., Edwards, A.M. (2006). Chemical screening methods to identify ligands that promote protein stability, protein crystallization, and structure determination. Proceedings of the National Academy of Sciences of the United States of America 103, 15835–15840.

Vrinten, P.L., and Nakamura, T. (2000). Wheat granule-bound starch synthase I and II are encoded by separate genes that are expressed in different tissues. Plant Physiology 122, 255–263.

Vu, N.T., Shimada, H., Kakuta, Y., Nakashima, T., Ida, H., Omori, T., Nishi, A., Satoh, H., and Kimura, M. (2008). Biochemical and crystallographic characterization of the starch branching enzyme I (BEI) from *Oryza sativa* L. Bioscience, Biotechnology, and Biochemistry 72, 2858–2866.

Waduge, R.N., Xu, S., Bertoft, E., and Seetharaman, K. (2013). Exploring the surface morphology of developing wheat starch granules by using Atomic Force Microscopy. Starch /Stärke 65, 398–409.

Waffenschmidt, S., and Jaenicke, L. (1987). Assay of reducing sugars in the nanomole range with 2,2'-bicinchoninate. Analytical Biochemistry 165, 337–340.

Wang, Y., and Li, Y. (2014). Cultivation to improve *in vivo* solubility of overexpressed arginine deiminases in *Escherichia coli* and the enzyme characteristics. BMC Biotechnology 14, 1–10.

Wattebled, F., Dong, Y., Dumez, S., Delvalle, D., Planchot, V., Berbezy, P., Vyas, D., Colonna, P., Chatterjee, M., Ball, S.G., D'Hulst, C. (2005). Mutants of *Arabidopsis* lacking a chloroplastic isoamylase accumulate phytoglycogen and an abnormal form of amylopectin. Plant Physiology 138, 184–195.

Webb, B., and Sali, A. (2014). Comparative protein structure modeling using Modeller. Current Protocols in Bioinformatics, John Wiley & Sons, Inc. 5.6.1-5.6.32.

Webb, B., and Sali, A. (2016). Modeller. Retrieved from https://salilab.org/modeller/9.16/release.html on 2011-06-20.

Weir, M.P., and Sparks, J. (1987). Purification and renaturation of recombinant human interleukin-2. Biochemical Journal 245, 85–91.

Wong, K., Kubo, A., Jane, J., and Harada, K. (2003). Structures and properties of amylopectin and phytoglycogen in the endosperm of *sugary-1* mutants of rice. Journal of Cereal Science 37, 139–149.

Yadav, B.S., Guleria, P., and Yadav, R.B. (2013). Hydrothermal modification of Indian water chestnut starch: Influence of heat-moisture treatment and annealing on the physicochemical, gelatinization and pasting characteristics. Food Science and Technology 53, 211–217.

Yan, B.X., and Sun, Y.Q. (1997). Glycine residues provide flexibility for enzyme active sites. Journal of Biological Chemistry 272, 3190–3194.

Yoshii, H., Furuta, T., Yonehara, T., Ito, D., Linko, Y., and Linko, P. (2000). Refolding of denatured/reduced lysozyme at high concentration with diafiltration. Bioscience, Biotechnology, and Biochemistry 64, 1159–1165.

Yu, D., Xiao, S., Tong, C., Chen, L., and Liu, X. (2007). Dialdehyde starch nanoparticles: Preparation and application in drug carrier. Chinese Science Bulletin 52, 2913–2918.

Yu, T., Kofler, H., Häusler, R.E., Hille, D., Flügge, U., Zeeman, S.C., Smith, A.M., Kossmann, J., Lloyd, J., Ritte, G., Steup, M., Lue, W., Chen, J., Weber, A. (2001). The Arabidopsis *sex1* mutant is defective in the R1 protein, a general regulator of starch degradation in plants, and not in the chloroplast hexose transporter. Plant Cell 13, 1917–1918.

SUPPLEMENTAL MATERIAL

Table S1: Variations of protein expression from *Escherichia coli*.

Protein	Volume of overnight culture (mL)	Volume of expressed culture (mL)	Yield of recombinant protein (mg)
Intein-tagged DrGBE	40	2,000	12.5
His-tagged DrGBE	5	250	0.65-0.88
$TtGBE_{cat}$-$mSBEI_{COO-}$ and $TtGBE_{cat}$-$mSBEI_{NH2}$	6-10	100-600	0-0.21

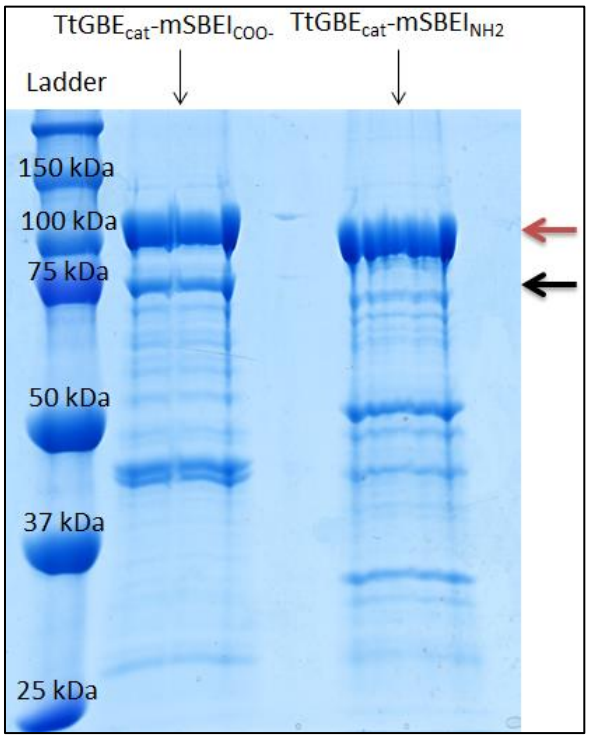

Figure S1: SDS-PAGE analysis of chimeric enzymes made using domains from *Thermus thermophilus* and *Zea mays* branching enzymes after protein refolding from inclusion bodies. The red arrow indicates the intein-tagged chimeric enzyme (~105 or 100 kDa for intein-tagged $TtGBE_{cat}$-$mSBEI_{COO-}$ and $TtGBE_{cat}$-$mSBEI_{NH2}$ respectively), and the black arrow indicates the tag-free chimeric enzyme (~77 or 72 kDa for $TtGBE_{cat}$-$mSBEI_{COO-}$ and $TtGBE_{cat}$-$mSBEI_{NH2}$ respectively). First lane: 5 µL Precision Plus Protein™ All Blue Standards protein ladder. Lanes 2 and 3: 20 µg of refolded protein.

Table S2: Variations of protein purification using chitin resin.

Protein	Chitin slurry per column (mL)	Protein sample loaded (mL)	Number of times chitin resin was agitated during wash step
DrGBE	12*	~50-70**	5-7
$TtGBE_{cat}$-$mSBEI_{COO-}$ and $TtGBE_{cat}$-$mSBEI_{NH2}$	4	~3-6**	1-3
Refolded $TtGBE_{cat}$-$mSBEI_{COO-}$ and $TtGBE_{cat}$-$mSBEI_{NH2}$	1.2-2	~0.2-5***	0 (unnecessary when using such little resin)

*Two columns used to purify DrGBE produced from 2 L of *E. coli* culture. Excess chitin resin was used to ensure enough chitin binding sites were present for nearly all DrGBE-intein tag fusions, as the amount of DrGBE within the soluble fraction was unknown at the time.
**Loaded with an approximately equal volume of column buffer.
***Loaded with ~5 mL of column buffer.

Table S3: Variations of SDS-PAGE analysis.

Sample	Preparation of SDS-PAGE samples			Volume of SDS-PAGE samples loaded onto gel (µL)
	Volume sample (µL)	Volume water (µL)	Volume Laemmli loading buffer (µL)	
Pre-induction control (lysate of *E. coli* cells before expressing recombinant protein)	Cell pellet from 1 mL *E. coli* culture	100-150	25-40	38-40
		50	10	20
Soluble fraction (before purification)	~5-15	~3-10	~2.5-7	~12-32
Inclusion bodies (before refolding)	5	150	40	40
Inclusion bodies (after refolding) (unknown protein content)	16-50	0-14	8-10	~19-60
Flow-through	4-50	3-30	2.5-10	12.5-60
Chitin or Ni-NTA resin	100	0	25	35-50
Eluate (~5-10 µg protein*)	~1-50	~0-30	~5-10	~10-60

*Or undetectable protein content for chimeric enzymes purified from refolded inclusion bodies

Table S4: PCR reagents used for site-directed mutagenesis.

Mutation	Concentration of reagents* in 20 µL of PCR reaction						
	Buffer	$MgCl_2$ (mM)	dNTPs (µM)	DMSO (v/v)	Polymerase (U/µL)	DNA** (ng/µL)	Forward and reverse primer (µM)
Q205H	1X	1	200	3.34%	0.0163	3.5-10	0.125
A310Q				0	0.0100	1.4-4	0.3
A310G							
A312T							

*Reagents from iProof™ High-Fidelity DNA Polymerase kit (Cat# 172-5301) and primers from University of Guelph Lab Services.
**DNA concentrations found using the Thermo Scientific NanoDrop 2000C Spectrophotometer.

Table S5: PCR temperatures used for site-directed mutagenesis.

Mutation	Temperature : time for each step*					
	Step 1	Step 2	Step 3	Step 4	Step 5	Step 6
Q205H	98°C : 30s	98°C : 15s	50°C : 30s	72°C : 6 min	Repeat steps 2-4 20 times	72°C : 10 min
A310Q			45°C : 30s	72°C : 10 min		72°C : 15 min
A310G						
A312T				72°C : 6 min		72°C : 10 min

*Temperature controlled using the PTC-150 MiniCycler (Cat# HBA-1152 from MJ Research Incorporation) or the Applied Biosystems Veriti 96-well thermal cycler (Cat# 4375786 from Thermo Fisher Scientific).

Table S6: PCR primers for site-directed mutagenesis and sequencing.

Purpose	Primer sequence* (yellow = difference in sequence relative to wild-type DrGBE) (underline = difference in codon relative to wild-type DrGBE)
SDM for Q205H	Forward: GGCTATCACGTCACGGGCTAC Reverse: GTAGCCCGTGACGTGATAGCC
SDM for A310Q	Forward: GTGGACCAGGTGGCCTCCAT Reverse: ATGGAGGCCACCTGGTCCAC
SDM for A310G	Forward: GTGGACGGAGTGGCCTCCAT Reverse: ATGGAGGCCACTCCGTCCAC
SDM for A312T	Forward: GTGGACGCGGTGACCTCCATGCTGTAC Reverse: GTACAGCATGGAGGTCACCGCGTCCAC
Sequencing primers**	T7 promoter and T7 terminator Forward starting at residue 262: CGCTACAAATTCCGCGTGACCG Reverse starting at residue 822: CCAGTCGTAGTGGTAGCCCTTGC Reverse starting at residue 957: AAAGTCCAGGTACAGCATGGAG Forward starting at residue 679: AACCATTTGCACTCGCTCG Forward starting at 1427: GCAGCGAGTGGAACCATGAC Reverse starting at 2012: ACCAGCCGCTGTTGCTCGTT Reverse starting at 1274: CTAATCGCCAGCACGTAGTTTTCAC Forward starting at 1019: TTCTCAAGCGCCTGAACGA

*Primers from University of Guelph Lab Services.
**More sequencing primers used than necessary because originally used a sequencing protocol that was inefficient for GC-rich sequences.

Table S7: Variations of transforming *Escherichia coli* with the pET28a vector.

	Transformation into DH5α			Transformation into BL21		
DrGBE variant	**DNA (µL)**	**Cells (µL)**	**Time for heat-shock (s)**	**DNA (µL)**	**Cells (µL)**	**Time for heat-shock (s)**
Q205H	5	50	60	2.5	50	45
A310Q	1	100				
A310G	1	100				
A312T	1.5	15				